ICT-619555 RESCUE

D1.2.1 Version 1.0

Assessment on Feasibility, Achievability, and Limits

Contractual Date of Delivery to the CEC:	04/2015 (M18)
Actual Date of Delivery to the CEC:	TBD
Editor	Xiaobo Zhou
Author(s)	Xiaobo Zhou, Na Yi, Xin He, Jiancao Hou, Tad Matsumoto, Szymon Szott, Diana Gonzáles, Albrecht Wolf, Maximilian Matthé, Sebastian Kühlmorgen, Olayinka Adigun
Participants	UOULU, UNIS, JAIST, TUD, AGH, UbiTech
Work package	WP1
Estimated person months	19
Security	**PU**
Nature	R
Version	1.0
Total number of pages	59

Abstract: In this deliverable some preliminary results on the achievable rate region and performance limit analysis of RESCUE system are presented. Based on the input of Task 1.1, we first identify four simple scenario assumptions, referred to as toy scenarios, that are suitable for evaluation of the links-on-the-fly concept. The underline supporting theories for the links-on-the-fly concept, including distributed lossless/lossy coding theorems and Shannon's lossy source/channel separation theorem are then introduced briefly. The achievable rate region, outage probability and/or error rate of the four toy scenarios are analyzed in details based on the supporting theories. The baselines of different protocol layers for the performance comparison with RESCUE system are also summarized. It is shown that with the links-on-the-fly concept, significant performance gains can be achieved.

Keyword list: links-on-the-fly, distributed lossless/lossy source coding, Shannon's lossy source/channel separation theorem, achievable rate region, outage probability

Disclaimer:

Executive Summary

This deliverable presents some preliminary theoretical results to demonstrate the potential performance gains of the links-on-the-fly concept introduced in the RESCUE project. Since the general network model for the RESCUE project is complicated in terms of densely deployed nodes and the mixture of lossless/lossy links, it is difficult to perform theoretical analysis to the general network model directly. Instead, first we focus on four representative toy scenarios, which are suitable for the evaluation of the links-on-the-fly concept. The baselines of different protocol layers used for performance comparison with the RESCUE system are also summarized. The distributed lossless/lossy coding and Shannon's lossy source/channel separation theorems are the keys to understanding the benefits of the links-on-the-fly concept, which are then introduced briefly. Sequentially, the performance assessment of the four toy scenarios based on these theorems are provided in details with rigorous mathematical derivations.

Toy Scenario 1 (TS1) we considered is a typical three-node one-way relay system. With the links-on-the-fly concept, the source-relay link is allowed to be lossy. The achievable rate region of TS1 is determined by the theorem for source coding with a helper, and the outage probability is expressed as triple integrals over the achievable rate region. By replacing the theorem for source coding with a helper, an approximated yet accurate enough outage probability can be obtained. Compared with the case where source-relay link is not allowed to be lossy, TS1 can achieve better outage performance. Based on the derivation of the outage probability, the optimal relay location is shifted to exactly the midpoint between the source and the destination. Furthermore, it is found that TS1 with lossy forwarding concept outperforms the conventional techniques in terms of the ε-outage capacity and throughput performance.

Toy scenario 2 (TS2) is a single-source multiple-relays and single-destination system, where there is no direct link between the source and the destination. We are interested in the performance of TS2 in the special case that all the source-relay links are lossy, which is also known as the chief executive officer (CEO) problem. We analyze the achievable rate-distortion region according to the Berger-Tung inner bound and derived the threshold limit of the bit error rate (BER) performance. Moreover, to better understand the performance in TS2, an approximation and a lower bound are proposed to predict the error floor. The outage probability of TS2 is also derived based on the Slepian-Wolf theorem, when the minimal distortion of TS2 is achieved.

Toy scenario 3 (TS3) is an extension of TS1, where multiple relays are deployed to help the information transmission from the source to the destination. With multiple relays and the links-on-the-fly concept, the achievable rate region and outage probability analysis involves extremely challenging theoretical work that does not have an optimal solution yet. Therefore, as an intermediate result, the Selective Decode-and-Forward (SDF) based multiple erroneous relaying is investigated. The initial performance analysis in terms of BER has been studied over Rayleigh fading channel environment.

Toy scenario 4 (TS4) is an orthogonal multiple access relay channel (MARC) with two sources, single relay and a common destination, where the source-relay links are allowed to be lossy with the links-on-the-fly concept. The achievable rate region is determined by the theorem for source coding with a helper, and the outage probability is derived based on the achievable rate region. It is shown through simulations that in the case one of the source nodes is far way from both the relay and the destination, TS4 outperforms the case where source-relay links are not allowed to be lossy.

Although the performance gains of the links-on-the-fly concept applied to TS3 is not provided in this deliverable, an initial theoretical framework that enables further extension has been established. The preliminary results obtained with TS2 are also of crucial importance to understand and demonstrate the benefits of the links-on-the-fly concept, which need to be further refined through some challenging theoretical work. One of the contributions of this deliverable is the rigorous theoretical analysis of TS1 and TS4 show that significant performance gains can be achieved with the links-on-the-fly concept. In summary, these results indicate that the links-on-the-fly concept is promising in the general network model of the RESCUE system that built upon the toy scenarios.

Authors

Partner	Name	Phone/Fax/e-mail
University of Oulu (UOULU)	Xiaobo Zhou	Phone: +358 41 490 3754 Fax: – e-mail: xiaobo.zhou@ee.oulu.fi
	Xin He	Phone: +358 41 490 0476 Fax: – e-mail: xin.he@ee.oulu.fi
University of Surrey (UNIS)	Na Yi	Phone: +44 1483 684703 Fax: +44 1483 686011 e-mail: n.yi@surrey.ac.uk
	Jiancao Hou	Phone: +44 1483 683658 Fax: +44 1483 686011 e-mail: jh0067@surrey.ac.uk
Japan Advanced Institute of Science and Technology (JAIST)	Tad Matsumoto	Phone: +81 761 51 1265 Fax: +81 761 51 1149 e-mail: matumoto@jaist.ac.jp
Technical University Dresden (TUD)	Albrecht Wolf	Phone: +49 351 463 41 047 Fax: – e-mail: albrecht.wolf@ifn.et.tu-dresden.de
	Maximilian Matthé	Phone: +49 351 463 41 071 Fax: – e-mail: maximilian.matthe@ifn.et.tu-dresden.de
	Sebastian Kühlmorgen	Phone: +49 351 463 41 047 Fax: – e-mail: Sebastian.Kuehlmorgen@tu-dresden.de
AGH University of Science and Technology (AGH)	Szymon Szott	Phone: +48126173538 Fax: +48126342372 e-mail: szott@kt.agh.edu.pl
UbiTech Ltd	Olayinka Adigun	Phone: Fax: e-mail: Olayinka@ubitechit.com

Table of Contents

List of Acronyms and Abbreviations

Term	Description
AF	Amplify-and-forward
AF-IR	Amplify-and-forward with incremental relaying
AWGN	Additive white Gaussian noise
BER	Bit error rate
BPSK	Binary phase-shift keying
BSC	Binary symmetric channel
CBF	Contention-based forwarding
CEO	Chief executive officer
CF	Compress-and-forward
CRC	Cyclic redundancy check
CSI	Channel state information
D	Destination
DACC	Doped-accumulator
DF	Decode-and-forward
DF-IE	Decode-and-forward relaying allowing intra-link errors
DF-IR	Decode-and-forward with incremental relaying
DTO	Data traffice overhead
ETED	End-to-end delay
FER	Frame error rate
GF	Greedy forwarding
i.i.d.	Indepently and identically distributed
IR	Incremental relaying
KPI	Key performance indicator
LLR	Log-likelihood ratio
LOS	Line-of-sight
MARC	Multiple access relay channel
MARC-IE	Multiple access relay channel allowing intra-link errors
MARC-NC	Network-coding-based multiple access relay channel
MARC-SDF	Multiple access relay channel with selective decode-and-forward relaying
MGF	Moment generating function
MP-OLSR	Multipath optimized link state routing
MRC	Maximum-ratio combine
NAK	Negative acknowledge
NDF	Non-cooperative decode-and-forward
NLOS	Non line-of-sight
ODF	Opportunistic decode-and-forward
pdf	Probability density function
PHY	Physical
pmf	Probability mass function
QoS	Quality of service
R	Relay
R-D	Relay destination
R-OLSR	RESCUE optimized link state routing
S	Source
S-D	Source-destination
SDF	Selective decode-and-forward
SGB	Simple geo-broadcast
SNCC	Separate network-and-channel coding
SNR	Signal-to-noise ratio
S-R	Source-relay
TH	Throughput
TS	Toy scenario

V2V	Vehicle-to-vehicle
WIR	Well-informed relay
WLAN	Wireless local area network
XOR	Exclusive-OR

1.   Introduction

1.1   Links-on-the-fly Concept and Identified Toy Scenarios

Two potential use case scenarios, i.e., public safety operations and vehicle-to-vehicle (V2V) communication, have been introduced in [D11] for the RESCUE system, where the former one takes place in areas where the communication infrastructure is partially inoperable due to natural disasters such as tsunami and earthquake, and the latter one is dedicated to applications where cars and other vehicles share safety-critical information about the road and traffic conditions with each other. The key functional requirements and design challenges of these two use cases are also identified based on their unique wireless characteristics. It was shown that in public safety operations, the remaining infrastructures have limited communication capacity, and the moving speed of the terminals can be safely assumed to be low enough. On the other hand, in V2V communication, a fast changing environment, including channel conditions and network topology, must be assumed due to the possible high moving speed of vehicles.

The objective of Task 1.2 is to identify the canonical network models suitable for public safety operations and V2V communications, and to assess the feasibility, achievability and limits of the links-on-the-fly concept within the canonical network models. Although the two use cases have unique characteristics as described above, they still share the common links-on-the-fly concept that as developed for networks expected to be dense in terms of node and link populations, and heterogeneous in terms of their built-in capabilities. In such networks, there are multiple sources communicating with multiple destinations that are most probably multi-hops away with the assistance of multiple intermediate nodes (relays). Since accurate/strict link budget design cannot be guaranteed, certain level of distortion is allowed at the relays and consequently multiple lossy links can be preserved. Another important factor is the channel conditions changing from line-of-sight (LOS) component to non-line-of-sight (NLOS) component, resulting in dynamic changes in the connectivity and the network topology. A general cooperative network model taking these features into account is depicted in Figure 1.1, where each node can be a rescuer or a base station in public safety operation, or a car or a road side equipment in V2V communication.
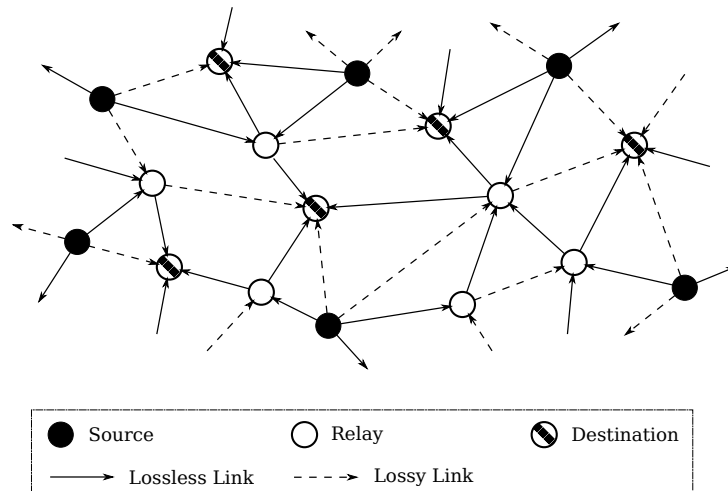
Figure 1.1: Abstract general network model for RESCUE system.

A major advantage of the links-on-the-fly concept is that the information sequences received at the relay found to contain errors are not discarded but further interleaved, re-encoded, and forward to the next stage. By allowing this source-relay link (referred to as intra-link) errors, many parallel links can be preserved and the network as a whole is converted into distributed codes, thus significant gains are expected. However, theoretical analysis and performance evaluation of the general cooperative network model with the links-on-the-fly concept shown in Figure 1.1 presents a lot of challenges due to its complicated and dynamic network topology. Instead, we first decompose this general network into basic network models that are widely studied in cooperative communications. In this deliverable, we refer the basic network models as toy scenarios. In total, four toy scenarios are considered, which are shown in Figure 1.2.
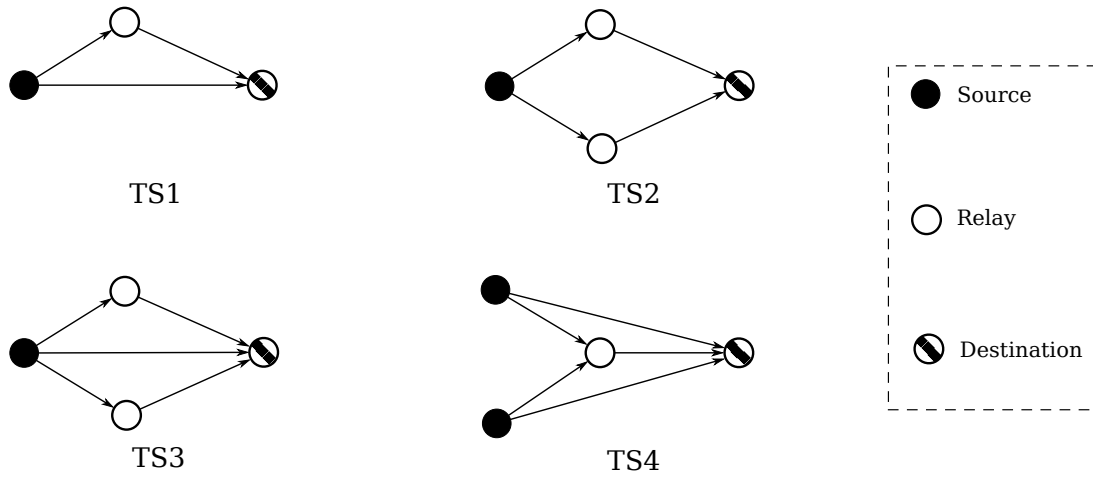
Figure 1.2: Four toy scenarios considered in this deliverable.

Toy Scenario 1 (TS1) This is a typical three-node one-way relay system, where a single source is communicating with a single destination with the help of a single relay. The basic idea of this simple relay channel was first introduced by Van der Meulen [Meu71] in 1970s. Nowadays, this typical three-node one-way relay system still serves as an important network model for investigating performance of new cooperative strategies.

Toy Scenarios 2 (TS2) This is a single source, multi-relay, single destination without direct link system. We are especially interested in the case when all the source-relay links are not perfect. In this case, the information forwarded by the relays contains certain errors about the original information sent from the source, and the destination tends to recover the original information after receiving signals from the relays. This problem is also referred to as chief executive officer (CEO) problem.

Toy Scenarios 3 (TS3) As an extension of TS1, multiple relays are available in TS3 to help the information transmission from the source to the relay. With the presence of multiple relays, there are multiple routes from the source to the destination, which is suitable for modeling the RESCUE system. Compared with TS2, there is a direct link between the source and the destination, therefore the destination has a chance to recover losslessly the original information transmitted from the source.

Toy Scenarios 4 (TS4) This is an multiple access relay channel (MARC), where multiple sources are transmitting their dedicated information to the common destination with the assistance of a single relay. In the MARC, the relay transmits the combination of signals received from the two sources, and diversity gain, as well as energy/spectrum efficiency can be achieved.

There are some assumptions made with the theoretical analysis for the four toy scenarios, which are listed as follow.

- The relays are working in half-duplex mode with single antenna, i.e., they cannot receive and transmit simultaneously.

- Strict synchronization at the destination, hence misalignment of the received signals is not considered.

- Error free channel estimation is assumed at the destination.

- Single carrier is assumed and complex waveform design is not considered in this deliverable. The communication links are assumed to be block Rayleigh/Rician fading channels with additive white Gaussian noise (AWGN) in TS1, TS3 and TS4, and only to be AWGN channels in TS2. Note that the optimal rate-distortion region of the binary CEO problem is still unknown in network information theory, therefore we only investigate the performance limits of TS2 in AWGN channels for simplicity in this deliverable.

1.2   Baseline Setup

The novel links-on-the-fly concept is promising in capacity and spectrum efficiency enhancement, and transmit power and outage probability reduction, by means of employing new designs of different protocol layers, from physical (PHY) layer to network layer. In order to demonstrate the performance gains of the links-on-the-fly concept, different baselines for different protocol layers are chosen from the state of the art approaches for performance comparison. A brief introduction of the baselines, together with key performance indicators (KPIs), are presented in this section.

1.2.1   PHY Layer Baseline

As described above, the RESCUE cooperative relaying protocol in the PHY layer consists of decode-and-forward (DF) that allows intra-link errors, combined with distributed codes that brings improved error protection. We consider the following state of the art DF based relaying protocols as the PHY layer baselines.

Non-cooperative DF (NDF) relaying The traditional target of relay-aided communication is to increase the coverage of the network. The state of the art for the relaying in the existing technologies and standards, such as cellular LTE-Advanced networks and TETRA networks, is NDF relaying, where a single route between the source and the destination is discovered and employed. The transmission from the source to the destination fails if either the relay or the destination fails in decoding. NDF can be used for performance comparison with RESCUE relaying protocol in terms of outage probability, frame error rate (FER), and throughput.

Selective DF (SDF) relaying In SDF relaying [LTW04], the relay forwards the received data selectively. More specifically, the relay forwards the data that was detected correctly to the destination to achieve full diversity, and discards the ones that were detected with errors in order to avoid error propagation.

In WP1, the relaying protocols are analyzed from purely information theory point of view with the assumption of infinite block length. This implies that an outage (i.e. code rate is larger than the channel capacity) is translated directly into a detection error at the relay. The KPIs of the comparison with the RESCUE relaying protocol are outage probability, outage capacity, and throughput.

The assumption of infinite block length is removed and practical channel coding/decoding algorithms are investigated in WP2. In this case, the forwarding decision is usually made based on the decoding result at the relay. One such technique is to use a cyclic redundancy check (CRC) check at the relay [LTW04], which is referred to as CRC-based SDF. Other measures that can be used for forwarding decision are link signal-to-noise ratio (SNR) and log-likelihood ratio (LLR), and the corresponding approach are referred to as SNR-based SDF [HZF04; OAF+08] and LLR-based SDF [KK06; PAR08], respectively. For SNR-based SDF (or LLR-based SDF), the relay will forward the data only if the received SNR (or LLR of the received signal) at the relay pass the predefined threshold. In both SNR-based and LLR-based SDF, the optimal threshold is globally determined based on the channel state information (CSI) of the source-destination and relay-destination links, which is impractical in large scale networks. Moreover, SNR-based and LLR-based SDF were analyzed in the case of uncoded transmission where the link-level bit error rate (BER) can be expressed as a closed-form function of the SNR. Note in WP2, where practical channel coding/decoding is used, we only apply the concept of SNR-based and LLR-based SDF, and the optimal threshold investigation is out of the scope of the project. The KPIs we consider are FER, sum rate, and throughput.

Opportunistic DF (ODF) relaying The opportunistic relaying was proposed by Bletsas et. al. [BKR+06] to reduce the system complexity, where the best relay is selected among available relay candidates according to a certain policy. It is shown that there is no loss in performance in terms of the diversity-multiplexing tradeoff if only the best relay participates in cooperation. The outage probability of opportunistic DF relaying was derived in [HKA08], where the relay selection policy is to maximize the minimum of the source-relay and relay-destination channel gains. The KPIs for performance comparison with RESCUE relaying protocol are outage probability, FER, and throughput.

In the above mentioned baselines, ODF is suitable for TS3 where there are multiple relays, while NDF and SDF can be applied in TS1, TS2, and TS4. Note for the binary CEO problem in TS2, the optimal rate-distortion region is a long-standing open problem. To the best of our knowledge, there is no baseline for the theoretical bound of the CEO problem. However, the performance of the coding/decoding algorithm will be compared with that proposed in [HBP08; RYA11] in terms of BER. The PHY layer baselines are summarized in Table 1.1.

Table 1.1: The PHY layer baselines.

PHY layer baseline		KPI		Toy scenario
		WP1	WP2	
NDF		- outage probability - throughput	- FER - throughput	TS1, TS3, TS4
SDF	CRC-based SDF	- outage probability - outage capacity - throughput	- FER - sum rate - throughput	TS1, TS3, TS4
	SNR-based SDF			
	LLR-based SDF			
ODF		- outage probability - throughput	- FER - throughput	TS3
Baseline for TS2		None	- BER	TS2

1.2.2   Message Transfer Baselines

1.2.2.1   Baseline for MAC

IEEE 802.11 [12] (commercially referred to as Wi-Fi) is the predominant standard for wireless local area networks (WLANs). It has achieved widespread adoption through ease of use and low cost of devices. It relies on uncoordinated, packet-based channel access for providing high transmission speeds for nomadic users.

802.11 has been chosen as the MAC baseline because of the following features:

- relative simplicity of medium access (an extended version of CSMA/CA which also serves as the basis of the RESCUE MAC design),

- packet-based operation,

- having been analysed in-depth by the research community (including partners of the RESCUE consortium) [NP00; KNP11; KNS+13],

- operation in unlicensed (free) spectrum,

- availability of software tools and hardware platforms.

As KPIs relevant to the comparison of the the MAC protocols designed in WP3 and 802.11 we consider:

- throughput – under lossless operation the RESCUE MAC should exhibit similar throughput as 802.11, whereas under lossy link conditions the RESCUE MAC should significantly outperform 802.11,

- delay – the difference in traffic latency as caused by 802.11 and the RESCUE MAC will serve as a metric of the overhead imposed by the use of the cooperative relaying approach,

- jitter – because the multipath approach adopted in RESCUE can lead to an increase in the variance of traffic latency, this metric will inform whether higher layer applications are operating within acceptable bounds,

- packet loss – a critical metric for operating under lossy link conditions and for providing appropriate QoS.

In terms of requirements, in order to make a meaningful comparison with 802.11 it is necessary for the MAC protocol under comparison to consider asynchronous, packet-based, half-duplex transmissions. This is in line with the initial design of RESCUE MAC protocols described in D3.1.

1.2.2.2   Baseline for geographic routing

The ESTI GeoNetworking protocol [ETS14] is a network protocol that provides single-hop and multi-hop communication in vehicular ad hoc networks based on IEEE 802.11p/ITS-G5. It is standardized by the ETSI Technical Committee ITS as part of its Release 1. The standards specify several optional forwarding algorithms. These algorithms make use of geographic positions for forwarding decisions. They enable the distribution of packets to all nodes inside a geographical area. Greedy Forwarding (GF) and Contention-Based Forwarding (CBF) are used for unicast and broadcast communication where the broadcast case is more relevant for vehicle safety applications. The forwarding scheme with the lowest complexity is Simple Geo-Broadcast (SGB), where a dedicated geographic area is flooded with a packet. Advanced forwarding is a combination of the GF and CBF algorithms; they use overhearing to decrease the network load.

Vehicular networks are inherently unreliable due to the frequently changing network topology and moving cars. GeoNetworking is intended for vehicle to vehicle communication. It is part of the protocol stack for cooperative ITS in Europe [Fes14] and it is expected that the protocol will be deployed in the next years. The theoretical results of the RESCUE approach indicate that its application in vehicular scenarios can improve the reliability and latency of the communication. In this context, ETSI GeoNetworking represents the state-of-the-art solution, which we regard as the baseline and compare GeoNetworking with the RESCUE approach. The metrics decsribed below will be used as KPIs.

Throughput (*TP*): In vehicular networks it is important to disseminate a message reliably to a neighbor or via multi-hop to a vehicle far away. For this reason a high throughput is important for all safety applications.

$$TP = \frac{\text{No. of messages received by the destination}}{\text{No. of sent messages by the source}} \qquad (1.1)$$

End-to-End Delay (*ETED*): In vehicular networks a small latency is critical for safety applications since the nodes change their positions continuously. In some cases, vehicles may have to react in a very short time. This requires the end-to-end delay being low.

$$ETED = t_{\text{Rx}} - t_{\text{Tx}} \qquad (1.2)$$

Data traffic overhead (*DTO*): To route a message through a network some control messages and retransmissions are needed. The simplest way is to retransmit every message in every node. This leads to a waste of bandwidth. Therefore the routing algorithm has to forward the message in a smart way to decrease the channel load.

$$DTO = \frac{\text{Total no. of frames at PHY/MAC layer}}{\text{No. of sent messages Tx}} \qquad (1.3)$$

GeoNetworking has been evaluated in [Küh15]. This paper can serve as a reference case to compare the RESCUE geographic routing algorithm with the standardized solutions. The assumptions necessary in order to perform a meaningful comparison include the existence of lossy links between the source and the destination and that corrupted packets are forwarded and not discarded in the MAC. In GeoNetworking the communication is only successful if at least one link is lossless. In [Küh15] a bidirectional freeway with three lanes per direction and a high node density was used. To accomplish lossy links the scenario has to be modified to one with a more sparse node density.

1.2.2.3   Baseline for RESCUE multi-path routing

Routing protocols are fundamental to determine the appropriate paths over which data is transmitted in ad hoc networks. RESCUE Optimized Link State Routing (R-OLSR) is a routing protocol being proposed for the RESCUE project and it considers multiple paths in its route calculation. Hence, it can increase network throughput, improve transmission reliability and provide load balancing. The Multipath Optimized Link State Routing (MP-OLSR) [YAD+11] protocol has been chosen as a baseline for comparison with R-OLSR.

MP-OLSR is a multipath routing protocol based on OLSR which is expected to provide more stable routes for a network using the concept of source suggested routing. It has been chosen as our baseline for comparison because it has the ability to provide multiple paths between the source and destination node as is the case with R-OLSR. This will enable a fair basis for comparison between these protocols and other known routing protocols in the literature.

In the comparison and analysis of R-OLSR, some key performance indicators to be considered are: throughput, end-to-end delay, and routing overhead. An assumption necessary in order to make a meaningful comparison with MP-OLSR is that joint turbo decoding at the destination node provides an error-free copy of the message.

1.3   Contributions and Outline

The primary goal of this deliverable is to establish a theoretical basis for analyzing the four toy scenarios, where the links-on-the-fly concept is applied, and define the baseline for performance comparison. The achievable rate region, performance limits such as threshold limit and outage probability, etc., are analysed within the framework of distributed lossless/lossy compression and Shannon's lossy source/channel separation theorem, which are all belonging to network information theory. Since the intra-links are allowed to be lossy, the theoretical analysis is different from the previous work focusing on perfect intra-links. The information theoretical understanding for these four toy scenarios provides insights into understanding and analysis of more complicated networks of the RESCUE system. Furthermore, it is shown through theoretical results that significant performance gains can be achieved in the toy scenarios with the links-on-the-fly concept.

This deliverable is organized as follows. In Chapter 1 (this chapter), we have reviewed the two use cases identified in [D11] and identified four toy scenarios that are suitable for the links-on-the-fly concept. The baselines for different protocol layers are also summarized. Chapter 2 briefly introduces the network information theoretical background for analyzing the performance of the toy scenarios, including distributed lossless/lossy source coding and Shannon's lossy source/channel separation theorems. Theoretical performance analysis of TS1, TS2, TS3, and TS4 are presented in Chapter 3, Chapter 4, Chapter 5, and Chapter 6, respectively. Finally, Chapter 7 summarizes the results presented in this deliverable that serve as the initial input to WP2 and WP3, and provides insights into the future work.

2.   Information Theoretical Background

This chapter describes the information theoretical background for analyzing the RESCUE system. With the links-on-the-fly concept, intra-link errors are allowed and many parallel routes between the source and the destination can be preserved in the four toy scenarios. The information sequences conveyed via the multiple routes are highly correlated with each other since they are transmitted from the same source. Hence, it is with higher probability to reconstruct the original information at the destination if the correlation knowledge can be utilized in the decoding process. To be able to understand the advantages of the links-on-the-fly concept and to quantitatively analyze the performance improvement, it is of crucial importance to identify the amount of the correlation knowledge (or the redundancy) among different routes connecting to the same destination.

Source coding is one of the most important signal processing problems in communication theory that deals with the source redundancy. In conventional source coding techniques, a single encoder or several encoders collaborate with each other to perform compression in order to remove the redundancy of the source, which is usually referred to as centralized source coding [DG09]. However, the advance of wireless sensor/mesh networks and ad-hoc networks brought new challenges to the source coding problem: the source information to be compressed appears at several separate terminals and it is not always feasible to communicate among these terminals. The resulting source coding problem is often referred to as distributed source coding [XLC04] in network information theory. The information transmission with the links-on-the-fly concept falls exactly into the category of distributed source coding.

Depending on whether a certain level of distortion is allowed at the destination after decoding, there are two different classes of distributed source coding: the lossless one and the lossy one. Distributed lossless source coding can be regarded as a special case of distributed lossy source coding by setting the distortion to be 0. Intuitively, be accepting a certain level of distortion at the destination, more redundancy can be removed, and the achievable rate region is enlarged. It should be emphasized that in this deliverable, unless otherwise specified, the *achievable rate region* refers to the achievable compression rate region for source coding.

2.1   Distributed Lossless Source Coding

In this section, we introduces two important theorems about distributed lossless source coding. First we consider the problem of transmitting correlated sources over parallel links to a common destination. The achievable rate region for separately encoding and joint decoding of these two correlated sources is identified by the Slepian-Wolf theorem. We then consider the problem of lossless source coding with a helper. Unlike the first problem, only one of the correlated sources is to be recovered at the destination and the other serves as a helper.

2.1.1   Slepian-Wolf Coding

Let $\{X_1^i, X_2^i\}_{i=1}^{\infty}$ be a sequence of independent and identically distributed (i.i.d.) discrete random pairs with a joint probability density function (pdf), i.e., $(X_1^i, X_2^i) \sim p(x_1, x_2)$. According to the source coding theorem [Sha48], if we want to transmit both X_1 and X_2 losslessly to the decoder, a rate $H(X_1, X_2)$ is sufficient if X_1 and X_2 are encoded together. For example, we can first describe X_1 at $H(X_1)$ bits per symbol and then describe X_2 at $H(X_2|X_1)$ bits per symbol based on the complete knowledge of X_1 at both the encoder and the decoder.
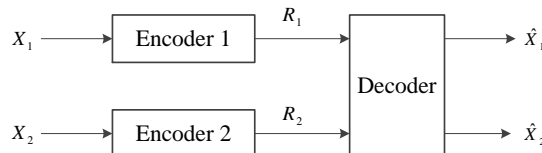
Figure 2.1: Distributed lossless source coding system.

However, if X_1 and X_2 are separately encoded at rates R_1 and R_2, respectively, and decoded jointly, as shown in

Figure 2.1, determining the sufficient rates for lossless recovery of X_1 and X_2 is not so straightforward. Clearly, X_1 and X_2 can be separately encoded at their corresponding entropy resulting in an overall rate $R = R_1 + R_2 = H(X_1) + H(X_2)$, but obviously this is greater than $H(X_1, X_2)$ when X_1 and X_2 are correlated. This problem has been theoretically investigated by Slepian and Wolf in their landmark paper [SW73], of which the results can be described as follow.

Theorem 1 (Slepian-Wolf Theorem). *For a sequence $\{X_1^i, X_2^i\}_{i=1}^{\infty}$ of discrete random pairs (X_1^i, X_2^i) drawing i.i.d. $\sim p(x_1, x_2)$, where $X_1^i \in \mathscr{X}_1$ and $X_2^i \in \mathscr{X}_2$. Then for any rate pair that satisfy*

$$\begin{cases} R_1 & \geq & H(X_1 | X_2), \\ R_2 & \geq & H(X_2 | X_1), \\ R_1 + R_2 & \geq & H(X_1, X_2), \end{cases} \tag{2.1}$$

there exists an integer n and mappings

$$\begin{array}{llll} i: & \mathscr{X}_1^n & \to & I = \{1, 2, \cdots, 2^{nR_1}\}, \\ j: & \mathscr{X}_2^n & \to & J = \{1, 2, \cdots, 2^{nR_2}\}, \\ g: & I \times J & \to & \mathscr{X}_1^n \times \mathscr{X}_2^n, \end{array} \tag{2.2}$$

such that

$$\Pr\{g(i(X_1^1, \cdot, X_1^n), j(X_2^1, \cdots, X_2^n)) \neq (X_1^1, \cdots, X_1^n, X_2^1, \cdots, X_2^n)\} \leq \varepsilon. \tag{2.3}$$

According to the Slepian-Wolf theorem, an achievable rate region is specified, as shown in Figure 2.2. Compared with independent decoding of X_1 and X_2, the achievable rate region specified by the Slepian-Wolf theorem is enlarged. It is well known that as long as the rate pair (R_1, R_2) falls inside the achievable rate region, the error probability after joint decoding can be made arbitrarily small. Therefore the decoding error probability can be greatly reduced with the joint decoding of X_1 and X_2 according to Slepian-Wolf theorem.
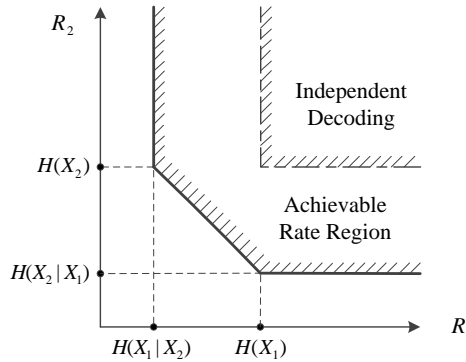
Figure 2.2: The achievable rate region of Slepian-Wolf theorem.

2.1.2 Lossless Source Coding with a Helper

In the correlated source transmission problem described in the previous section, if only one of the two sources is to be recovered at the destination while the other one serves as a helper, Slepian-Wolf theorem does not hold any more. Without loss of generality, we assume X_1 and X_2 are separately encoded and transmitted to the same destination, and only X_1 is to be recovered losslessly while the encoder for X_2 provides *coded side information* to the decoder to help the decoding of X_1, as shown in Figure 2.3. The question is if we encode X_2 at rate R_2, then what is the optimal rate R_1 for encoding X_1.

Consider two extreme case: (1) if $R_2 = 0$, there is no helper at the decoder, then X_1 must be encoded at a rate equal to or larger than its entropy, i.e., $R_1 \geq H(X_1)$; (2) if $R_2 \geq H(X_2)$, X_2 can be losslessly transmitted to the decoder, then $R_1 \geq H(X_1 | X_2)$ is sufficient and necessary according to the Slepian-Wolf theorem. In general, if X_2 can provide more information about X_1, R_1 can be further reduced, leading to the following theorem [GK11, Theorem 10.2].
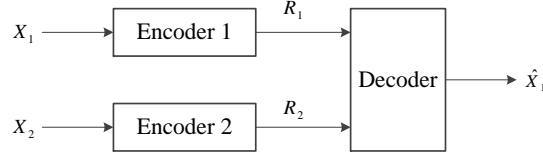
Figure 2.3: Distributed lossless source coding with a helper.

Theorem 2. *For a sequence $\{X_1^i, X_2^i\}_{i=1}^{\infty}$ of discrete random pairs (X_1^i, X_2^i) drawing i.i.d. $\sim p(x_1, x_2)$, where $X_1^i \in \mathscr{X}_1$ and $X_2^i \in \mathscr{X}_2$. Then for any rate pair that satisfy*

$$\begin{cases} R_1 & \geq & H(X_1|U), \\ R_2 & \geq & I(X_2;U), \end{cases} \tag{2.4}$$

there exists an integer n and mappings

$$\begin{array}{rcl} i: & \mathscr{X}_1^n & \to & I = \{1, 2, \cdots, 2^{nR_1}\}, \\ j: & \mathscr{X}_2^n & \to & J = \{1, 2, \cdots, 2^{nR_2}\}, \\ g: & I \times J & \to & \mathscr{X}_1^n, \end{array} \tag{2.5}$$

such that

$$\Pr\{g(i(X_1^1, \cdot, X_1^n), j(X_2^1, \cdots, X_2^n)) \neq (X_1^1, \cdots, X_1^n)\} \leq \varepsilon. \tag{2.6}$$

for some conditional probability mass function (pmf) $p(u|x_2)$, where $|\mathscr{U}| \leq |\mathscr{X}_2| + 1$.

The achievable rate region specified by the theorem for lossless source coding with a helper is depicted in Figure 2.4.
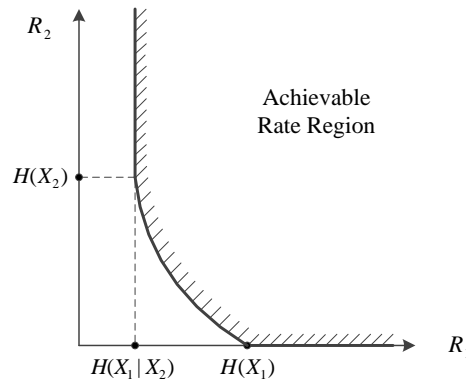
Figure 2.4: The achievable rate region of lossless source coding with a helper.

2.2   Distributed Lossy Source Coding

In the previous section, it is assumed that at least one of the correlated sources is to be recovered at the destination. In this section, we remove this constraint by accepting specific distortions associated with different sources, which belongs to distributed lossy source coding problem. The distributed lossy source coding is usually used in the system where quality of service (QoS) requirement is concerned, such as some distortion is allowed in RESCUE systems in some emergency situation.
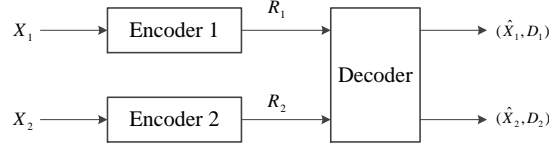
Figure 2.5: Distributed lossy source coding system with two sources.

A distributed lossy source coding system with two correlated sources X_1 and X_2 is shown in Figure 2.5. X_1 and X_2 are encoded at rates R_1 and R_2, respectively, and transmitted to the same destination. The destination obtains two estimations, $\hat{X}_1$ and $\hat{X}_2$, after joint decoding. Let $d_1(X_1, \hat{X}_1)$ and $d_2(X_2, \hat{X}_2)$ be the distortion measures, determining the achievable rate region within which the predefined distortion constraints can be satisfied, i.e., $E[d_1(X_1, \hat{X}_1)] \leq D_1$ and $E[d_2(X_2, \hat{X}_2)] \leq D_2$, with D_1 and D_2 denoting the allowed distortion for X_1 and X_2, respectively, is a challenging topic. Unlike the two distributed lossless source coding problems described in the previous section, the rate-distortion region of the distributed lossy source coding problem is still not known in general [GK11]. In the following, however, an inner and outer bound on the rate-distortion region is introduced.

2.2.1 Berger-Tung Inner Bound

Theorem 3 (Berger-Tung Inner Bound). *For a sequence $\{X_1^i, X_2^i\}_{i=1}^{\infty}$ of discrete random pairs (X_1^i, X_2^i) drawing i.i.d. $\sim p(x_1, x_2)$, where $X_1^i \in \mathcal{X}_1$ and $X_2^i \in \mathcal{X}_2$. Then for any rate pair that satisfy*

$$\left\{ \begin{array}{rcl} R_1 & \geq & I(X_1; U_1 | U_2, Q), \\ R_2 & \geq & I(X_2; U_2 | U_1, Q), \\ R_1 + R_2 & \geq & I(X_1, X_2; U_1, U_2 | Q), \end{array} \right. \tag{2.7}$$

there exists an integer n and mappings

$$\begin{array}{rcll} i: & \mathcal{X}_1^n & \rightarrow & I = \{1, 2, \cdots, 2^{nR_1}\}, \\ j: & \mathcal{X}_2^n & \rightarrow & J = \{1, 2, \cdots, 2^{nR_2}\}, \\ g: & I \times J & \rightarrow & \mathcal{X}_1^n \times \mathcal{X}_2^n, \end{array} \tag{2.8}$$

such that

$$E[d_1(X_1, \hat{X}_1)] \leq D_1 \text{ and } E[d_2(X_2, \hat{X}_2)] \leq D_2, \tag{2.9}$$

for some conditional pmf $p(q)p(u_1|x_1, q)p(u_2|x_2, q)$ with $|\mathcal{U}_i| \leq |\mathcal{X}_i| + 4$, $i = 1, 2$.

It is easy to see that the Slepian-Wolf theorem is a special case of the Berger-Tung inner bound by setting $D_1 = D_2 = 0$.

2.2.2 Berger-Tung Outer Bound

As stated before, the rate-distortion region of lossy source coding problem is still not known in general. The lower convex envelope of the Berger-Tung inner bound determines an upper bound of the rate-distortion region, while the lower convex envelop of the Berger-Tung outer bound determines an lower bound of the rate-distortion region. In this subsection, the Berger-Tung outer bound is reviewed.

Theorem 4 (Berger-Tung Outer Bound). *For distributed lossy source coding problem, a rate pair (R_1, R_2) is achievable with given distortion pair (D_1, D_2) only if there exists two auxiliary random variables U_1 and U_2 which satisfy the inequalities*

$$\left\{ \begin{array}{rcl} R_1 & \geq & I(X_1, X_2; U_1 | U_2), \\ R_2 & \geq & I(X_1, X_2; U_2 | U_1) \\ R_1 + R_2 & \geq & I(X_1, X_2; U_1, U_2), \end{array} \right. \tag{2.10}$$

for some conditional pmf $p(u_1, u_2 | x_1, x_2)$ such that $U_1 \rightarrow X_1 \rightarrow X_2$ and $X_1 \rightarrow X_2 \rightarrow U_2$ form two independent Markov chains and $E[d_i(X_i, \hat{X}_i)] \leq D_i$ with $\hat{X}_i = f_i(U_1, U_2)$, $i = 1, 2$.

The expression of the outer bound is very similar to the Berger-Tung inner bound except requiring the time sharing variable Q to ensure the convexity of the envelope of the outer bound. Furthermore, the Markov condition is weaker than that in Berger-Tung inner bound.

2.3 Shannon's Lossy Source/Channel Separation Theorem

Recall that with the links-on-the-fly concept, intra-link errors are allowed. The information transmission with the source-relay or relay-relay link can be well modelled by Shannon's lossy source-channel separation theorem [Sha59; VFC+14]. This theorem states that if a transmitter intends to transmit a message to a certain receiver with a distortion level $\mathscr{D}$, then the following inequality must be satisfied:

$$R_c \cdot R(\mathscr{D}) \leq C(\gamma), \tag{2.11}$$

where R_c is the spectrum efficiency that includes both the channel coding rate and the modulation multiplicity, $R(\mathscr{D})$ the source rate-distortion function [CT06], and $C(\gamma)$ the channel capacity of the link between the transmitter and the receiver with a SNR γ. Assuming Gaussian codebook is used for modulation, $C(\gamma) = (N_D/2)\log_2(1 + 2\gamma/N_D)$ with N_D denoting the dimensionality of the channel input.

Note in high SNR region, it is possible to losslessly transmit X to the receiver and the distortion $\mathscr{D}$ always equals to 0. In this case, the inequality of Equation (2.11) always holds and is independent of γ. On the other hand, in low SNR region, most probably X cannot be losslessly transmitted. In this case, for a given value γ and by taking the equality of Equation (2.11), the minimum distortion $\mathscr{D}_{min}$ for the given channel SNR can be determined.

In RESCUE systems, binary sources are assumed and hence Hamming distortion measure is used, which result in $R(\mathscr{D}) = 1 - H_b(\mathscr{D})$, where $H_b(x) = -x\log_2(x) - (1-x)\log_2(1-x)$ is the binary entropy function. By taking the above descriptions into consideration, we can identify the relationship between $\mathscr{D}_{min}$ and γ as

$$\mathscr{D}_{min} = \begin{cases} H_b^{-1}[1 - C(\gamma)/R_c], & \text{for } 0 \leq \gamma \leq \gamma^*, \\ 0, & \text{for } \gamma \geq \gamma^*, \end{cases} \tag{2.12}$$

where γ^* is the threshold SNR.

Assume $R_c = 1/2$ and one-dimensional channel input, the source distortion curve with respect to the channel SNR is shown in Figure 2.6. As can be seen the figure, if the channel SNR γ is larger than the threshold ($\gamma^* = -3.01$ dB in this case), the distortion $\mathscr{D}_{min}$ is always 0. It can also been seen that as γ gets below the threshold, $\mathscr{D}_{min}$ increases as γ decreases. Intuitively, as the channel condition gets worse, less information can be conveyed from the transmitter to the receiver. It is expected that as $\gamma \to -\infty$, the source distortion finally goes to 0.5, which is not shown in this figure.
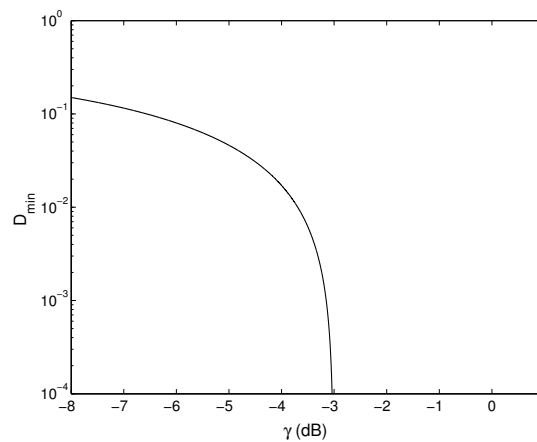
Figure 2.6: Source distortion vs. channel SNR.

3.   Performance Analysis of TS1

In this chapter, we theoretically analyze the outage probability of TS1, as shown in Figure 1.2. With the links-on-the-fly concept, the relay always forwards the decoder output to the destination regardless of whether errors are detected after decoding in the information part or not. Using the theorems for lossy source/channel separation and for source coding with a helper, the exact outage probability is derived. It is then shown that the exact expression can be reduced to a simple, yet accurate approximation by replacing the theorem for source coding with a helper by the Slepian-Wolf theorem. Compared with SDF and NDF relaying, the proposed scheme can achieve even lower outage probability. Moreover, by allowing intra-link errors, the optimal position of the relay is found to be exactly the midpoint between the source and destination. Finally, the ε-outage capacity and the throughput of TS1 are compared with the corresponding baselines. Results of the simulations are provided to verify the accuracy of the analytical results.

3.1   System Model

3.1.1   DF-IE System
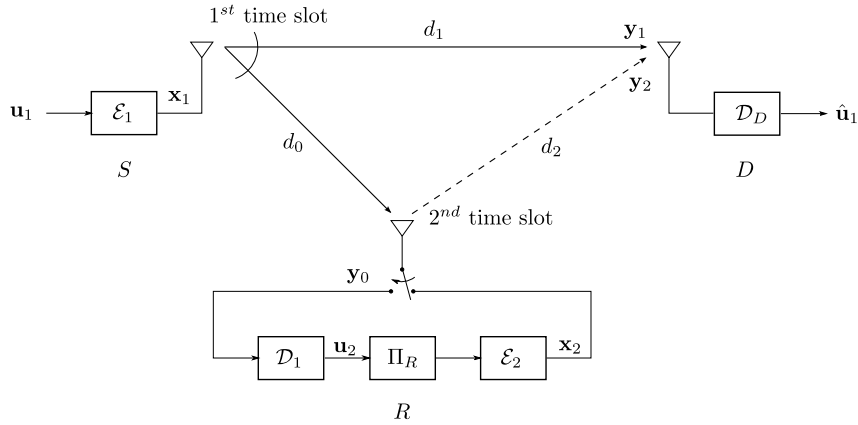
Figure 3.1: The block diagram of the three-node one-way relay system.

In the three-node one-way orthogonal half-duplex relay system, a source S and a relay R cooperate to transmit a message to a destination D, as shown in Figure 3.1. To guarantee orthogonal transmission, a time-division channel allocation is assumed; the transmission consists of two time slots. During the first time slot, S first performs a serial concatenation of channel coding and modulation, which is denoted as $\mathscr{E}_1(\cdot)$, on the original data sequence $\mathbf{u}_1$. The coded signal sequence $\mathbf{x}_1 = \mathscr{E}_1(\mathbf{u}_1)$ is then broadcasted to both R and D. During the second time slot, R first applies signal detection and decoding, which is dented as $\mathscr{D}_1(\cdot)$, on the received signal $\mathbf{y}_0$. The estimate of $\mathbf{u}_1$, i.e., $\mathbf{u}_2 = \mathscr{D}_1(\mathbf{y}_0)$, is then interleaved and re-encoded to obtain the coded signal $\mathbf{x}_2$, i.e., $\mathbf{x}_2 = \mathscr{E}_2[\Pi_R(\mathbf{u}_2)]$, where $\mathscr{E}_2(\cdot)$ is the signaling scheme applied at R and Π_R the random interleaver. The coded signal $\mathbf{x}_2$ is always forwarded to D, even though the $\mathbf{u}_2$ may contain errors about $\mathbf{u}_1$ (such errors are referred to as intra-link errors). Note that the decoder output at R is highly correlated with the original message sent from S. This correlation is referred to as *source-relay correlation* in this chapter.

After receiving signals $\mathbf{y}_1$ and $\mathbf{y}_2$ from S and R, respectively, D performs joint decoding by exploiting the source-relay correlation to retrieve $\mathbf{u}_1$ sent from S. The relay system assumed in this chapter, as a whole, can be seen as a distributed Turbo code. Hence, an iterative decoding process is required at D between the decoders for the codes used by S and R [AM12]. We refer this relay system as DF relaying system allowing intra-link errors (DF-IE).

3.1.2   Channel Model

The links between S and R, S and D, and R and D are assumed to suffer from independent block Rayleigh fading, where the channel gains keep constant within one transmission block but vary transmission-by-transmission. The

received signals at R and D can be expressed as

$$\mathbf{y}_0 = \sqrt{G_0} \cdot h_0 \cdot \mathbf{x}_1 + \mathbf{n}_0, \tag{3.1}$$

$$\mathbf{y}_1 = \sqrt{G_1} \cdot h_1 \cdot \mathbf{x}_1 + \mathbf{n}_1, \tag{3.2}$$

$$\mathbf{y}_2 = \sqrt{G_2} \cdot h_2 \cdot \mathbf{x}_2 + \mathbf{n}_2, \tag{3.3}$$

where h_i and $\mathbf{n}_i$ denote the complex channel gain and the zero-mean AWGN vector with the variance σ_i^2 per dimension, with $i \in \{0, 1, 2\}$ denotes the source-relay (*SR*), source-destination (*SD*) and relay-destination (*RD*) links, respectively. It is assumed that $\sigma_0^2 = \sigma_1^2 = \sigma_2^2 = N_0/2$ without loss of generality. The geometric-gain of each link is also considered in this chapter, which is represented by G_i. With d_i denoting the distance of its corresponding link and G_1 being normalized to the unity, G_0 and G_2 can be defined as $G_0 = (d_1/d_0)^l$ and $G_2 = (d_1/d_2)^l$, respectively, where l is the pathloss exponent, which is empirically set at 3.52 as in [YG11]. The geometric-gain between two nodes with distance d is defined as $G = (\frac{1}{d})^l$ according to [YG11]. Note further that we assume the transmit power per symbol at S and R is the same, which is denoted as E_s.

With the definitions described above, the instantaneous and average SNRs of *SD* link are expressed as $\gamma_1 = G_1|h_1|^2 E_s/N_0$ and $\Gamma_1 = G_1 E_s/N_0$, respectively. Similar definitions apply to γ_0, Γ_0, γ_2 and Γ_2. With Rayleigh fading assumption, the pdf of γ_i is given by [SBS96]

$$p(\gamma_i) = \frac{1}{\Gamma_i} \exp\left(-\frac{\gamma_i}{\Gamma_i}\right), \; i = 0, 1, 2. \tag{3.4}$$

3.2   Achievable Rate Region Analysis

With the block Rayleigh fading assumption, the intra-link error probability p stays constant over one block, but varies transmission-by-transmission. Note we set p as the minimum source distortion with hamming distortion measure [ZA06; ZCH+14], the relationship between p and the instantaneous SNR of the intra-link, γ_0, can be identified by Equation (2.12). In this section, we consider only one transmission, and hence p is regarded as a fixed parameter. As described above, $\mathbf{u}_2$ may contain some errors. Hence, $\mathbf{u}_2$ can be regarded as the bit-flipped version of $\mathbf{u}_1$, as $\mathbf{u}_2 = \mathbf{u}_1 \oplus \mathbf{e}$, where $\oplus$ indicates modulus-2 addition and $\mathbf{e}$ is a binary random variable vector with probability $\text{Pr}(e_k = 1) = 1 - \text{Pr}(e_k = 0) = p$. The correlation between $\mathbf{u}_1$ and $\mathbf{u}_2$ is characterized by p, where $p = 0$ indicates perfect decoding at R, and $0 < p \le 0.5$ indicates errors occurring in the intra-link. Assuming $\mathbf{u}_1$ and $\mathbf{u}_2$ are described with rates R_1 and R_2, respectively, the achievable rate region for R_1 and R_2 is derived in this section.
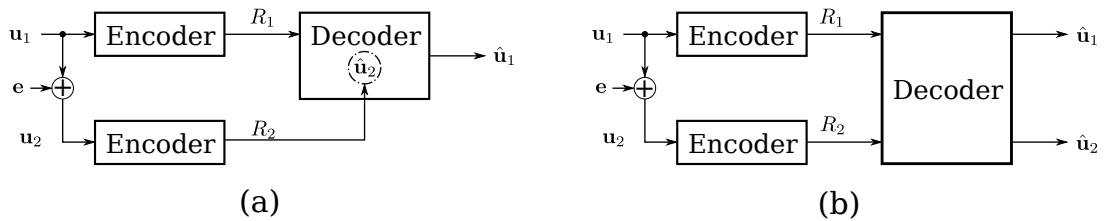
Figure 3.2: Abstract model for the coding/decoding of $\mathbf{u}_1$ and $\mathbf{u}_2$ from the viewpoint of (a) source coding with a helper, and (b) Slepian-Wolf theorm. $\mathbf{u}_2$ is the bit-flipped version of $\mathbf{u}_1$.

3.2.1   Exact Rate Region

As stated before, in the DF-IE system, the objective of D is only to retrieve $\mathbf{u}_1$, which was sent from S. On the other hand, $\mathbf{u}_2$ sent from R does not need to be successfully recovered at D. The coding/decoding of $\mathbf{u}_1$ and $\mathbf{u}_2$ falls exactly into the category of source coding with a helper problem [GK11], where two correlated sources are encoded separately and transmitted to the same decoder at the destination, but only one of the two sources is to be recovered at the destination and the other one serves as a helper. Obviously, in DF-IE system, $\mathbf{u}_2$ helps to decode of $\mathbf{u}_1$ at the destination, as shown in Figure 3.2(a). According to Theorem 2, successful recovery of $\mathbf{u}_1$ after joint

decoding at D can be achieved if R_1 and R_2 satisfy

$$\begin{cases} R_1 & \geq & H(\mathbf{u}_1|\hat{\mathbf{u}}_2), \\ R_2 & \geq & I(\mathbf{u}_2;\hat{\mathbf{u}}_2), \end{cases} \tag{3.5}$$

where $\hat{\mathbf{u}}_2$ is the estimate of $\mathbf{u}_2$ at the final output, as shown in Figure 3.2(a). The relationship between $\mathbf{u}_2$ and $\hat{\mathbf{u}}_2$ can also be expressed as a bit-flipping model with a error probability α, where $\alpha \in [0, 0.5]$. Let $H(\mathbf{u}_1|\hat{\mathbf{u}}_2)$ and $I(\mathbf{u}_2;\hat{\mathbf{u}}_2)$ denote the entropy of $\mathbf{u}_1$ conditioned on $\hat{\mathbf{u}}_2$ and the mutual information between $\mathbf{u}_2$ and $\hat{\mathbf{u}}_2$, respectively. It is easily found that $H(\mathbf{u}_1|\hat{\mathbf{u}}_2) = H_b(\alpha * p)$ and $I(\mathbf{u}_2;\hat{\mathbf{u}}_2) = H(\hat{\mathbf{u}}_2) - H(\hat{\mathbf{u}}_2|\mathbf{u}_2) = 1 - H_b(\alpha)$, where $\alpha * p = (1-\alpha)p + \alpha(1-p)$ is the binary convolution of α and p.
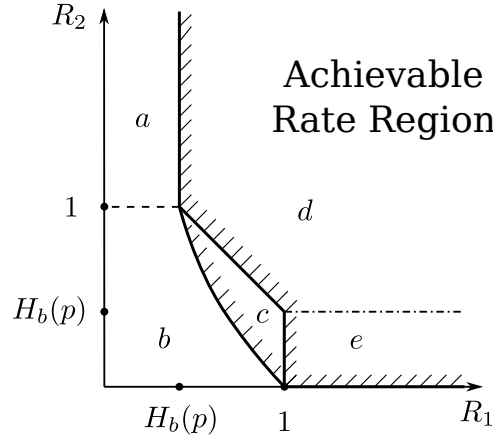
Figure 3.3: The achievable rate region for S and R.

Let $\mathscr{R}_{SCwH}$ denote the admissible rate region specified by (3.5). To facilitate the rate region comparison to be provided later in this section, we divide the entire rate region into five sub-regions, $\mathscr{R}_a$, $\mathscr{R}_b$, $\mathscr{R}_c$, $\mathscr{R}_d$ and $\mathscr{R}_e$, as shown in Figure 3.3. From this figure, we have $\mathscr{R}_{SCwH} = \mathscr{R}_c \cup \mathscr{R}_d \cup \mathscr{R}_e$. Consider two extreme cases: (1) In the case $\mathbf{u}_2$ can be successfully decoded at the decoder, $\hat{\mathbf{u}}_2 = \mathbf{u}_2$ and $\alpha = 0$. Therefore, the conditions become as $R_1 \geq H_b(0 * p) = H_b(p)$ and $R_2 \geq 1 - H_b(0) = 1$, which corresponds to the linear boundary between $\mathscr{R}_a$ and $\mathscr{R}_d$. (2) In the case the estimate $\hat{\mathbf{u}}_2$ of $\mathbf{u}_2$ after decoding is totally wrong, $\hat{\mathbf{u}}_2$ does not contain any information about $\mathbf{u}_2$ and $\alpha = 0.5$. Therefore, the conditions become as $R_1 \geq H_b(0.5 * p) = 1$ and $R_2 = 1 - H_b(0.5) = 0$, which corresponds to the lower linear boundary of $\mathscr{R}_e$. In all other cases $(0 < \alpha < 0.5)$, it is easily to know the conditions become as $R_1 \geq H_b(\alpha * p)$ and $R_2 = 1 - H_b(\alpha)$, which corresponds to the nonlinear boundary between $\mathscr{R}_b$ and $\mathscr{R}_c$. According to the discussions presented above, $\mathscr{R}_{SCwH}$ can be expressed even in an explicit way as

$$R_1 \geq \begin{cases} H_b(p), & \text{for} \quad R_2 \geq 1, \\ H_b[H_b^{-1}(1-R_2) * p], & \text{for} \quad 0 \leq R_2 \leq 1. \end{cases} \tag{3.6}$$

The three boundaries between $\mathscr{R}_d$ and $\mathscr{R}_c$, $\mathscr{R}_d$ and $\mathscr{R}_e$, and $\mathscr{R}_c$ and $\mathscr{R}_e$ will be discussed in Section 3.2.2.

3.2.2   Approximated Rate Region

The Slepian-Wolf theorem is well known for lossless transmission of correlated sources. Unlike *the theorem for source coding with a helper*, the Slepian-Wolf theorem provides the achievable rate region required to recover all the correlated sources. In this subsection, we show that the rate region of the DF-IE system can also be approximated by the Slepian-Wolf theorem. With this assumption, the boundary can be expressed by a connection of linear lines.

First of all, we consider the successful transmission of both $\mathbf{u}_1$ and $\mathbf{u}_2$ from the viewpoint of Slepian-Wolf theorem, as shown in Figure 3.2(b). According to Theorem 1, successful recovery of both $\mathbf{u}_1$ and $\mathbf{u}_2$ after joint decoding at D is possible if R_1 and R_2 satisfies

$$\begin{cases} R_1 & \geq & H(\mathbf{u}_1|\mathbf{u}_2), \\ R_2 & \geq & H(\mathbf{u}_2|\mathbf{u}_1), \\ R_1 + R_2 & \geq & H(\mathbf{u}_1, \mathbf{u}_2), \end{cases} \tag{3.7}$$

where $H(\mathbf{u}_1|\mathbf{u}_2)$ $(H(\mathbf{u}_2|\mathbf{u}_1))$ denotes the conditional entropy of $\mathbf{u}_1$ $(\mathbf{u}_2)$ given $\mathbf{u}_2$ $(\mathbf{u}_1)$, and $H(\mathbf{u}_1,\mathbf{u}_2)$ denotes the joint entropy of $\mathbf{u}_1$ and $\mathbf{u}_2$. It is obvious that $H(\mathbf{u}_1) = H(\mathbf{u}_2) = 1$, $H(\mathbf{u}_1|\mathbf{u}_2) = H(\mathbf{u}_2|\mathbf{u}_1) = H_b(p)$ and $H(\mathbf{u}_1,\mathbf{u}_2) = 1 + H_b(p)$. The achievable rate region identified by (3.7) is represented by $\mathscr{R}_d$, which is an unbounded polygon, as shown in Fig. 3.3. However, $\mathscr{R}_e$ should also be included as the admissible rate region for DF-IE system [CAM13; ZCH+14], since we only focus on the transmission of $\mathbf{u}_1$ and an arbitrary value of R_2 is satisfactory as long as $R_1 \geq H(\mathbf{u}_1)$.

Let $\mathscr{R}_{SW}$ denote the admissible rate region that includes both $\mathscr{R}_d$ and $\mathscr{R}_e$ ($\mathscr{R}_{SW} = \mathscr{R}_d \cup \mathscr{R}_e$), $\mathscr{R}_{SW}$ can be expressed as

$$R_1 \geq \begin{cases} H_b(p), & \text{for} \quad R_2 \geq 1, \\ 1 + H_b(p) - R_2, & \text{for} \quad H_b(p) \leq R_2 \leq 1, \\ 1, & \text{for} \quad 0 \leq R_2 \leq H_b(p). \end{cases} \tag{3.8}$$

According to Equation (3.8), if $0 \leq R_2 \leq H_b(p)$, R_1 should always be larger than 1 to guarantee successful recovery of $\mathbf{u}_1$ at the receiver. However, $\mathbf{u}_2$ can be partially recovered at the receiver as long as $R_2 > 0$, and the partially recovered $\mathbf{u}_2$ can serve as side information for recovering $\mathbf{u}_1$. Intuitively, with the help of the side information at the receiver, R_1 can be further reduced to less than 1 while keeping the possibility that $\mathbf{u}_1$ still can be successfully recovered at the receiver, which is obviously excluded in Equation (3.8). This shows that $\mathscr{R}_{SW}$ is an approximation of the admissible rate region for S and R.

Note the size of both $\mathscr{R}_{SCwH}$ and $\mathscr{R}_{SW}$ are uniquely determined by p, we use $\mathscr{R}_{SCwH}(p)$ and $\mathscr{R}_{SW}(p)$ to explicitly indicate the achievable rate regions are functions of p. As shown in Figure 3.3, $\mathscr{R}_{SCwH}(p) \geq \mathscr{R}_{SW}(p)$, and the difference is represented by $\mathscr{R}_c$. The proof of $\mathscr{R}_{SCwH}(p) \geq \mathscr{R}_{SW}(p)$ is provided in Appendix A. Although $\mathscr{R}_{SW}(p)$ is an approximation of $\mathscr{R}_{SCwH}(p)$, if we set $p = 0$ and according to Equation (3.6) and Equation (3.8), the boundaries of $\mathscr{R}_{SCwH}(0)$ and $\mathscr{R}_{SW}(0)$ become the same, and $\mathscr{R}_c$ vanishes.

3.3 Outage Probability Analysis

3.3.1 Relationship Between R_1, R_2 and Their Corresponding Channel SNRs

It should be emphasized here that, in the DF-IE system considered, specific source coding for compression is performed neither at S nor at R. Instead, the correlation knowledge between $\mathbf{u}_1$ and $\mathbf{u}_2$ is exploited at D to enhance the error correction capability of the system. Now consider the transmission of the SD and RD links. According to Shannon's separation theorem, if the *total* information transmission rates over these two independent channels satisfy [GZ05]

$$\begin{cases} R_1 R_{c,1} & \leq & C(\gamma_1), \\ R_2 R_{c,2} & \leq & C(\gamma_2), \end{cases} \tag{3.9}$$

the message error probability can be made arbitrarily small. Here, $R_{c,1}$ and $R_{c,2}$ indicate the spectrum efficiencies of $\mathscr{E}_1(\cdot)$ and $\mathscr{E}_2(\cdot)$ that include both the channel coding rate and the modulation multiplicity, respectively. $C(\gamma_1)$ and $C(\gamma_2)$ denote the channel capacity of the SD and RD links, respectively, given the instantaneous SNRs of the SD and RD links being γ_1 and γ_2.

In the theoretical analysis, we only consider the equality of (3.9). The relationship between rate R_i and its corresponding instantaneous channel SNR γ_i is given by

$$R_i = \Phi_i(\gamma_i) = \frac{C(\gamma_i)}{R_{c,i}}, \tag{3.10}$$

with its inverse function

$$\gamma_i = \Phi_i^{-1}(R_i) = C^{-1}(R_i R_{c,i}), \tag{3.11}$$

where $i = 1, 2$ and $C^{-1}(\cdot)$ denotes the inverse function of channel capacity.

3.3.2 Outage Probability Calculation

Within one transmission and for a given p value, the outage event happens when (R_1, R_2) falls outside the achievable rate region. Note that the intra-link error probability p changes, according to the variation of γ_0, as described

in Section 2.3. Taking into account the impact of the variation of the intra-link, the outage probability of the system is defined by taking the average over all the transmissions. Based on the exact and approximated achievable rate region obtained in Section 3.2, the exact and approximated outage probability can be defined as

$$
\begin{aligned}
P_{out}^{SCwH} &= \Pr\{0 \leq p \leq 0.5,\ (R_1, R_2) \notin \mathscr{R}_{SCwH}(p)\} \\
&= \Pr\{p = 0, (R_1, R_2) \in \mathscr{R}_a \cup \mathscr{R}_b\} + \Pr\{0 < p \leq 0.5, (R_1, R_2) \in \mathscr{R}_a \cup \mathscr{R}_b\} \\
&= \underbrace{\Pr\{p = 0, (R_1, R_2) \in \mathscr{R}_a\}}_{P_{1,a}} + \underbrace{\Pr\{p = 0, (R_1, R_2) \in \mathscr{R}_b\}}_{P_{1,b}} \\
&\quad + \underbrace{\Pr\{0 < p \leq 0.5, (R_1, R_2) \in \mathscr{R}_a\}}_{P_{2,a}} + \underbrace{\Pr\{0 < p \leq 0.5, (R_1, R_2) \in \mathscr{R}_b\}}_{P_{2,b}},
\end{aligned}
\tag{3.12}
$$

and

$$
\begin{aligned}
P_{out}^{SW} &= \Pr\{0 \leq p \leq 0.5,\ (R_1, R_2) \notin \mathscr{R}_{SW}(p)\} \\
&= \Pr\{p = 0, (R_1, R_2) \in \mathscr{R}_a \cup \mathscr{R}_b \cup \mathscr{R}_c\} + \Pr\{0 < p \leq 0.5, (R_1, R_2) \in \mathscr{R}_a \cup \mathscr{R}_b \cup \mathscr{R}_c\} \\
&= \underbrace{\Pr\{p = 0, (R_1, R_2) \in \mathscr{R}_{ab'}\}}_{P_{1,ab'}} + \underbrace{\Pr\{p = 0, (R_1, R_2) \in \mathscr{R}_{b''c}\}}_{P_{1,b''c}} \\
&\quad + \underbrace{\Pr\{0 < p \leq 0.5, (R_1, R_2) \in \mathscr{R}_{ab'}\}}_{P_{2,ab'}} + \underbrace{\Pr\{0 < p \leq 0.5, (R_1, R_2) \in \mathscr{R}_{b''c}\}}_{P_{2,b''c}},
\end{aligned}
\tag{3.13}
$$

respectively. To simplify the calculation of P_{out}^{SW}, we further divide $\mathscr{R}_b$ into two subregions, $\mathscr{R}_{b'}$ and $\mathscr{R}_{b''}$, i.e., $\mathscr{R}_b = \mathscr{R}_{b'} \cup \mathscr{R}_{b''}$, as shown in Fig. 3.4. In (3.13), $\mathscr{R}_{ab'}$ and $\mathscr{R}_{b''c}$ are defined as $\mathscr{R}_{ab'} = \mathscr{R}_a \cup \mathscr{R}_{b'}$ and $\mathscr{R}_{b''c} = \mathscr{R}_c \cup \mathscr{R}_{b''}$, respectively. It is obvious that $\mathscr{R}_{ab'} = \{(R_1, R_2) : 0 \leq R_1 \leq H_b(p), R_2 \geq 0\}$, and $\mathscr{R}_{b''c} = \{(R_1, R_2) : H_b(p) \leq R_1 \leq 1, R_1 + R_2 \leq 1 + H_b(p)\}$.
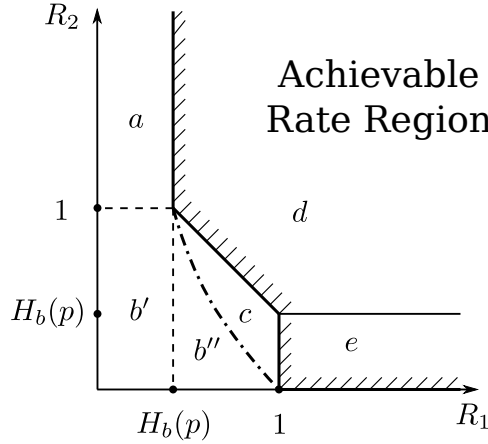
Figure 3.4: The achievable rate region for S and R determined by the Slepian-Wolf theorem.

Note that the intra-link error probability p and the rates R_1, R_2 can be converted into the instantaneous channel SNR of their corresponding links, as shown in Section 2.3 and 3.3.1. Moreover, since all the three links are suffering from statistically independent block Rayleigh fading, the joint pdf of the instantaneous SNRs can be expressed as $p(\gamma_0, \gamma_1, \gamma_2) = p(\gamma_0) \cdot p(\gamma_1) \cdot p(\gamma_2)$. After some mathematical manipulations (please refer to Appendix B for more details), $P_{1,a}$, $P_{1,b}$, $P_{2,a}$, $P_{2,b}$, $P_{1,ab'}$, $P_{1,b''c}$, $P_{2,ab'}$ and $P_{2,b''c}$ can be further expressed as

$$
P_{1,a} = 0,
\tag{3.14}
$$

$$
P_{1,b} = \frac{1}{\Gamma_2} \exp\left[-\frac{\Phi_1^{-1}(1)}{\Gamma_0}\right] \int_0^{\Phi_2^{-1}(1)} \exp(-\frac{\gamma_2}{\Gamma_2}) \left[1 - \exp(-\frac{\Phi_1^{-1}[1 - \Phi_2(\gamma_2)]}{\Gamma_1})\right] d\gamma_2,
\tag{3.15}
$$

$$P_{2,a} = \frac{1}{\Gamma_0} \exp\left[-\frac{\Phi_2^{-1}(1)}{\Gamma_2}\right] \int_0^{\Phi_1^{-1}(1)} \exp(-\frac{\gamma_0}{\Gamma_0}) \left[1 - \exp(-\frac{\Phi_1^{-1}[1-\Phi_1(\gamma_0)]}{\Gamma_1})\right] d\gamma_0, \qquad (3.16)$$

$$P_{2,b} = \frac{1}{\Gamma_0\Gamma_2} \int_0^{\Phi_1^{-1}(1)} \int_0^{\Phi_2^{-1}(1)} \exp(-\frac{\gamma_0}{\Gamma_0} - \frac{\gamma_2}{\Gamma_2}) \left\{1 - \exp\left[-\frac{\Phi_1^{-1}[\Psi(\gamma_0,\gamma_2)]}{\Gamma_1}\right]\right\} d\gamma_0 d\gamma_2, \qquad (3.17)$$

$$P_{1,ab'} = 0, \qquad (3.18)$$

$$P_{1,b''c} = \frac{1}{\Gamma_1} \exp\left[-\frac{\Phi_1^{-1}(1)}{\Gamma_0}\right] \int_0^{\Phi_1^{-1}(1)} \exp(-\frac{\gamma_1}{\Gamma_1}) \left[1 - \exp(-\frac{\Phi_2^{-1}[1-\Phi_1(\gamma_1)]}{\Gamma_2})\right] d\gamma_1, \qquad (3.19)$$

$$P_{2,ab'} = \frac{1}{\Gamma_0} \int_0^{\Phi_1^{-1}(1)} \exp(-\frac{\gamma_0}{\Gamma_0}) \left[1 - \exp(-\frac{\Phi_1^{-1}[1-\Phi_1(\gamma_0)]}{\Gamma_1})\right] d\gamma_1, \qquad (3.20)$$

and

$$P_{2,b''c} = \frac{1}{\Gamma_0\Gamma_1} \int_0^{\Phi_1^{-1}(1)} \int_{\Phi_1^{-1}[1-\Phi_1(\gamma_0)]}^{\Phi_1^{-1}(1)} \exp(-\frac{\gamma_0}{\Gamma_0} - \frac{\gamma_1}{\Gamma_1}) \left[1 - \exp(-\frac{\Phi_2^{-1}[2-\Phi_1(\gamma_0)-\Phi_1(\gamma_1)]}{\Gamma_2})\right] d\gamma_1 d\gamma_0. \qquad (3.21)$$

respectively, with $\Psi(\gamma_0,\gamma_2) = H_b\{H_b^{-1}[1-\Phi_1(\gamma_0)] * H_b^{-1}[1-\Phi_2(\gamma_2)]\}$. As indicated by (3.14) and (3.18), the values of $P_{1,a}$ and $P_{1,ab'}$ are found to be always equal to 0. Since the derivation for the explicit expressions of the integrals in (3.15), (3.16), (3.17), (3.19), (3.20) and (3.21) may not be possible, we use a numerical method [Sha08] to calculated the values of $P_{1,b}$, $P_{2,a}$, $P_{2,b}$, $P_{1,b''c}$, $P_{2,ab'}$ and $P_{2,b''c}$.

Note that the boundary between $\mathscr{R}_b$ and $\mathscr{R}_c$ is nonlinear, and the calculation of P_{out}^{SCwH} requires an inverse binary entropy function $H_b^{-1}(\cdot)$. However, it is difficult to derive an explicit expression of $H_b^{-1}(\cdot)$ and we use an approximation technique which is described in Appendix C. With the approximated achievable rate region, the boundary can be expressed by a connection of linear lines, which eliminates the difficulty in numerical calculation. Note that the outage probability P_{out}^{SW} and P_{out}^{SCwH} both include the average SNR and the spectrum efficiency of all the three links, only as parameters, i.e., $P_{out} = g(\Gamma_0,\Gamma_1,\Gamma_2,R_{c,1},R_{c,2})$. Therefore, they both can be applied to arbitrary relay location cases. However, since $\mathscr{R}_{SCwH}(p)$ is larger than $\mathscr{R}_{SW}(p)$, it is expected that P_{out}^{SCwH} is smaller than P_{out}^{SW}.

3.4   Numerical Results

In this section, we show the numerical results of the theoretical outage probability calculation and the simulation results using Monte Carlo method. In the simulations, $R_{c,1}$ and $R_{c,2}$ both are set at $1/2$. It should be emphasized here that the capacity achieving code is assumed to be used in the simulations.

The outage curves of DF-IE, obtained using the analytical expressions of P_{out}^{SCwH} and P_{out}^{SW}, respectively, are shown in Figure. 3.5 (a). Here, two different relay location scenarios are considered: in Location A, $d_0 = d_1 = d_2$; in Location B, $d_0 = \frac{1}{4}d_1$ and $d_2 = \frac{3}{4}d_1$. According to (5), we have $\Gamma_0 = \Gamma_1 + 10\log_{10}[(d_1/d_0)^{3.52}]$ (dB) and $\Gamma_2 = \Gamma_1 + 10\log_{10}[(d_1/d_2)^{3.52}]$ (dB), respectively. From the figure we can see the difference between P_{out}^{SW} and P_{out}^{SCwH} is roughly 0.01 dB in Location A, and 0.001 dB in Location B. This observation indicates P_{out}^{SW} is an accurate approximation to the exact outage probability P_{out}^{SCwH}. Moreover, it is found that P_{out}^{SCwH} is always smaller than P_{out}^{SW}, which is consistent with the theoretical analysis provided in Section 3.3.2. As references, the outage probabilities of the SDF system [BH06] and the NDF system are also provided in the same figure. As can be seen from the figure, DF-IE system can achieve better performance than the SDF and NDF systems, which also agrees with the theoretical analysis. Note that the DF-IE system causes more complexity or energy consumption than SDF and NDF systems when the intra-link errors are detected. However, the increase in complexity or energy consumption
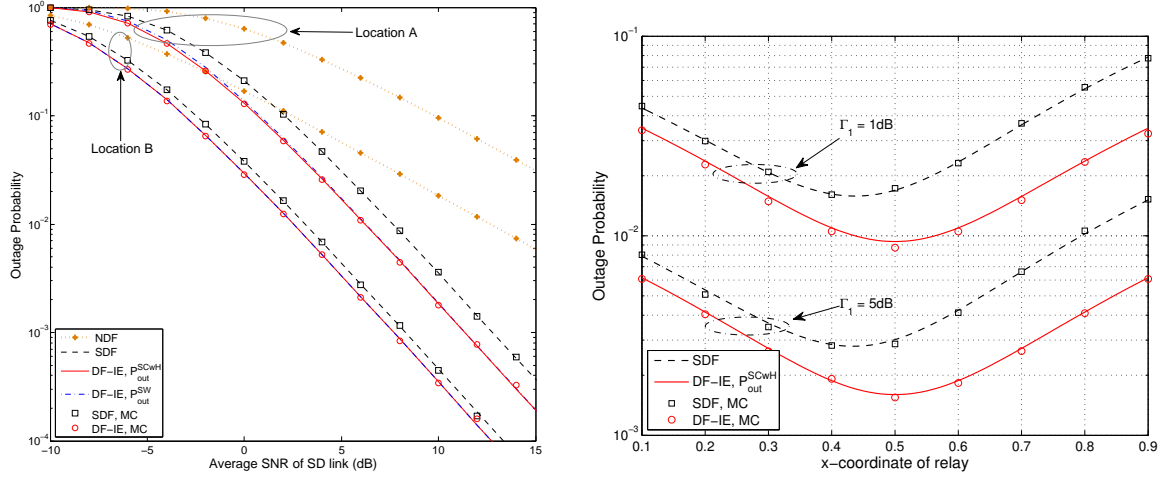
Figure 3.5: (a) Comparison of the outage probability of the DF-IE and SDF systems, and (b) Outage probability versus the relay location, where $\Gamma_1 = 1$ dB and $\Gamma_1 = 5$ dB.

over SDF is negligible, especially in high SNR regime. However, the performance gain obtained in Location B (≈ 0.6 dB) is smaller than that obtained in Location A (≈ 1.5 dB). This is because, in Location B, the quality of the intra-link is better than that in Location A, resulting in lower probability of the intra-link transmission failure. Note that the theoretical outage probabilities of the both DF-IE and SDF system are in excellent agreement with their corresponding simulation results, respectively.

The impact of the relay location on the outage probability of both the DF-IE and SDF systems is depicted in Figure. 3.5 (b), where the average SNR of *SD* link is kept at $\Gamma_1 = 1$ dB and $\Gamma_1 = 5$ dB. Here, the position of *R* is assumed to vary along the line between *S* ($x = 0$) and *D* ($x = 1$). With SDF relaying system, the lowest outage probability is achieved at a certain point ($x \approx 0.43$) between *S* and the midpoint. With DF-IE system, interestingly, we found that when the relay is located at the midpoint ($x = 0.5$), the lowest outage probability can be achieved. In general, the lowest outage probability can be achieved at a point where the contributions of both *SR* and *RD* links to outage are balanced. Since in SDF, the relay stops forwarding the information sequence when errors are found, the quality of the *SR* link has to be good enough, which results in the optimal position shifted more closer to the side of the source. In DF-IE system, the contributions of the two links to the outage probability are balanced because there is a chance that the errors occurring in the *SR* link can be corrected at the destination, and as a consequence, the optimal location is the midpoint.

The ε-outage capacity and throughput are further analyzed for the DF-IE, SDF and NDF systems. We fixed the relay location to be Location B where the relay node is located closer to the source node. The ε-outage capacity is obtained by solving the equation

$$R_c^\varepsilon = \sup\{R_c : P_{out} \leq \varepsilon\}. \tag{3.22}$$

It is the largest rate of transmission such that the outage probability P_{out} is not greater than ε. The results of the ε-outage capacity are illustrated in Figure. 3.6 (a), where ε is set to 0.01. It can be found from the figure that the DF-IE system outperforms the other two systems in terms of the ε-outage capacity. On the other hand, the throughput, denoted by TP, is calculated by

$$TP = R_c(1 - P_{out}). \tag{3.23}$$

The throughput performances of the DF-IE, SDF and NDF systems are shown in Figure. 3.6 (b). It can be also seen from the figure that the DF-IE system has the best throughput compared to the baselines.
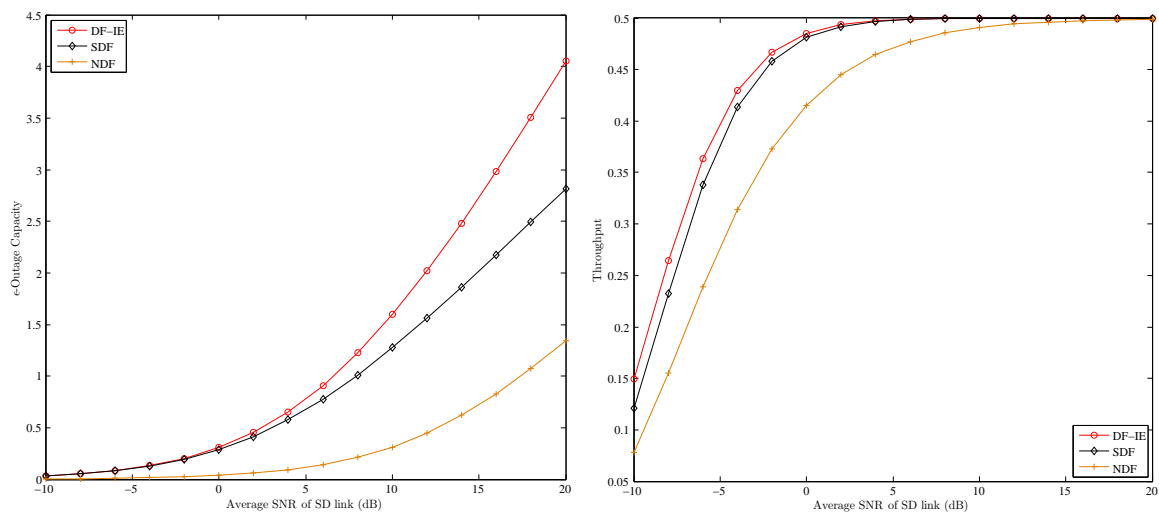
Figure 3.6: (a) ε-outage capacity of the DF-IE, SDF and NDF systems, where ε is set to 0.01, and (b) throughput performances of the DF-IE, SDF and NDF systems.

4.   Performance Analysis of TS2

In this chapter, the achievable rate-distortion region of TS2, as shown in Figure 1.2, is derived based on Theorem 3. We also derive the approximated bit error probability floor from Poisson-binomial distribution, and the theoretical lower bound of the error floor using conventional rate-distortion function for the binary source. Furthermore, the outage probability of TS2 is analytically derived based on the Slepian-Wolf theorem by assuming the minimal distortion is achieved.

4.1   Data and Error Rate Bounds for Binary CEO Problem

In this section, the rate-distortion region of TS2 having two relays is derived. Furthermore, the error floor of TS2 is approximated based on Poisson binomial distribution.

4.1.1   Problem definition

As can be seen from Figure 1.2, there is no direct link between the source and the destination. Moreover, the intra-links are allowed to be lossy with the links-on-the-fly concept. If there is no error happening in one of the intra-links, the problem is equivalent to TS1. Therefore, in this section, we assume that errors happen in both intra-links with fixed error probability, which is also known as the CEO problem in network information theory [GK11]. The abstract model of the CEO problem is depicted in Figure 4.1. An i.i.d. random data sequence $\mathbf{u}$ taking values from a binary set $\{0,1\}$ with equal probability is observed by two encoders. Let $\mathbf{u}_1$ and $\mathbf{u}_2$ be the output random data sequences of the two independent binary symmetric channels with associated crossover probabilities p_1 and p_2, respectively. Therefore, the joint pmf $\Pr(\mathbf{u}, \mathbf{u}_1, \mathbf{u}_2) = \Pr(\mathbf{u}) \Pr(\mathbf{u}_1 | \mathbf{u}) \Pr(\mathbf{u}_2 | \mathbf{u})$.
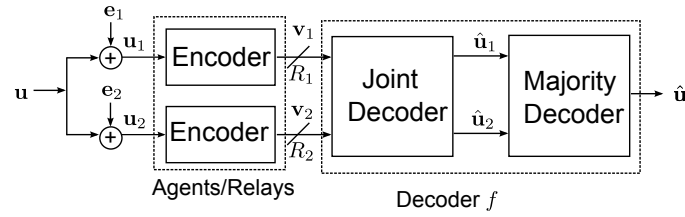
Figure 4.1: An abstract model of a binary CEO problem.

Two encoders independently encode $\mathbf{u}_1$ and $\mathbf{u}_2$ at rates R_1 and R_2 and send to a common decoder. The common decoder f jointly produces the estimates $\hat{\mathbf{u}}_1$ and $\hat{\mathbf{u}}_2$ of $\mathbf{u}_1$ and $\mathbf{u}_2$, under specified distortion measures d_1 and d_2, respectively, based on the received descriptions $\mathbf{v}_1$ and $\mathbf{v}_2$ [GK11]. Let $d_1 = Ed(\mathbf{u}_1, \hat{\mathbf{u}}_1)$ and $d_2 = Ed(\mathbf{u}_2, \hat{\mathbf{u}}_2)$ be the average Hamming distortions of $\mathbf{u}_1$ and $\mathbf{u}_2$, respectively. Finally, the estimate $\hat{\mathbf{u}}$ of $\mathbf{u}$ is obtained by using the majority logic decoding.

4.1.2   Threshold for Two Relays Case

As stated in Chapter 2.2, Berger [Ber78] and Tung [Tun78] characterize the inner and outer bounds of the information rate region, necessary and sufficient, respectively, to construct the codes that can achieve the acceptable distortions. We apply the inner bound to the case the binary sources are estimated under given Hamming distortions d_1 and d_2.

Corollary 5. *Given that $d_1, d_2 \in [0, \frac{1}{2}]$, the Berger-Tung inner bound for binary sources is expressed as*

$$R_1 \geq H_b(d_1 * p_1 * p_2 * d_2) - H_b(d_1) \tag{4.1a}$$

$$R_2 \geq H_b(d_1 * p_1 * p_2 * d_2) - H_b(d_2) \tag{4.1b}$$

$$R_{sum} \geq 1 + H_b(d_1 * p_1 * p_2 * d_2) - H_b(d_1) - H_b(d_2) \tag{4.1c}$$

where p_i is the probability $p(e_i = 1)$, $i = 1, 2$.
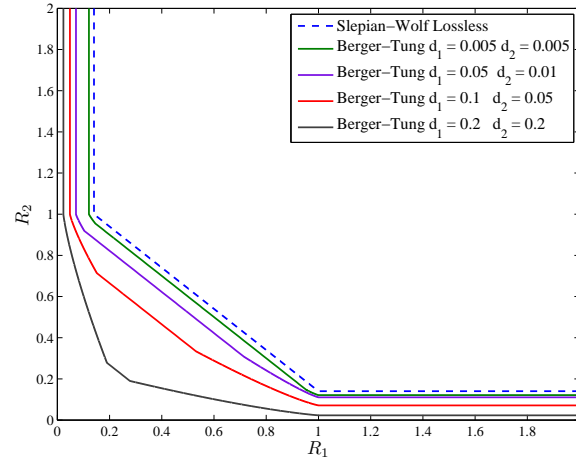
Figure 4.2: Rate-distortion regions of Berger-Tung inner bound with different required pairs of distortion levels. The source correlation parameters $p_1 = p_2 = 0.01$. The rate region of Slepian-Wolf lossless case is also plotted as a reference with $p_1 = 0$ and $p_2 = 0.01 * 0.01 = 0.0198$.

Proof. By using the Markov property and the chain rules of entropy and mutual information, the Berger-Tung inner bound shown in (4.1) is obtained in the following way

$$R_1 \geq I(\mathbf{u}_1; \mathbf{v}_1 | \mathbf{v}_2)$$
$$= H(\mathbf{v}_1 | \mathbf{v}_2) - H(\mathbf{v}_1 | \mathbf{u}_1, \mathbf{v}_2) \tag{4.2}$$
$$= H(\mathbf{v}_1 | \mathbf{v}_2) - H(\mathbf{v}_1 | \mathbf{u}_1) \tag{4.3}$$
$$= H_b(d_1 * p_1 * p_2 * d_2) - H_b(d_1)$$
$$R_2 \geq H_b(d_1 * p_1 * p_2 * d_2) - H_b(d_2) \tag{4.4}$$

$$R_{\text{sum}} \geq I(\mathbf{u}_1, \mathbf{u}_2; \mathbf{v}_1, \mathbf{v}_2)$$
$$= H(\mathbf{v}_1, \mathbf{v}_2) - H(\mathbf{v}_1, \mathbf{v}_2 | \mathbf{u}_1, \mathbf{u}_2)$$
$$= H(\mathbf{v}_1) + H(\mathbf{v}_1 | \mathbf{v}_2) - H(\mathbf{v}_1 | \mathbf{u}_1, \mathbf{u}_2)$$
$$- H(\mathbf{v}_2 | \mathbf{u}_1, \mathbf{u}_2, \mathbf{v}_1) \tag{4.5}$$
$$= 1 + H_b(d_1 * p_1 * p_2 * d_2) - H(\mathbf{v}_1 | \mathbf{u}_1)$$
$$- H(\mathbf{v}_2 | \mathbf{u}_1, \mathbf{u}_2) \tag{4.6}$$
$$= 1 + H_b(d_1 * p_1 * p_2 * d_2) - H(\mathbf{v}_1 | \mathbf{u}_1)$$
$$- H(\mathbf{v}_2 | \mathbf{u}_2) \tag{4.7}$$
$$= 1 + H_b(d_1 * p_1 * p_2 * d_2) - H_b(d_1) - H_b(d_2)$$

where the steps are justified, with:
(4.2) the chain rule for mutual information,
(4.3) given $\mathbf{u}_1$, $\mathbf{v}_1$ and $\mathbf{v}_2$ are conditionally independent,
(4.4) symmetric to the calculation of R_1,
(4.5) the chain rule for entropy,
(4.6) given $\mathbf{u}_1$, $\mathbf{u}_2$ and $\mathbf{v}_1$ are conditionally independent, $\mathbf{v}_1$ and $\mathbf{v}_2$ are conditionally independent given $\mathbf{u}_1$ and $\mathbf{u}_2$,
(4.7) given $\mathbf{u}_2$, $\mathbf{u}_1$ and $\mathbf{v}_2$ are conditionally independent. $\qquad\square$

In order to easily compare the rate-distortion region shown in (4.1) with the Slepian-Wolf lossless rate region, we further visualize the rate-distortion region in the (R_1, R_2)-plane, where the method for plotting the rate-distortion region is described in Appendix F. The terminology *"lossless"* does not mean end-to-end lossless transmission, due to the fact that errors are inserted in the observation data. The Slepian-Wolf lossless rate region only corresponds the case with $p_k = 0$, $k = 1$. The rate pair (R_1, R_2) is plotted in Figure 4.2 with some specified distortion measures d_1 and d_2. From Figure 4.2, it is clearly found that the source can be further compressed if we allow certain distortion levels d_1 and d_2, i.e., the transmission power can be further reduced compared to the Slepian-Wolf lossless case.
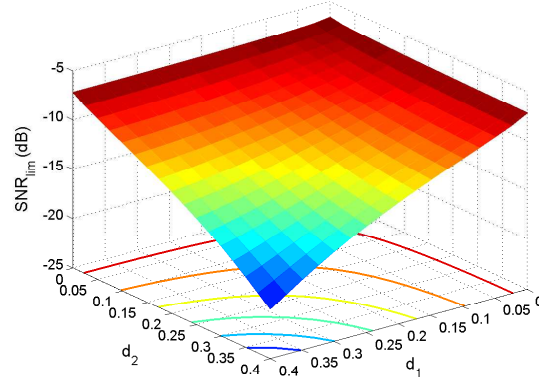
Figure 4.3: The effect of d_1 and d_2 onto SNR_{lim}. $p_1 = p_2 = 0.01$. The channel coding rate R_{c_k} is $1/2$.

The threshold SNR is then calculated based on source and channel separation theorem [GZ05], as

$$SNR_{\lim} = 10\log_{10}\left(2^{\frac{R_{sum}}{\Sigma_k 1/R_{c_k}}} - 1\right),$$

(4.8)

where R_{c_k} represents the channel coding rate of k-th relay node. For the purpose of examining the effect of d_1 and d_2 onto the threshold SNR value, we plot $SNR_{\lim}$ versus d_1 and d_2 in Figure 4.3. It is found through Figure 4.3 that $SNR_{\lim}$ decreases as d_1 and d_2 increase, i.e., the required transmission power is reduced if we allow a specified distortion level, which is consistent with the tendency shown in Figure 4.2.

In general, the derivation of the Berger-Tung inner bound for multiple users with Hamming distortion measure is still an open problem, and hence, we just provide a derivation for a special case $d_k = 0$, $k = 1, \cdots, K$, which is detailed in Appendix G.

4.1.3   Threshold SNR versus K

It is expected that the threshold SNR becomes smaller as the number of relays K increases [RYA11; ZHA+12; HZA+13]. We provide a proof of this through examining the helper information evaluated in the form of the mutual information. It is shown that the mutual information is monotonically increasing in terms of K, i.e., $I(\mathbf{U}_{\kappa\backslash k}; \mathbf{u}_k) \leq I(\mathbf{U}_{\kappa\backslash k}, \mathbf{u}_{K+1}; \mathbf{u}_k)$, where $\mathbf{U} = [\mathbf{u}_1, \mathbf{u}_2, \cdots, \mathbf{u}_K]^T$ with $[\cdot]^T$ denoting the transposition of its argument matrix and $\kappa = \{1, 2, \cdots, K\}$.

Lemma 6. *The threshold SNR is monotonically decreasing as the number of relays K increases.*

Proof.

$$\begin{aligned}
I(\mathbf{U}_{\kappa\backslash k}, \mathbf{u}_{K+1}; \mathbf{u}_k) &= H(\mathbf{U}_{\kappa\backslash k}, \mathbf{u}_{K+1}) + H(\mathbf{u}_k) - H(\mathbf{U}_{\kappa\backslash k}, \mathbf{u}_{K+1}, \mathbf{u}_k) \\
&= H(\mathbf{U}_{\kappa\backslash k}) + H(\mathbf{u}_{K+1}|\mathbf{U}_{\kappa\backslash k}) + H(\mathbf{u}_k) - H(\mathbf{U}_{\kappa\backslash k}, \mathbf{u}_k) - H(\mathbf{u}_{K+1}|\mathbf{U}_{\kappa\backslash k}, \mathbf{u}_k) \\
&= I(\mathbf{U}_{\kappa\backslash k}; \mathbf{u}_k) + H(\mathbf{u}_{K+1}|\mathbf{U}_{\kappa\backslash k}) - H(\mathbf{u}_{K+1}|\mathbf{U}_{\kappa\backslash k}, \mathbf{u}_k) \\
&\geq I(\mathbf{U}_{\kappa\backslash k}; \mathbf{u}_k),
\end{aligned}$$

(4.9)

where (4.9) is due to the fact that conditioning reduces entropy with the equality hold if and only if $p_{K+1} = 0.5$, meaning that the sequence $\mathbf{u}_{K+1}$ is uncorrelated to $\mathbf{U}$. □

4.1.4   Error Floor Analysis

4.1.4.1   *Approximation by Poisson Binomial Distribution*

To analyze the error floor that appears in the BER performance curve of the coding/decoding technique proposed in [ZHA+12] and [HZA+13], we assume the channels between the relays and the destination are noiseless and

hence the error floor is only determined by the observation error probabilities.

Without loss of generality, we assume the source $\mathbf{u}$ is an all zero sequence with n bits. The majority decision rule to generate $\hat{u}(i)$ is

$$\hat{u}(i) = \begin{cases} 1, & \text{if } \mathbf{1}(\mathbf{U}_i) > \mathbf{0}(\mathbf{U}_i), \\ 0, & \text{otherwise,} \end{cases} \tag{4.10}$$

where $\mathbf{1}(\mathbf{U}_i)$ and $\mathbf{0}(\mathbf{U}_i)$ represent the number of 1's and 0's in the i-th column of $\mathbf{U}$, respectively.

The decision error occurs when $\hat{u}(i)$ is decided to be 1. Hence, the error floor is analyzed by determining the probability of the number of 1's from K independent Bernoulli sequences having different probabilities of "1". In the statistics, the Poisson-binomial distribution is the probability distribution of the sum of independent Bernoulli trials that are not necessarily identically distributed. The probability of J-times occurrence of the error in K-times repeated binary trials with different crossover probabilities is [Wan93]

$$\Pr(J = j) = \begin{cases} \prod_{k=1}^{K} (1 - p_k), & \text{for } j = 0, \\ \frac{1}{j} \sum_{k=1}^{j} (-1)^{(k-1)} \Pr(J = j - k) L(k), & \text{for } j > 0, \end{cases} \tag{4.11}$$

where $L(k) = \sum_{l=1}^{K} \left(\frac{p_l}{1 - p_l} \right)^k$ and $0 \le j \le K$.

Hence, the error floor with different observation error probabilities is calculated by

$$\Pr(\hat{u}(i) \ne u(i)) = \begin{cases} \sum_{j=\frac{K+1}{2}}^{K} \Pr(J = j), & \text{if } K \text{ is odd,} \\ \frac{1}{2} \Pr(J = \frac{K}{2}) + \sum_{j=\frac{K}{2}+1}^{K} \Pr(J = j), & \text{if } K \text{ is even.} \end{cases} \tag{4.12}$$

4.1.4.2   Theoretical Lower Bound of Error Floor

The theoretical error floor analysis provided in the previous subsection is based only on the generalized majority logic (Poisson-binomial) analysis. We further provide a theoretical lower bound of the error floor p_{lb} by invoking the rate-distortion function, taking the error probabilities of observations into account. This lower bound is independent of any practical decoding technique.

Lemma 7. $p_{lb} = H^{-1}[1 + H_b(p_1) + \cdots + H_b(p_K) - H(\mathbf{U})]$.

Proof.

$$1 - H_b(\tilde{d}) = I(\mathbf{u}; \hat{\mathbf{u}}) \tag{4.13}$$
$$\le I(\mathbf{u}; \mathbf{U}) \tag{4.14}$$
$$= H(\mathbf{u}) - H(\mathbf{u}|\mathbf{U})$$
$$= 1 - H(\mathbf{u}, \mathbf{U}) + H(\mathbf{U})$$
$$= 1 - [H(\mathbf{u}) + H(\mathbf{u}_1|\mathbf{u}) + \cdots + H(\mathbf{u}_K|\mathbf{u})] + H(\mathbf{U}) \tag{4.15}$$
$$= 1 - [1 + H_b(p_1) + \cdots + H_b(p_K)] + H(\mathbf{U}), \tag{4.16}$$

where $\tilde{d}$ is a dummy variable, and the steps are justified as:
(4.13) rate-distortion function for the binary source,
(4.14) there exists information loss in the process of obtaining $\hat{\mathbf{u}}$ from $\mathbf{U}$,
(4.15) assume $\mathbf{u}_k \to \mathbf{u} \to \mathbf{U}_{K \setminus k}$ forms Markov chains, $k = 1, \cdots, K$.

Thus, it is obvious from (4.16) that $\tilde{d} \ge H^{-1}[1 + H_b(p_1) + \cdots + H_b(p_K) - H(\mathbf{U})]$ with $H^{-1}[\cdot]$ represents the inverse of the binary entropy function. Therefore, the lower bound of the error floor p_{lb} is the minimal value of $\tilde{d}$, as

$$p_{lb} = H^{-1}[1 + H_b(p_1) + \cdots + H_b(p_K) - H(\mathbf{U})] . \tag{4.17}$$

□

4.1.5   Results

A series of analytical results that serve as a reference for performance evaluation in RESCUE Deliverable D2.1.1 is shown in this subsection. The analytical results for different number of relays and error probabilities are summarized in Table 4.1. The channel coding rates of relays are simply set at $1/2$.

Table 4.1: The analytical results of the threshold SNR and the error floor.

K	$[p_1, \cdots, p_K]$	SNR_{lim} (dB)	Approximated error floor	p_{lb}
2	[0.01, 0.01]	-6.6	1×10^{-2}	2.1×10^{-3}
3	[0.025, 0.075, 0.002]	-7.02	2.1×10^{-3}	4.44×10^{-4}
4	[0.01, 0.01, 0.01, 0.01]	-9.157	2.98×10^{-4}	4.03×10^{-5}
5	[0.0145,0.005,0.025,0.015,0.03]	-9.223	4.6×10^{-5}	1.58×10^{-5}
6	[0.01, 0.01, 0.01, 0.01, 0.01, 0.01]	-10.48	9.85×10^{-6}	1.01×10^{-6}
7	[0.01,0.015,0.02,0.05,0.005,0.0003,0.02]	-10.28	1.33×10^{-6}	8.37×10^{-8}
8	[0.01, 0.01, 0.01, 0.01,0.01,0.01,0.01,0.01]	-11.31	3.42×10^{-7}	2.84×10^{-8}

4.2   Slepian-Wolf Admissible Rate Region Based Outage Probability Derivation for CEO Problem

In this section, we derive the outage probability for TS2 also referred to as CEO problem [BZV96]. The outage probability, in the case of minimal distortion is achieved, can be associated with the Slepian-Wolf admissible rate region, which is demonstrated in this section for a three relay scenario.

4.2.1   System Model

Fig. 4.4 (a) represents the system model, where an i.i.d. binary Bernoulli information sequence $\mathbf{u}_0$ is originated by the source (S) with $\Pr[\mathbf{u}_0 = 0] = \Pr[\mathbf{u}_0 = 1] = 0.5$. The information sequence is corrupted by independent binary Bernoulli distributed errors $\mathbf{e}_i$ via binary symmetric channel (BSC). The information sequence $\mathbf{u}_i = \mathbf{u}_0 \oplus \mathbf{e}_i$, $i \in \{1,2,3\}$ is observed by relay (R) i and can be associated with the bit flipping probability $p_i = \Pr[\mathbf{e}_i = 1]$ and $p_i \in (0, 0.5)$. "$\oplus$" denotes the binary exclusive OR operation. The correlated information sequences $\mathbf{u}_i, \forall i$ are transmitted via Rayleigh fading channels to the destination (D). The pdf of the Rayleigh fading channel is given by

$$p(\gamma_i) = \frac{1}{\Gamma_i} \exp(-\frac{\gamma_i}{\Gamma_i}), \forall i, \tag{4.18}$$

with instantaneous signal-to-noise ratio (SNR) γ_i and average SNR

$$\Gamma_i = \frac{E_{\text{i}}}{N_0} \cdot d_i^{-\eta}, \tag{4.19}$$

where E_i is the transmit power of relay i, N_0 is the variance of AWGN, d_i the distance between relay i and destination and η the path loss exponent. Best performed recovery of $\mathbf{u}_0$ at the destination can be achieved if all information sequences $\hat{\mathbf{u}}_1$, $\hat{\mathbf{u}}_2$ and $\hat{\mathbf{u}}_3$ are recovered error free [WMF15].

Assuming channel codes with Gaussian codebooks, the relationship between the source rate at relay i and instantaneous SNR i is given by [GZ05]

$$R_i = \frac{1}{R_{ci}} \log (1 + \gamma_i), \ i = 1, 2, 3, \tag{4.20}$$
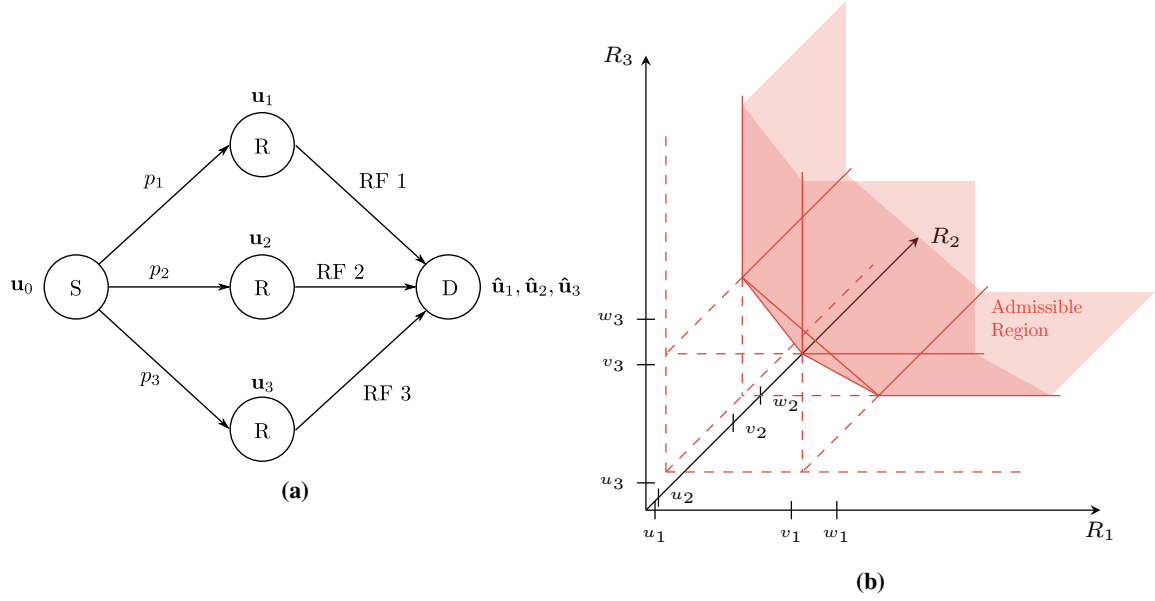
Figure 4.4: (a) System model for CEO problem, and (b) Slepian-Wolf admissible rate region, where $u_1 = H(\mathbf{u}_1 \mid \mathbf{u}_2, \mathbf{u}_3)$, $u_2 = H(\mathbf{u}_2 \mid \mathbf{u}_1, \mathbf{u}_3)$, $u_3 = H(\mathbf{u}_1 \mid \mathbf{u}_1, \mathbf{u}_2)$, $v_1 = H(\mathbf{u}_1)$, $v_2 = H(\mathbf{u}_2)$, $v_3 = H(\mathbf{u}_3)$, $w_1 = H(\mathbf{u}_1, \mathbf{u}_3, \mathbf{u}_2)$, $w_2 = H(\mathbf{u}_1, \mathbf{u}_2, \mathbf{u}_3)$, $w_3 = H(\mathbf{u}_2, \mathbf{u}_3, \mathbf{u}_1)$.

where R_{ci} represents the spectrum efficiency of RF channel i, considering the channel coding scheme and the modulation multiplicity [CAM13]. If and only if all Slepian-Wolf source rate inequality constraints

$$R_1 \geq H(\mathbf{u}_1 \mid \mathbf{u}_2, \mathbf{u}_3), \tag{4.21}$$

$$R_2 \geq H(\mathbf{u}_2 \mid \mathbf{u}_1, \mathbf{u}_3), \tag{4.22}$$

$$R_3 \geq H(\mathbf{u}_3 \mid \mathbf{u}_1, \mathbf{u}_2), \tag{4.23}$$

$$R_1 + R_2 \geq H(\mathbf{u}_1, \mathbf{u}_2 \mid \mathbf{u}_3), \tag{4.24}$$

$$R_1 + R_3 \geq H(\mathbf{u}_1, \mathbf{u}_3 \mid \mathbf{u}_2), \tag{4.25}$$

$$R_2 + R_3 \geq H(\mathbf{u}_2, \mathbf{u}_3 \mid \mathbf{u}_1), \tag{4.26}$$

$$R_1 + R_2 + R_3 \geq H(\mathbf{u}_1, \mathbf{u}_2, \mathbf{u}_3) \tag{4.27}$$

are fulfilled, $\hat{\mathbf{u}}_1$, $\hat{\mathbf{u}}_2$ and $\hat{\mathbf{u}}_3$ can be recovered error free [Cov75]. Therefore all sets (R_1, R_2, R_3) which satisfy all inequality constraints (4.21) - (4.27) are known as the admissible region (cf. Fig. 4.4 (b)). For the system model the entropy properties are defined as [SW73]

$$H(\mathbf{u}_1) = H(\mathbf{u}_2) = H(\mathbf{u}_3) = 1, \tag{4.28}$$

$$H(\mathbf{u}_1 \mid \mathbf{u}_2, \mathbf{u}_3) = H(\mathbf{u}_1, \mathbf{u}_2, \mathbf{u}_3) - H(\mathbf{u}_2 \mid \mathbf{u}_3) - 1, \tag{4.29}$$

$$H(\mathbf{u}_2 \mid \mathbf{u}_1, \mathbf{u}_3) = H(\mathbf{u}_1, \mathbf{u}_2, \mathbf{u}_3) - H(\mathbf{u}_1 \mid \mathbf{u}_3) - 1, \tag{4.30}$$

$$H(\mathbf{u}_3 \mid \mathbf{u}_1, \mathbf{u}_2) = H(\mathbf{u}_1, \mathbf{u}_2, \mathbf{u}_3) - H(\mathbf{u}_1 \mid \mathbf{u}_2) - 1, \tag{4.31}$$

$$H(\mathbf{u}_1, \mathbf{u}_2 \mid \mathbf{u}_3) = H(\mathbf{u}_1, \mathbf{u}_3 \mid \mathbf{u}_2) = H(\mathbf{u}_2, \mathbf{u}_3 \mid \mathbf{u}_1) = H(\mathbf{u}_1, \mathbf{u}_2, \mathbf{u}_3) - 1. \tag{4.32}$$

The entropies for the system model can be calculated with bit flipping probabilities p_i, p_j, p_l of the BSCs and $i, j, l \in \{1, 2, 3\}$ by

$$H(\mathbf{u}_i \mid \mathbf{u}_j) = H(\mathbf{u}_j \mid \mathbf{u}_i) = H_b(q_{i,j}), \tag{4.33}$$

$$q_{i,j} = p_i + p_j - 2p_i p_j,$$

$$H(\mathbf{u}_i, \mathbf{u}_j, \mathbf{u}_l) = -2\sum_{i=1}^{4} a_i \log(a_i), \tag{4.34}$$

$$a_1 = 0.5\big(p_i p_j p_l + (1-p_i)(1-p_j)(1-p_l)\big),$$

$$a_2 = 0.5\big(p_i p_j (1-p_l) + (1-p_i)(1-p_j)p_l\big),$$

$$a_3 = 0.5\big(p_i (1-p_j)p_l + (1-p_i)p_j (1-p_l)\big),$$

$$a_4 = 0.5\big((1-p_i)p_j p_l + p_i (1-p_j)(1-p_l)\big),$$

where $H_b(\cdot)$ is the binary entropy function and j, j, l are pairwise not equal. Furthermore if

$$p_i < p_j < p_l \tag{4.35}$$

then

$$H(\mathbf{u}_j \mid \mathbf{u}_l) > H(\mathbf{u}_i \mid \mathbf{u}_l) > H(\mathbf{u}_i \mid \mathbf{u}_j) \tag{4.36}$$

and

$$H(\mathbf{u}_i \mid \mathbf{u}_j, \mathbf{u}_l) < H(\mathbf{u}_j \mid \mathbf{u}_i, \mathbf{u}_l) < H(\mathbf{u}_l \mid \mathbf{u}_i, \mathbf{u}_j). \tag{4.37}$$

Thus, u_1, u_2 and u_3 in Fig. 4.4 (b) have different values. The Slepian-Wolf regions are dependent on p_1, p_2 and p_3. By influencing RF channel conditions via power allocation, the admissible region can be maximized.

4.2.2   Outage Probability Derivation

If at least one relay information sequence can not be recovered error free, the information recovery of the source is considered to be unsuccessful also referred to as outage. The outage probability is defined by the inadmissible region which includes all sets of (R_1, R_2, R_3) that violate at least one Slepian-Wolf inequality constraint of Eq. (4.21) - Eq. (4.27). Fig. 4.5 shows the inadmissible region which can be divided into 5 volumes and thus, outage probability can be formulated as

$$P_{\text{out}} = P_1 + P_2 + P_3 + P_4 + P_5. \tag{4.38}$$
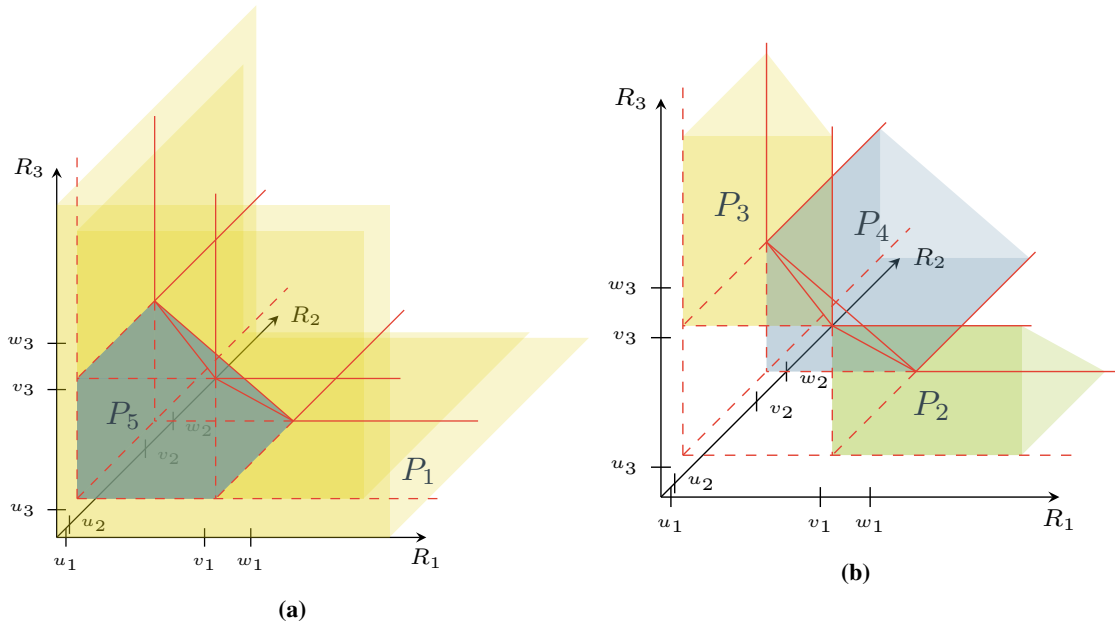
Figure 4.5: Slepian-Wolf inadmissible rate region divided into five volumes.

Substituting Eq. (4.20) into the Slepian-Wolf inequalities (4.21) - (4.27), the volumes P_1, P_2 , P_3, P_4 and P_5 can be

obtained as

$$P_1 = 1 - \Pr\left[R_1 > H\left(\mathbf{u}_1|\mathbf{u}_2,\mathbf{u}_3\right), R_2 > H\left(\mathbf{u}_2|\mathbf{u}_1,\mathbf{u}_3\right), R_3 > H\left(\mathbf{u}_3|\mathbf{u}_1,\mathbf{u}_2\right)\right]$$
$$= 1 - \Pr\left[2^{R_{c1}H(\mathbf{u}_1|\mathbf{u}_2,\mathbf{u}_3)} - 1 < \gamma_1 < \infty, 2^{R_{c2}H(\mathbf{u}_2|\mathbf{u}_1,\mathbf{u}_3)} - 1 < \gamma_2 < \infty, 2^{R_{c3}H(\mathbf{u}_3|\mathbf{u}_1,\mathbf{u}_2)} - 1 < \gamma_3 < \infty\right], \quad (4.39)$$

$$P_2 = \Pr\left[R_1 > H\left(\mathbf{u}_1\right), H\left(\mathbf{u}_2|\mathbf{u}_1,\mathbf{u}_3\right) \le R_2 < H\left(\mathbf{u}_2|\mathbf{u}_1\right), H\left(\mathbf{u}_3|\mathbf{u}_1,\mathbf{u}_2\right) \le R_3 < H\left(\mathbf{u}_2,\mathbf{u}_3|\mathbf{u}_1\right) - R_2\right]$$
$$= \Pr\left[2^{R_{c1}H(\mathbf{u}_1)} - 1 \le \gamma_1 < \infty, 2^{R_{c2}H(\mathbf{u}_2|\mathbf{u}_1,\mathbf{u}_3)} - 1 \le \gamma_2 < 2^{R_{c2}H(\mathbf{u}_2|\mathbf{u}_1)} - 1,\right.$$
$$\left. 2^{R_{c3}H(\mathbf{u}_3|\mathbf{u}_1,\mathbf{u}_2)} - 1 \le \gamma_3 < 2^{R_{c3}H(\mathbf{u}_2,\mathbf{u}_3|\mathbf{u}_1) - \frac{R_{c3}}{R_{c2}}\log(1+\gamma_2)} - 1\right], \quad (4.40)$$

$$P_3 = \Pr\left[H\left(\mathbf{u}_1|\mathbf{u}_2,\mathbf{u}_3\right) \le R_1 < H\left(\mathbf{u}_1|\mathbf{u}_3\right), H\left(\mathbf{u}_2|\mathbf{u}_1,\mathbf{u}_3\right) \le R_2 < H\left(\mathbf{u}_1,\mathbf{u}_2|\mathbf{u}_3\right) - R_1, R_3 > H\left(\mathbf{u}_3\right)\right]$$
$$= \Pr\left[2^{R_{c1}H(\mathbf{u}_1|\mathbf{u}_2,\mathbf{u}_3)} - 1 \le \gamma_1 < 2^{R_{c1}H(\mathbf{u}_1|\mathbf{u}_3)} - 1, 2^{R_{c2}H(\mathbf{u}_2|\mathbf{u}_1,\mathbf{u}_3)} - 1 \le \gamma_2 < 2^{R_{c2}H(\mathbf{u}_1,\mathbf{u}_2|\mathbf{u}_3) - \frac{R_{c2}}{R_{c1}}\log(1+\gamma_1)} - 1,\right.$$
$$\left. 2^{R_{c3}H(\mathbf{u}_3)} - 1 \le \gamma_3 < \infty\right], \quad (4.41)$$

$$P_4 = \Pr\left[H\left(\mathbf{u}_1|\mathbf{u}_2,\mathbf{u}_3\right) \le R_1 < H\left(\mathbf{u}_3,\mathbf{u}_1|\mathbf{u}_2\right) - R_3, R_2 > H\left(\mathbf{u}_2\right), H\left(\mathbf{u}_3|\mathbf{u}_1,\mathbf{u}_2\right) \le R_3 < H\left(\mathbf{u}_3|\mathbf{u}_2\right)\right]$$
$$= \Pr\left[2^{R_{c1}H(\mathbf{u}_1|\mathbf{u}_2,\mathbf{u}_3)} - 1 \le \gamma_1 < 2^{R_{c1}H(\mathbf{u}_3,\mathbf{u}_1|\mathbf{u}_2) - \frac{R_{c1}}{R_{c3}}\log(1+\gamma_3)} - 1, 2^{R_{c2}H(\mathbf{u}_2)} - 1 \le \gamma_2 < \infty,\right.$$
$$\left. 2^{R_{c3}H(\mathbf{u}_3|\mathbf{u}_1,\mathbf{u}_2)} - 1 \le \gamma_3 < 2^{R_{c3}H(\mathbf{u}_3|\mathbf{u}_2)} - 1\right]. \quad (4.42)$$

The definition of P_5 depends on 3 volumes related as

$$P_5 = P_{5a} - P_{5b} - P_{5c}, \quad (4.43)$$

where P_{5a}, P_{5b} and P_{5c} are given by

$$P_{5a} = \Pr\left[H\left(\mathbf{u}_1|\mathbf{u}_2,\mathbf{u}_3\right) \le R_1 < H\left(\mathbf{u}_1\right), H\left(\mathbf{u}_2|\mathbf{u}_1,\mathbf{u}_3\right) \le R_2 < H\left(\mathbf{u}_3,\mathbf{u}_1,\mathbf{u}_2\right) - R_1 - R_3,\right.$$
$$\left. H\left(\mathbf{u}_3|\mathbf{u}_1,\mathbf{u}_2\right) \le R_3 < H\left(\mathbf{u}_1,\mathbf{u}_2,\mathbf{u}_3\right) - H\left(\mathbf{u}_2|\mathbf{u}_1,\mathbf{u}_3\right) - R_1\right],$$
$$= \Pr\left[2^{R_{c2}H(\mathbf{u}_1|\mathbf{u}_2,\mathbf{u}_3)} - 1 \le \gamma_1 < 2^{R_{c1}H(\mathbf{u}_1)} - 1, 2^{R_{c2}H(\mathbf{u}_2|\mathbf{u}_1,\mathbf{u}_3)} \le \gamma_2 < 2^{R_{c2}H(\mathbf{u}_1,\mathbf{u}_2,\mathbf{u}_3) - \frac{R_{c2}}{R_{c3}}\log(1+\gamma_3) - \frac{R_{c2}}{R_{c1}}\log(1+\gamma_1)},\right.$$
$$\left. 2^{R_{c3}H(\mathbf{u}_3|\mathbf{u}_1,\mathbf{u}_2)} - 1 \le \gamma_3 < 2^{R_{c3}(H(\mathbf{u}_1,\mathbf{u}_2,\mathbf{u}_3) - H(\mathbf{u}_2|\mathbf{u}_1,\mathbf{u}_3)) - \frac{R_{c3}}{R_{c1}}\log(1+\gamma_1)} - 1\right], \quad (4.44)$$

$$P_{5b} = \Pr\left[H\left(\mathbf{u}_1|\mathbf{u}_2,\mathbf{u}_3\right) \le R_1 < H\left(\mathbf{u}_1|\mathbf{u}_2\right), H\left(\mathbf{u}_2\right) \le R_2 < H\left(\mathbf{u}_1,\mathbf{u}_2,\mathbf{u}_3\right) - R_1 - R_3,\right.$$
$$\left. H\left(\mathbf{u}_3|\mathbf{u}_1,\mathbf{u}_2\right) \le R_3 < H\left(\mathbf{u}_1,\mathbf{u}_3|\mathbf{u}_2\right) - R_1\right],$$
$$= \Pr\left[2^{R_{c2}H(\mathbf{u}_1|\mathbf{u}_2,\mathbf{u}_3)} - 1 \le \gamma_1 < 2^{R_{c1}H(\mathbf{u}_1|\mathbf{u}_2)} - 1, 2^{R_{c2}H(\mathbf{u}_2)} - 1 \le \gamma_2 < 2^{R_{c2}H(\mathbf{u}_1,\mathbf{u}_2,\mathbf{u}_3) - \frac{R_{c2}}{R_{c3}}\log(1+\gamma_3) - \frac{R_{c2}}{R_{c1}}\log(1+\gamma_1)} - 1,\right.$$
$$\left. 2^{R_{c3}H(\mathbf{u}_3|\mathbf{u}_1,\mathbf{u}_2)} - 1 \le \gamma_3 < 2^{R_{c3}H(\mathbf{u}_1,\mathbf{u}_2|\mathbf{u}_3) - \frac{R_{c3}}{R_{c1}}\log(1+\gamma_1)} - 1\right], \quad (4.45)$$

$$P_{5c} = \Pr\left[H\left(\mathbf{u}_1|\mathbf{u}_2,\mathbf{u}_3\right) \le R_1 < H\left(\mathbf{u}_1|\mathbf{u}_3\right), H\left(\mathbf{u}_2|\mathbf{u}_1,\mathbf{u}_3\right) \le R_2 < H\left(\mathbf{u}_1,\mathbf{u}_2,\mathbf{u}_3\right) - R_1 - R_3,\right.$$
$$\left. H\left(\mathbf{u}_3|\mathbf{u}_1,\mathbf{u}_2\right) \le R_3 < H\left(\mathbf{u}_1,\mathbf{u}_2,\mathbf{u}_3\right) - H\left(\mathbf{u}_2|\mathbf{u}_2,\mathbf{u}_3\right) - R_1\right],$$
$$= \Pr\left[2^{R_{c2}H(\mathbf{u}_1|\mathbf{u}_2,\mathbf{u}_3)} - 1 \le \gamma_1 < 2^{R_{c1}H(\mathbf{u}_1|\mathbf{u}_3)} - 1, 2^{R_{c2}H(\mathbf{u}_2|\mathbf{u}_1,\mathbf{u}_3)} - 1 \le \gamma_2 < 2^{R_{c2}H(\mathbf{u}_1,\mathbf{u}_2,\mathbf{u}_3) - \frac{R_{c2}}{R_{c3}}\log(1+\gamma_3) - \frac{R_{c2}}{R_{c1}}\log(1+\gamma_1)} - 1\right.$$
$$\left. 2^{R_{c3}H(\mathbf{u}_3|\mathbf{u}_1,\mathbf{u}_2)} - 1 \le \gamma_3 < 2^{R_{c3}(H(\mathbf{u}_1,\mathbf{u}_2,\mathbf{u}_3) - H(\mathbf{u}_2|\mathbf{u}_2,\mathbf{u}_3)) - \frac{R_{c3}}{R_{c1}}\log(1+\gamma_1)} - 1\right]. \quad (4.46)$$

Assuming the channel 1, channel 2 and channel 3 undergo independent Rayleigh flat fading, the outage probability can be obtained by the integral of the joint pdf of the instantaneous SNR $p(\gamma_1,\gamma_2,\gamma_3) = p(\gamma_1)p(\gamma_2)p(\gamma_3)$ over the range defined in Equations (4.39)-(4.43). Therefore, the outage probability for each region can be mathematically formulated as

$$P_1 = \left(1 - e^{-\frac{2^{R_c H(\mathbf{u}_1|\mathbf{u}_2,\mathbf{u}_3)}-1}{\Gamma_1} - \frac{2^{R_c H(\mathbf{u}_2|\mathbf{u}_1,\mathbf{u}_3)}-1}{\Gamma_2} - \frac{2^{R_c H(\mathbf{u}_3|\mathbf{u}_1,\mathbf{u}_2)}-1}{\Gamma_3}}\right), \quad (4.47)$$

$$P_2 = \frac{1}{\Gamma_2} e^{-\frac{2^{R_c H(\mathbf{u}_3|\mathbf{u}_1,\mathbf{u}_2)}-1}{\Gamma_3}} e^{-\frac{2^{R_c}-1}{\Gamma_1}} \int_{2^{R_c H(\mathbf{u}_2|\mathbf{u}_1,\mathbf{u}_3)}-1}^{2^{R_c H(\mathbf{u}_1|\mathbf{u}_2)}-1} e^{-\frac{\gamma_2}{\Gamma_2}} \left(1 - e^{\frac{2^{R_c H(\mathbf{u}_3|\mathbf{u}_1,\mathbf{u}_2)}}{\Gamma_3} - \frac{2^{R_c H(\mathbf{u}_2,\mathbf{u}_2|\mathbf{u}_1)}}{(\gamma_2+1)\Gamma_3}} \right) d\gamma_2, \quad (4.48)$$

$$P_3 = \frac{1}{\Gamma_1} e^{-\frac{2^{R_c H(\mathbf{u}_2|\mathbf{u}_1,\mathbf{u}_3)}-1}{\Gamma_2}} e^{-\frac{2^{R_c}-1}{\Gamma_3}} \int_{2^{R_c H(\mathbf{u}_1|\mathbf{u}_2,\mathbf{u}_3)}-1}^{2^{R_c H(\mathbf{u}_1|\mathbf{u}_3)}-1} e^{-\frac{\gamma_1}{\Gamma_1}} \left(1 - e^{\frac{2^{R_c H(\mathbf{u}_2|\mathbf{u}_1,\mathbf{u}_3)}}{\Gamma_2} - \frac{2^{R_c H(\mathbf{u}_1,\mathbf{u}_2|\mathbf{u}_3)}}{(\gamma_1+1)\Gamma_2}} \right) d\gamma_1, \quad (4.49)$$

$$P_4 = \frac{1}{\Gamma_3} e^{-\frac{2^{R_c H(\mathbf{u}_1|\mathbf{u}_2,\mathbf{u}_3)}-1}{\Gamma_1}} e^{-\frac{2^{R_c}-1}{\Gamma_2}} \int_{2^{R_c H(\mathbf{u}_3|\mathbf{u}_1,\mathbf{u}_2)}-1}^{2^{R_c H(\mathbf{u}_2|\mathbf{u}_3)}-1} e^{-\frac{\gamma_3}{\Gamma_3}} \left(1 - e^{\frac{2^{R_c H(\mathbf{u}_1|\mathbf{u}_2,\mathbf{u}_3)}}{\Gamma_1} - \frac{2^{R_c H(\mathbf{u}_3,\mathbf{u}_1|\mathbf{u}_2)}}{(\gamma_3+1)\Gamma_1}} \right) d\gamma_3, \quad (4.50)$$

$$P_{5a} = \frac{1}{\Gamma_1\Gamma_3} e^{-\frac{2^{R_c H(\mathbf{u}_2|\mathbf{u}_1,\mathbf{u}_3)}-1}{\Gamma_2}} \int_{2^{R_c H(\mathbf{u}_1|\mathbf{u}_2,\mathbf{u}_3)}-1}^{2^{R_c}-1} \int_{2^{R_c H(\mathbf{u}_3|\mathbf{u}_1,\mathbf{u}_2)}-1}^{\frac{2^{R_c(H(\mathbf{u}_1|\mathbf{u}_3)+1)}}{(\gamma_1+1)}-1} e^{-\frac{\gamma_1}{\Gamma_1}} e^{-\frac{\gamma_3}{\Gamma_3}} \left(1 - e^{\frac{2^{R_c H(\mathbf{u}_2|\mathbf{u}_1,\mathbf{u}_3)}}{\Gamma_2} - \frac{2^{R_c H(\mathbf{u}_1,\mathbf{u}_2,\mathbf{u}_3)}}{(\gamma_1+1)(\gamma_3+1)\Gamma_2}} \right) d\gamma_3 d\gamma_1, \quad (4.51)$$

$$P_{5b} = \frac{1}{\Gamma_1\Gamma_3} e^{-\frac{2^{R_c}-1}{\Gamma_2}} \int_{2^{R_c H(\mathbf{u}_1|\mathbf{u}_2,\mathbf{u}_3)}-1}^{2^{R_c H(\mathbf{u}_1|\mathbf{u}_2)}-1} \int_{2^{R_c H(\mathbf{u}_3|\mathbf{u}_2,\mathbf{u}_1)}-1}^{\frac{2^{R_c H(\mathbf{u}_1,\mathbf{u}_3|\mathbf{u}_2)}}{(\gamma_1+1)}-1} e^{-\frac{\gamma_1}{\Gamma_1}} e^{-\frac{\gamma_3}{\Gamma_3}} \left(1 - e^{\frac{2^{R_c 1}}{\Gamma_2} - \frac{2^{R_c H(\mathbf{u}_1,\mathbf{u}_2,\mathbf{u}_3)}}{(\gamma_1+1)(\gamma_3+1)\Gamma_2}} \right) d\gamma_3 d\gamma_1, \quad (4.52)$$

$$P_{5c} = \frac{1}{\Gamma_1\Gamma_3} e^{-\frac{2^{R_c H(\mathbf{u}_2|\mathbf{u}_1,\mathbf{u}_3)}-1}{\Gamma_2}} \int_{2^{R_c H(\mathbf{u}_1|\mathbf{u}_2,\mathbf{u}_3)}-1}^{2^{R_c H(\mathbf{u}_1|\mathbf{u}_3)}-1} \int_{2^{R_c H(\mathbf{u}_3|\mathbf{u}_1,\mathbf{u}_2)}-1}^{\frac{2^{R_c(H(\mathbf{u}_1|\mathbf{u}_3)+1)}}{(\gamma_1+1)}-1} e^{-\frac{\gamma_1}{\Gamma_1}} e^{-\frac{\gamma_3}{\Gamma_3}} \left(1 - e^{\frac{2^{R_c H(\mathbf{u}_2|\mathbf{u}_1,\mathbf{u}_3)}}{\Gamma_2} - \frac{2^{R_c H(\mathbf{u}_1,\mathbf{u}_2,\mathbf{u}_3)}}{(\gamma_1+1)(\gamma_3+1)\Gamma_2}} \right) d\gamma_3 d\gamma_1, \quad (4.53)$$

where $R_{c1} = R_{c2} = R_{c3} = R_c$ is assumed . Unfortunately, exact closed-form expressions for P_2, P_3, P_4 and P_5 are sophisticated to achieve.. Focusing on the high-SNR behaviour, an asymptotic analysis of P_{out} is performed with the approximation $e^{-x} \approx 1 - x$ for very small x (MacLaurin series of exponential function). The closed-form expressions are provided in Appendix D. For high-SNR the asymptotic behaviour is mostly influence by first and second order terms. Consequently, third and higher order terms can be neglected and thus achieve a simplification of the equation.

As a result, the outage probability of the system model can be expressed as

$$P_{out} \approx \frac{C_1-1}{\Gamma_1} + \frac{C_2-1}{\Gamma_2} + \frac{C_3-1}{\Gamma_3} + \frac{C_1 C_2 - C_{1,2}}{\Gamma_1\Gamma_2} + \frac{C_2 C_3 - C_{2,3}}{\Gamma_2\Gamma_3} + \frac{C_1 C_3 - C_{1,3}}{\Gamma_1\Gamma_3} \quad (4.54)$$

where the constants are defined as

$$C_1 = 2^{R_c H(\mathbf{u}_1|\mathbf{u}_2,\mathbf{u}_3)}, \quad (4.55)$$

$$C_2 = 2^{R_c H(\mathbf{u}_2|\mathbf{u}_1,\mathbf{u}_3)}, \quad (4.56)$$

$$C_3 = 2^{R_c H(\mathbf{u}_3|\mathbf{u}_1,\mathbf{u}_2)}, \quad (4.57)$$

$$C_{2,3} = 2^{R_c H(\mathbf{u}_2,\mathbf{u}_3|\mathbf{u}_1)} - 2^{R_c H(\mathbf{u}_2,\mathbf{u}_3|\mathbf{u}_1)} \left(\ln 2^{R_c H(\mathbf{u}_1|\mathbf{u}_2)} - \ln 2^{R_c H(\mathbf{u}_2|\mathbf{u}_1,\mathbf{u}_3)} \right), \quad (4.58)$$

$$C_{1,2} = 2^{R_c H(\mathbf{u}_1,\mathbf{u}_2|\mathbf{u}_3)} - 2^{R_c H(\mathbf{u}_1,\mathbf{u}_2|\mathbf{u}_3)} \left(\ln 2^{R_c H(\mathbf{u}_1|\mathbf{u}_3)} - \ln 2^{R_c H(\mathbf{u}_1|\mathbf{u}_2,\mathbf{u}_3)} \right), \quad (4.59)$$

$$C_{1,3} = 2^{R_c H(\mathbf{u}_1,\mathbf{u}_3|\mathbf{u}_2)} - 2^{R_c H(\mathbf{u}_1,\mathbf{u}_3|\mathbf{u}_2)} \left(\ln 2^{R_c H(\mathbf{u}_2|\mathbf{u}_3)} - \ln 2^{R_c H(\mathbf{u}_3|\mathbf{u}_1,\mathbf{u}_2)} \right). \quad (4.60)$$

5.   Performance Analysis of TS3

In this chapter, TS3 will be studied (as shown in Figure 1.2), which contains one source, one destination and multiple relay nodes. As one of the conventional relaying protocols, the DF relaying protocol has been very popular due to its simplicity and good performance in the case of successful decoding at the relay [LTW04]. However, conventional DF relaying protocol based cooperative systems might suffer error propagation phenomenon.

To overcome this shortcoming, authors in [FL13] proposed to apply the iterative joint decoding of correlated sources to relay networks. In the proposed approach, relay detects all the information sent by the source before forwarding it to the destination. An iterative joint decoder has been considered at the destination node. It will iteratively decode, estimate and exploit the correlation between the source and the relay nodes based on the incoming messages from the SD and RD links. There also has been another fold of contributions to combat the error propagation at the relay nodes. Authors proposed a threshold-based relaying protocol in coded cooperative networks [AgH+11]. In the proposed technique, the relay calculates the LLR values for the bits sent from the source. These values are subjected to a threshold to distinguish the reliable bits from the unreliable bits. The relay then forwards the bits that are deemed reliable and discards the bits that are not, resulting in fewer errors propagating to the destination. However, the proposed approach in [AgH+11] still need CRC code to help at the relay, also the proposed approach only considers a single relay node. In the super dense wireless networks, it is easy to have more than one relay node to receive the broadcasting message from the source node. This motivated us to consider a SNR threshold based SDF protocol in TS3.

5.1   System Model

Figure 5.1 illustrates an example of the DF based multiple relaying network accommodating one source (S), one destination (D), and M half-duplex relays(Rs). The communication procedure consists of two phases. In the first phase, the source sends signals to the destination at the rate of R_s. Due to the broadcasting nature of wireless communications, there are L relays who can successfully re-produce the original signals. Those are called well-informed relays (WIRs) here. In the next step, SNR threshold based selection will be considered to take into account the error occurred at the relay. In the second phase, WIRs sequentially retransmit the original signals to the destination. The destination employs the maximum-ratio combine (MRC) of all signals received at both phases to attain the achievable cooperative diversity gain.

The discrete-time equivalent form of received signals at different relays as well at the destination are described by

$$\text{SD Link :} y^{(sd)} = h^{(sd)} x^{(s)} + v^{(sd)} \tag{5.1}$$

$$\text{SR}_m \text{ Link :} y_m^{(sr)} = h_m^{(sr)} x^{(s)} + v_m^{(sr)}, \text{ for } m = 1, 2, \ldots, M \tag{5.2}$$

$$\text{R}_l \text{D Link :} y_l^{(rd)} = h_l^{(rd)} x_l^{(r)} + v_l^{(rd)}, \text{ for } l = 1, 2, \ldots, L \tag{5.3}$$

where $y^{(sd)}$, $y_m^{(sr)}$ and $y_l^{(rd)}$ denote the signals received through the SD channel, $h^{(sd)}$, SR$_m$ channel, $h_m^{(sr)}$, and R$_l$D channel, $h_l^{(rd)}$, respectively; $x^{(s)}$ denotes the signal sent by the source and $x_l^{(r)}$ the signal sent by the lth relay nodes; v denotes the additive white Gaussian noise of corresponding links with the variance N_0; and the subscript $_m$ denotes the index of the relay nodes and $_l$ the index of the WIRs.

At the source transmitter, the binary information is encoded, interleaved, and then fed into a doped-accumulator (DACC) with a doping rate 1. The DACC employs a memory 1 SRCC and the decoder employs BCJR algorithm[BCJ+74]. For the rest of or work, we assume the binary phase-shift keying (BPSK) modulation, although the technique is expandable to higher order modulation schemes.

5.2   SDF based Multiple Erroneous Relaying

As depicted in Figure 5.1, we employ multiple selection-DF relays to help the SD link communication. The relays first perform the demodulation, then go through DACC decoder, de-interleaver and ACC decoder. The result
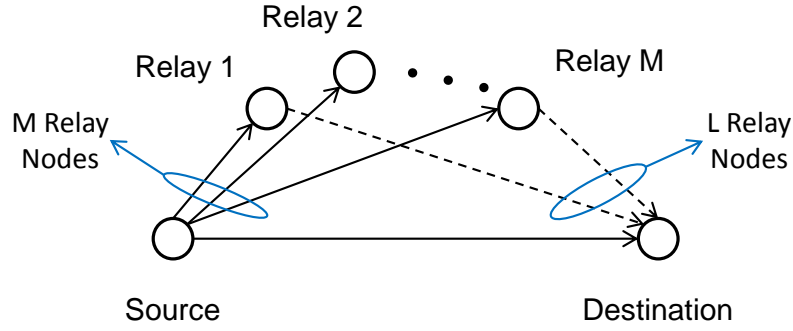
Figure 5.1: **System block diagram of DF based multiple relaying network**

obtained at relay nodes is

$$s_l^{(r)} = s^{(s)} + e_l^{(r)} \tag{5.4}$$

where $e^{(r)}$ denotes the error. Then the symbols are encoded and interleaved again, and the output is fed into DACC with a doping rate 1 if the received SNR for the SR link (denoted by $\gamma_m^{(sr)}$) is larger than the threshold γ^t.

When $\gamma_m^{(sr)}$ is smaller than γ^t, the m th relay will transmit nothing to the destination node. The probability for this event is the outage probability, which has been given in [LTW04], i.e.,

$$\Pr\left(\gamma_m^{(sr)} < \gamma^t\right) = 1 - e^{\frac{-\gamma^t}{\bar{\gamma}_m^{(sr)}}} \tag{5.5}$$

In the case of $\gamma^{(sr)} \geqslant \gamma^t$, the destination can receive a symbol block from the mth relay. Then, the destination can perform the combination of $y^{(sd)}$ and y_l^{sr} ($l = 1, \ldots, L$, i.e., the WIRs) for exploiting the achievable diversity-gain, i.e.,

$$y^{(mrc)} = w^{(sd)} y^{(sd)} + \sum_{l=1}^{L} w_l^{(rd)} y_l^{(rd)} \tag{5.6}$$

where $w^{(sd)}$ and $w_l^{(rd)}$ are the weighted coefficients. MRC is considered in our work, which is not optimal in TS3. However, because the location of the selected/de-selected bits is not known at the receiver, it is a good compromise with respect to complexity. Thus, the output of the MRC combiner can be expressed as

$$\gamma^{(mrc)} = \left(h^{(sd)}\right)^* y^{(sd)} + \sum_{l=1}^{L} \left(h_l^{(rd)}\right)^* y_l^{(rd)} \tag{5.7}$$

We can use ((5.5)) to obtain the probability

$$\Pr(\gamma_m^{(sr)} \geqslant \gamma^t) = \exp\left(\frac{-\gamma^t}{\bar{\gamma}_m^{(sr)}}\right). \tag{5.8}$$

The event $\gamma_m^{(sr)}$ include two cases, i.e., $e_m = 0$ and $e_m \neq 0$. The probability for the fore case can be upper bounded by 1. For the latter case, the error probability at the destination can be upper bounded by 1. As a summary of the above analysis, the overall performance can be upper bounded as

$$\overline{\mathscr{P}} \leqslant \prod_{m=1}^{M} \Pr\left(\gamma_m^{(sr)} < \gamma^t\right) \overline{\mathscr{P}}^{(sd)} + \sum_{m=1}^{\binom{M}{L}} \Pr\left(\gamma_m^{(sr)} \geqslant \gamma^t\right) \left(\Pr\left(e_m \neq 0 | \gamma_m^{(sr)} \geqslant \gamma^t\right) + \overline{\mathscr{P}}^{(comb)}\right) \tag{5.9}$$

where $\overline{\mathscr{P}}^{(comb)}$ is related to the specific combiner, and in our work MRC is considered.

5.3   Simulation Results

Computer based Monte Carlo simulations were used to demonstrate pros/cons of the proposed approach in TS3. All transmitters use equal transmission power. The main metric of interest was the end-to-end BER. The total E_b/N_0 was defined as the total trasmitted energy (i.e. at source and relay nodes) to noise raio.This set up is for fair comparation to have the same power gain. The simulation results were produced by carefully designed experiments having $50,000$ Monte Carlo trials. All the communication channels were generated independently according to Rayleigh distribution with unit variance. The SNR configuration of SR, SD and RD links have been set up as identical due to the super dense network assumption. The SNR threshold has been set up as 2 dB and 3 dB to demonstrate the effect of threshold setup. Each frame contrins 128 BPSK symbols.
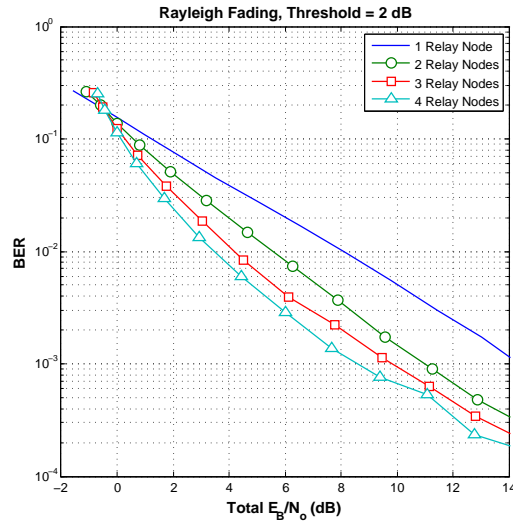
Figure 5.2: BER performance vs. total E_b/N_0 (dB) over Rayleigh fading channel $\gamma_t = 2$ dB
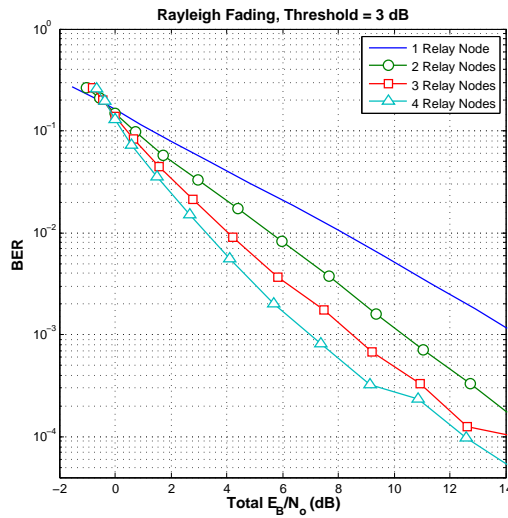
Figure 5.3: BER performance vs. total E_b/N_0 (dB) over Rayleigh fading channel $\gamma_t = 3$ dB

Figure 5.2 displays the end-to-end BER versus total E_b/N_o over a Rayleigh fading channel. The γ^t has been chosen as 2 dB at relays. It was observed that the general performance was increased as the number of relay nodes increased except for the lower E_b/N_0 range ($<$ 0 dB).

Figure 5.3 displays the end-to-end BER versus total E_b/N_o over a Rayleigh fading channel. The SNR threshold at relays are set up as 3 dB. Similar phenomena as in Figure 5.2 can be observed, but slightly better performance.

6.   Performance Analysis of TS4

In this chapter, the achievable rate region and outage probability of TS4, as shown in Figure 1.2, is analysed according to the framework of lossless source coding with a helper. The outage probability of the system considered is then compared with network-coding-based orthogonal MARC systems (MARC-NC) [WK07] and orthogonal MARC with selective decode-and-forward relaying (MARC-SDF) [IH11] in terms of the outage performance. It is observed through simulations that TS4 is superior to MARC-NC. Furthermore, it is found that in some cases, e.g., when one of the source nodes is far away from both the relay and the destination, model B achieves better performance than MARC-SDF.

6.1   System Model
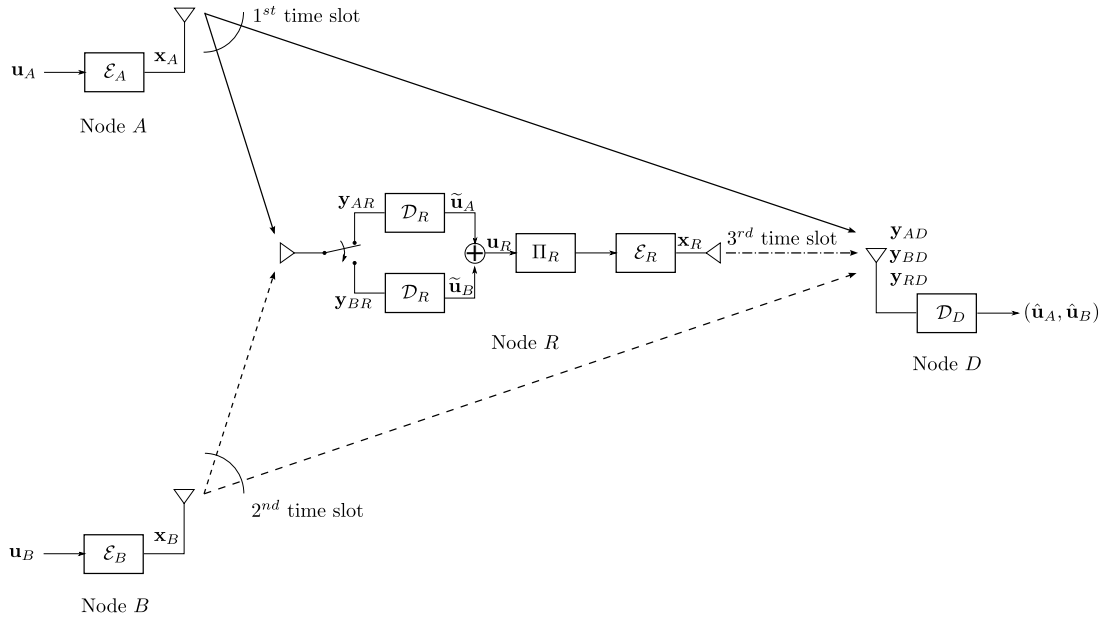
Figure 6.1: System model of an orthogonal multiple access relay channel.

Figure 6.1 illustrates a basic model of the orthogonal MARC system assumed in this section, where there are two source nodes A and B, a single relay node R, and one common destination node D. The K-bit length i.i.d. binary information sequences generated from nodes A and B are denoted as $\mathbf{u}_A = \{u_A(k)\}_{k=1}^K$ and $\mathbf{u}_B = \{u_B(k)\}_{k=1}^K$, respectively. The signaling scheme used at the A and B are denoted as $\mathscr{E}_A(\cdot)$ and $\mathscr{E}_B(\cdot)$, respectively, which consist of a serial concatenation of channel coding and modulation. There are three time slots in one transmission cycle. In the first two time slots, nodes A and B respectively broadcast their coded signal sequences $\mathbf{x}_A = \mathscr{E}_A(\mathbf{u}_A) = \{x_A(m)\}_{m=1}^M$ and $\mathbf{x}_B = \mathscr{E}_B(\mathbf{u}_B) = \{x_B(m)\}_{m=1}^M$ to the relay R and destination D, and the corresponding received signals obtained at R and D are $\mathbf{y}_{AR}$ and $\mathbf{y}_{BR}$, respectively.

In the third time slot, the relay R first applies signal detection and decoding on the received signals, which is denoted as $\mathscr{D}_R(\cdot)$. The estimates $\widetilde{\mathbf{u}}_A = \mathscr{D}_R(\mathbf{y}_{AR})$ and $\widetilde{\mathbf{u}}_B = \mathscr{D}_R(\mathbf{y}_{BR})$ may contain errors due to the variation of the two intra-links. In the system considered, $\widetilde{\mathbf{u}}_A$ and $\widetilde{\mathbf{u}}_B$ are always jointly network-channel coded regardless of whether they are correct or not, as $\mathbf{x}_R = \mathscr{E}_R(\mathbf{u}_R) = \mathscr{E}_R(\widetilde{\mathbf{u}}_A \oplus \widetilde{\mathbf{u}}_B)$, where the notation $\oplus$ denotes a binary exclusive-OR (XOR) operation and $\mathscr{E}_R(\cdot)$ represents the signaling scheme applied at R, including channel encoding and modulation. Finally, after receiving signals from A, B, and R, which are denoted as $\mathbf{y}_{AD}$, $\mathbf{y}_{BD}$, and $\mathbf{y}_{RD}$, respectively, the destination D performs joint network/channel decoding [LZA+14] on the received signals to retrieve $\mathbf{u}_A$ and $\mathbf{u}_B$ that transmitted from A and B, respectively. This system is referred to as MARC allowing intra-link errors (MARC-IE) in this section.

The spectrum efficiency of the signaling schemes $\mathscr{E}_A(\cdot)$, $\mathscr{E}_B(\cdot)$ and $\mathscr{E}_R(\cdot)$ are denoted as $R_{c,A}$, $R_{c,B}$ and $R_{c,R}$, respectively. Let $L_{i,j}$, $i \in \{A, B, R\}$, $j \in \{R, D\}$, $i \neq j$, denote the link between node i and j. The received signal of $L_{i,j}$

is expressed as

$$\mathbf{y}_{i,j} = h_{i,j} \cdot \mathbf{x}_i + \mathbf{n}_{i,j}, \tag{6.1}$$

where $h_{i,j}$ and $\mathbf{n}_{i,j}$ indicate the channel coefficients and the vector of independent zero-mean complex AWGN noise with variance $\sigma_{i,j}^2 = N_0/2$ per dimension of $L_{i,j}$. In this section, we assume all the links suffer from independent block Rayleigh fading, thus $h_{i,j}$ is constant over one transmission cycle, but varies transmission-by-transmission. Without loss of generality, we further assume the transmit power per symbol at A, B and R is the same, which is denoted as E_s. The instantaneous and average SNR of $L_{i,j}$ are given as $\gamma_{i,j} = |h_{i,j}|^2 \Gamma_{i,j}$ and $\Gamma_{i,j} = E_s/N_0$, respectively.

The error probabilities of L_{AR} and L_{BR} are expressed as

$$p_A = \mathfrak{B}(\mathbf{u}_A, \widetilde{\mathbf{u}}_A) = \frac{\sum_{k=1}^{K} |u_A(k) - \widetilde{u}_A(k)|}{K}, \tag{6.2}$$

and

$$p_B = \mathfrak{B}(\mathbf{u}_B, \widetilde{\mathbf{u}}_B) = \frac{\sum_{k=1}^{K} |u_B(k) - \widetilde{u}_B(k)|}{K}, \tag{6.3}$$

respectively.

6.2   Achievable Rate Region

In this subsection, we analyze the achievable rate region of the MARC-IE system within one transmission and temporarily set p_A and p_B with fixed values. The MARC-IE system model shown in Fig. 6.1 can be viewed as a system having two source nodes A and B, and one helper R. Letting R_A and R_B be the source coding rates of A and B, respectively. To investigate the admissible rate region for the two sources with one helper, we thus invoke the theorem [GK11, Theorem 10.4], according to which the information sequences $\mathbf{u}_A$ and $\mathbf{u}_B$ can be successfully recovered at the destination with the help of $\mathbf{u}_R$ if

$$\begin{cases} R_A & \geq & H(\mathbf{u}_A | \mathbf{u}_B, \hat{\mathbf{u}}_R), \\ R_B & \geq & H(\mathbf{u}_B | \mathbf{u}_A, \hat{\mathbf{u}}_R), \\ R_A + R_B & \geq & H(\mathbf{u}_A, \mathbf{u}_B | \hat{\mathbf{u}}_R), \\ R_R & \geq & I(\mathbf{u}_R; \hat{\mathbf{u}}_R), \end{cases} \tag{6.4}$$

where R_R represents the source coding rate at R, and $\hat{\mathbf{u}}_R$ is the estimate of $\mathbf{u}_R$ at D after joint decoding. According to (6.4) the side information provided by the relay R ($\hat{\mathbf{u}}_R$) helps reduce the rate R_A and R_B. Then, by using the chain rule, (6.4) can be re-formulated (see Appendix E) as follows

$$\begin{cases} R_A & \geq & \delta, \\ R_B & \geq & \delta, \\ R_A + R_B & \geq & \delta + 1, \\ R_R & \geq & 1 - H_b(p_R), \end{cases} \tag{6.5}$$

where

$$\delta = H_b(p_A * p_B * p_R), \tag{6.6}$$

and p_R is the error probability between $\mathbf{u}_R$ and $\hat{\mathbf{u}}_R$, i.e., $p_R = \mathfrak{B}(\mathbf{u}_R, \hat{\mathbf{u}}_R)$. As can be seen from (6.5), the achievable rate region is a 3-dimensional space with axis R_A, R_B and R_R. To simplify the analysis to be provided later, we first project the 3-dimensional rate region into the $R_A - R_B$ plane by fixing R_R. For a given R_R value, we can find the minimum p_R that satisfies the inequality $R_R \geq 1 - H_b(p_R)$. In this case, the achievable rate region of (R_A, R_B) for each transmission cycle is obtained, as shown in Figure 6.2.

6.3   Outage Probability

6.3.1   Outage Event for Each Transmission Cycle

For a transmission cycle, the outage event is defined as: one or both of the information sequences $\mathbf{u}_A$ and $\mathbf{u}_B$ cannot be successfully recovered at the destination. Therefore, given a fixed value of R_R, the outage event happens when
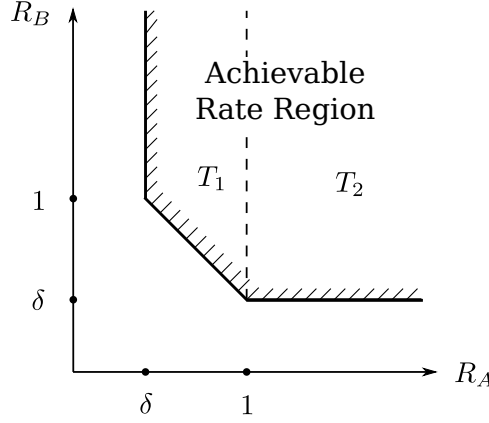
Figure 6.2: The projection of the achievable rate region of MARC-IE system into $R_A - R_B$ plane, given fixed R_R value. $\delta = H_b(p_A * p_B * p_R)$.

the pair (R_A, R_B) falls outside the achievable rate region. As shown in Figure 6.2, the entire achievable rate region can be divided into two parts T_1 and T_2. ε_1 and ε_2 denote the events that the rate pair (R_A, R_B) falls into T_1 and T_2, respectively, as

$$\begin{aligned} \varepsilon_1 &= \{(R_A, R_B) \in T_1\} = \{\delta \leq R_A \leq 1\} \cap \{R_A + R_B \geq \delta + 1\} \\ \varepsilon_2 &= \{(R_A, R_B) \in T_2\} = \{R_A \geq 1\} \cap \{R_B \geq \delta\}. \end{aligned} \tag{6.7}$$

Using the same method presented in Section 3.3.1, the relationship between R_A, R_B and γ_{AD}, γ_{BD} is identified as $R_A = \Phi_A(\gamma_{AD})$ and $R_B = \Phi_B(\gamma_{BD})$, respectively. The events ε_1 and ε_2 can be, respectively, expressed as

$$\begin{aligned} \varepsilon_1 &= \{\Phi_A^{-1}(\delta) \leq \gamma_{AD} \leq \Phi_A^{-1}(1)\} \cap \{\Phi_B^{-1}(\omega) \leq \gamma_{BD}\} \\ \varepsilon_2 &= \{\Phi_A^{-1}(1) \leq \gamma_{AD}\} \cap \{\Phi_B^{-1}(\delta) \leq \gamma_{BD}\}, \end{aligned} \tag{6.8}$$

where

$$\omega = \delta + 1 - \Phi_A(\gamma_{AD}). \tag{6.9}$$

The outage event of the MARC-IE system for each transmission cycle is defined as

$$\mathrm{OUT} = \overline{\{\varepsilon_1 \cup \varepsilon_2\}}. \tag{6.10}$$

where the $\overline{\{\varepsilon_1 \cup \varepsilon_2\}}$ denotes the complement of event $\{\varepsilon_1 \cup \varepsilon_2\}$.

6.3.2   Outage Calculation

In this subsection, the assumption that p_A, p_B and p_R are fixed values is eliminated, such that the channel variations of L_{AR}, L_{BR} and L_{RD} can be taken into account. According to Section 2.3, p_A and p_B can be expressed as functions of γ_{AR} and γ_{BR} as

$$p_A = \begin{cases} H_b^{-1}[1 - \Phi_A(\gamma_{AR})], & \text{for } 0 \leq \gamma_{AR} \leq \gamma_{AR}^*, \\ 0, & \text{for } \gamma_{AR} \geq \gamma_{AR}^*, \end{cases} \tag{6.11}$$

and

$$p_B = \begin{cases} H_b^{-1}[1 - \Phi_B(\gamma_{BR})], & \text{for } 0 \leq \gamma_{BR} \leq \gamma_{BR}^*, \\ 0, & \text{for } \gamma_{BR} \geq \gamma_{BR}^*, \end{cases} \tag{6.12}$$

respectively, where $\gamma_{AR}^* = \Phi_A^{-1}(1)$ and $\gamma_{BR}^* = \Phi_B^{-1}(1)$.

Now consider the constraint imposed on R_R, i.e., $R_R \geq 1 - H_b(p_R)$ in (6.5). It is found that if $R \geq 1$, the inequality always holds by setting $p_R = 0$. Otherwise, if $0 \leq R < 1$, p_R can be obtained by taking the equality of the constraint.

Since $R_R = \Phi_R(\gamma_{RD})$, R_R a one-to-one mapping to γ_{RD}, therefore the relationship between p_R and γ_{RD} can be expressed as

$$p_R = \begin{cases} H_b^{-1}[1 - \Phi_R(\gamma_{RD})], & \text{for } 0 \leq \gamma_{RD} \leq \gamma_{RD}^*, \\ 0, & \text{for } \gamma_{RD} \geq \gamma_{RD}^*, \end{cases} \qquad (6.13)$$

Recall that all the links are assumed to suffer from statistically independent block Rayleigh fading, we have $p(\gamma_{AD}, \gamma_{BD}, \gamma_{RD}) = p(\gamma_{AD}) \cdot p(\gamma_{BD}) \cdot p(\gamma_{RD})$. By replacing p_A, p_B and p_R with (6.11), (6.12) and (6.13), respectively, the probabilities of ε_1 and ε_2 are calculated, as

$$\begin{aligned} \Pr(\varepsilon_1) &= \Pr\left(\{\Phi_A^{-1}(\delta) \leq \gamma_{AD} \leq \Phi_A^{-1}(1)\} \cap \{\Phi_B^{-1}(\omega) \leq \gamma_{BD}\}\right) \\ &= \iiint_V \underbrace{\int_{\Phi_A^{-1}(\delta)}^{\Phi_A^{-1}(1)} p(\gamma_{AD})d\gamma_{AD} \int_{\Phi_B^{-1}(\omega)}^{\infty} p(\gamma_{BD})d\gamma_{BD}}_{g_1} \cdot p(\gamma_{AR}, \gamma_{BR}, \gamma_{RD})d\gamma_{AR}d\gamma_{BR}d\gamma_{RD} \\ &= \sum_{n=1}^{8} \iiint_{V_n} \underbrace{\frac{1}{\Gamma_{AD}} \int_{\Phi_A^{-1}(\delta)}^{\Phi_A^{-1}(1)} \exp\left(-\frac{\Phi_B^{-1}(\omega)}{\Gamma_{BD}} - \frac{\gamma_{AD}}{\Gamma_{AD}}\right) d\gamma_{AD}}_{g_1} \cdot p(\gamma_{AR})p(\gamma_{BR})p(\gamma_{RD})d\gamma_{AR}d\gamma_{BR}d\gamma_{RD}, \qquad (6.14) \end{aligned}$$

and

$$\begin{aligned} \Pr(\varepsilon_2) &= \Pr\left(\{\Phi_A^{-1}(1) \leq \gamma_{AD}\} \cap \{\Phi_B^{-1}(\delta) \leq \gamma_{BD}\}\right) \\ &= \iiint_V \underbrace{\int_{\Phi_A^{-1}(1)}^{\infty} p(\gamma_{AD})d\gamma_{AD} \int_{\Phi_B^{-1}(\delta)}^{\infty} p(\gamma_{BD})d\gamma_{BD}}_{g_2} \cdot p(\gamma_{AR}, \gamma_{BR}, \gamma_{RD})d\gamma_{AR}d\gamma_{BR}d\gamma_{RD} \\ &= \sum_{n=1}^{8} \iiint_{V_n} \underbrace{\exp\left(-\frac{\Phi_A^{-1}(1)}{\Gamma_{AD}} - \frac{\Phi_B^{-1}(\delta)}{\Gamma_{BD}}\right)}_{g_2} \cdot p(\gamma_{AR})p(\gamma_{BR})p(\gamma_{RD})d\gamma_{AR}d\gamma_{BR}d\gamma_{RD}, \qquad (6.15) \end{aligned}$$

respectively, where the domain of the threefold integral is

$$V = \{(\gamma_{AR}, \gamma_{BR}, \gamma_{RD}) : \gamma_{AR} \in [0, +\infty), \gamma_{BR} \in [0, +\infty), \gamma_{RD} \in [0, +\infty)\}. \qquad (6.16)$$

Finally, the outage probability of the MARC-IE system can be obtained, as

$$P_{\text{out}} = 1 - (\Pr(\varepsilon_1) + \Pr(\varepsilon_2)). \qquad (6.17)$$

It may be difficult to calculate the integrals shown in (6.14) and (6.15) in closed form. Hence, the results of (6.14) and (6.15) are numerically obtained by using functions provided in [Sha08]. Moreover, (6.14) and (6.15) can be respectively divided into eight sub-integrals with different sub-domains, which makes the numerical calculation of (6.14) and (6.15) tractable. The sub-domains of (6.14) and (6.15) are defined as

$$\begin{aligned} V_1 &= \{(\gamma_{AR}, \gamma_{BR}, \gamma_{RD}) : \gamma_{AR} \in [\gamma_{AR}^*, +\infty), \gamma_{BR} \in [\gamma_{BR}^*, +\infty), \gamma_{RD} \in [\gamma_{RD}^*, +\infty)\}, \\ V_2 &= \{(\gamma_{AR}, \gamma_{BR}, \gamma_{RD}) : \gamma_{AR} \in [\gamma_{AR}^*, +\infty), \gamma_{BR} \in [0, \gamma_{BR}^*), \gamma_{RD} \in [\gamma_{RD}^*, +\infty)\}, \\ V_3 &= \{(\gamma_{AR}, \gamma_{BR}, \gamma_{RD}) : \gamma_{AR} \in [0, \gamma_{AR}^*), \gamma_{BR} \in [\gamma_{BR}^*, +\infty), \gamma_{RD} \in [\gamma_{RD}^*, +\infty)\}, \\ V_4 &= \{(\gamma_{AR}, \gamma_{BR}, \gamma_{RD}) : \gamma_{AR} \in [0, \gamma_{AR}^*), \gamma_{BR} \in [0, \gamma_{BR}^*), \gamma_{RD} \in [\gamma_{RD}^*, +\infty)\}, \\ V_5 &= \{(\gamma_{AR}, \gamma_{BR}, \gamma_{RD}) : \gamma_{AR} \in [\gamma_{AR}^*, +\infty), \gamma_{BR} \in [\gamma_{BR}^*, +\infty), \gamma_{RD} \in [0, \gamma_{RD}^*)\}, \\ V_6 &= \{(\gamma_{AR}, \gamma_{BR}, \gamma_{RD}) : \gamma_{AR} \in [\gamma_{AR}^*, +\infty), \gamma_{BR} \in [0, \gamma_{BR}^*), \gamma_{RD} \in [0, \gamma_{RD}^*)\}, \\ V_7 &= \{(\gamma_{AR}, \gamma_{BR}, \gamma_{RD}) : \gamma_{AR} \in [0, \gamma_{AR}^*), \gamma_{BR} \in [\gamma_{BR}^*, +\infty), \gamma_{RD} \in [0, \gamma_{RD}^*)\}, \\ V_8 &= \{(\gamma_{AR}, \gamma_{BR}, \gamma_{RD}) : \gamma_{AR} \in [0, \gamma_{AR}^*), \gamma_{BR} \in [0, \gamma_{BR}^*), \gamma_{RD} \in [0, \gamma_{RD}^*)\}. \end{aligned} \qquad (6.18)$$
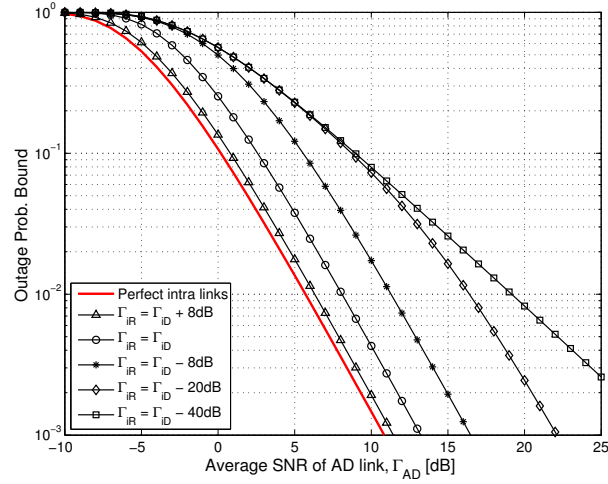
Figure 6.3: Outage probability of MARC-IE system, where $\Gamma_{AD} = \Gamma_{BD}$, $\Gamma_{RD} = \Gamma_{AD} + 3$ dB, and $R_{c,A} = R_{c,B} = R_{c,R} = 1/2$.

6.4   Numerical Results

Figure 6.3 shows the numerical results of the outage probability of the MARC-IE system that are independent of signaling schemes, obtained by calculating from (6.17) with (6.14) and (6.15) shown in Section 6.3.2, where $\Gamma_{AD} = \Gamma_{BD}$ and $\Gamma_{RD} = \Gamma_{AD} + 3$ dB is assumed. The values of $R_{c,A}$, $R_{c,B}$ and $R_{c,R}$ are all set to $1/2$. The curve of the probability with perfect intra-links [ZLA+14] is also provided in the same figure as a reference. It is found that as the quality of intra-links degrades, the gap increases between the reference curve and the outage curve with MARC-IE.
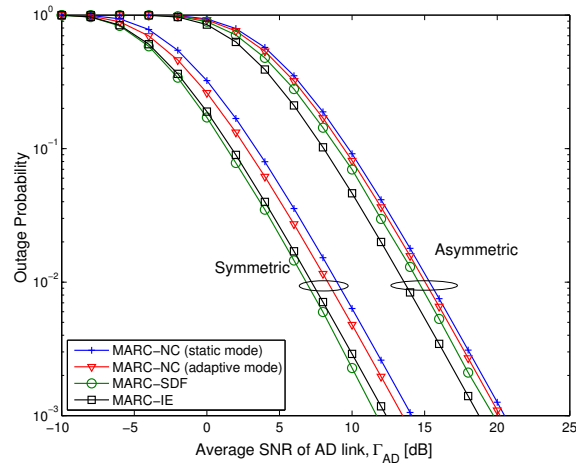
Figure 6.4: Outage probability of MARC-IE compared with that of MARC-NC and MARC-SDF. Both symmetric and asymmetric scenarios are considered. $R_{c,A} = R_{c,B} = R_{c,R} = 1/2$

Table 6.1: Settings of symmetric and asymmetric scenarios.

Scenario	Γ_{AD}	Γ_{BD}	Γ_{AR}	Γ_{BR}	Γ_{RD}
Symmetric	X	X	$X+\Delta$	$X+\Delta$	$X+\Delta$
Asymmetric	X	X-L	$X+\Delta$	$X+\Delta$-L	$X+\Delta$

To evaluate the benefit of MARC-IE system, we also compare its outage probability with that of MARC-NC [WK07] and MARC-SDF [IH11]. Results of the outage probability analysis in symmetric and asymmetric scenarios are demonstrated in Figure 6.4 for comparisons. The settings of the both scenarios are summarized in

Table 6.1, where *X* represents the average SNR of the *AD* link in dB; Δ and *L* denoting additional gain and loss due to the shorter and longer distance, respectively, and are set to 3 dB and 10 dB in this subsection.

The theoretical outage probabilities of MARC-NC, analyzed in a separate network-and-channel coding (SNCC) framework, were included in Figure 6.4. The outage probabilities in static and adaptive modes are obtained by [WK07, eqs. (4)-(5)] and [WK07, eqs. (4),(8)-(9),(11)], respectively. It is found that the MARC-IE system outperforms MARC-NC in terms of outage performance.

In principle, as stated in [IH11], a header (i.e., flag) is used at the relay in MARC-SDF to identify the correctly decoded source nodes, and furthermore, the header has to be protected with a very powerful error correction code. On the other hand, the relay in MARC-IE always performs network-coding and does not add header to the XOR-ed sequence to be forwarded to the destination. Therefore, it is not reasonable to make comparisons between MARC-SDF and MARC-IE, because MARC-SDF and MARC-IE belong to different categories of MARC (i.e., MARC-SDF is address-based, while MARC-IE is non-address-based).

Up to our best knowledge, there is no explicit mathematical expressions to calculate the theoretical outage probability of MARC-SDF. Deriving explicit mathematical expression of the outage probability with MARC-SDF is out of the scope of this section. Nevertheless, it is still meaningful to include MARC-SDF performance curves as a reference. The performance results with MARC-SDF, shown in Figure 6.4, are all based on the Monte Carlo method according to [IH11, eqs. (4)-(6)] with a modification of [SKM04, eq. (12)], while all the curves for MARC-IE are the theoretical results. It is emphasized that the conclusions for the superiority/inferiority of MARC-IE related to MARC-SDF in the Asymmetric/Symmetric scenarios are only based on simulations.

7.   Conclusion and Outlook

In this deliverable, based on the input from [D11], first we identified four toy scenarios TS1, TS2, TS3 and TS4 to demonstrated the benefits of the links-on-the-fly concept. The baselines of different protocols that are used for performance comparison with RESCUE system are presented. The distributed lossless/lossy source coding theorems and Shannon's lossy source/channel separation theorem are the key points to analyze the performance of the toy scenarios, which are then briefly introduced. The performance assessments of the four toy scenarios based on these theorems are provided with solid mathematical derivations and numerical results.

TS1 is a typical three-node one-way relay system. The outage probability of TS1 with decode-and-forward (DF) relaying allowing intra-link errors (DF-IE) was theoretically analyzed, where all the links between source, relay and destination are subject to independent block Rayleigh fading. The exact and approximated outage probabilities are derived from the viewpoint of the theorem for source coding with a helper and the Slepian-Wolf theorem, respectively. The admissible rate region is determined by the theorem for source coding with a helper, and found to be larger than that determined by the Slepian-Wolf theorem. The exact outage probability is lower than its approximation by the Slepian-Wolf theorem, however, the difference is negligible. Compared with the selective DF system, DF-IE can always achieve better outage performance. The most significant finding is, with the DF-IE system, the optimal relay location is shifted to exactly the midpoint between the source and destination, where the contributions of the source-relay and relay-destination links are balanced. The accuracy of the theoretical analysis has been verified through computer simulations. Furthermore, based on the numerical analysis, the DF-IE system can achieve better ε-outage capacity and throughput performance than the Selective DF (SDF) and Non-cooperative DF (NDF) systems.

TS2 is a single-source, multiple-relays, and single-destination system with no direct link between the source and the destination. With the links-on-the-fly concept, TS2 is also known as the chief executive officer (CEO) problem. The achievable rate-distortion region is derived according to Berger-Tung inner bound. The threshold limit of the bit error rate (BER) performance of TS2 is calculated based on the achievable rate-distortion region. Furthermore, we proposed two different methods to predict the error floor of the BER performance, one is the approximation of the error floor from Poisson Binomial distribution, and the other one is the theoretical lower bound determined by the rate-distortion function. In addition, the outage probability of TS2 in Rayleigh fading channels was derived from the viewpoint of the Slepian-Wolf theorem.

As an extension of TS1, there are multiple relays in TS3 to help the information transmission from the source to the destination. As an initial work, the SDF based multiple erroneous relaying were investigated. The initial performance analysis in terms of BER has been studied over Rayleigh fading channel environment.

TS4 is an orthogonal multiple access relay channel (MARC) allowing intra-link errors (MARC-IE), and the outage probability of MARC-IE is derived. The theoretical outage probabilities of network-coding-based MARC (MARC-NC) and MARC with selective decode-and-forward relaying (MARC-SDF) were also included for comparisons. It has been observed through simulations that the outage probability of MARC-NC is inferior to that of MARC-IE. Moreover, it has been found through simulations that if one of the source nodes is far away from both the relay and the destination, MARC-IE performs better than MARC-SDF.

The theoretical results of the four toy scenarios serve as preliminary input into WP2 and WP3 of the RESCUE project. Especially, the outage probability and error floor analysis plays an important role in higher layer simulations. In unpredictable environments assumed in RESCUE, strict link budget can not be guaranteed and the links are allowed to be lossy. The theoretical results of TS1 and TS4 demonstrated the potential benefits of preserving the lossy links in the network. It is expected that in more complicated network models that build upon the toy scenarios, significant performance gains can be achieved. As a future work, more accurate error rate analysis of TS2 will be provided, and lossy source-relay links will be included in TS3. Another extension is to investigate more toy scenarios that are suitable for RESUCE system, e.g., multi-way relay system.

8.   References

[12]   *IEEE Standard for Information technology—Telecommunications and information exchange between systems—Local and metropolitan area networks—Specific requirements—Part 11: Wireless LAN Medium Access Control (MAC) and Physical Layer (PHY) Specifications, March 2012*. 2012.

[AgH+11]   G. Al-Habian, A. ghrayeb, M. Hasna, and A. Abu-Dayya. "Threshold-based relaying in coded cooperative networks". In: *IEEE Trans. Veh. Technol.* 1.60 (2011), pp. 123–135.

[AM12]   K. Anwar and T. Matsumoto. "Accumulator-assisted distributed Turbo codes for relay system exploiting source-relay correlations". In: *IEEE Commun. Lett.* 16.7 (July 2012), pp. 1114–1117.

[BCJ+74]   L. Bahl, J. Cocke, F. Jelinek, and J. Raviv. "Optiaml decoding of linear codes for minimizing symbol error rate". In: *IEEE Trans. Inf. Theory* 20.2 (Mar. 1974), pp. 284–287.

[Ber78]   Toby Berger. "Multiterminal source coding". In: *The Information Theory Approach to Communications, G. Longo*. Vol. 229. Ed. New York, Springer-Verlag, 1978, pp. 171–231.

[BH06]   Norman C. Beaulieu and Jeremiah Hu. "A closed-form expression for the outage probability of decode-and-forward relaying in dissimilar Rayleigh fading channels". In: *IEEE Commun. Lett.* 10.12 (Dec. 2006), pp. 813–815.

[BKR+06]   A. Bletsas, A. Khisti, D.P. Reed, and Andrew Lippman. "A simple Cooperative diversity method based on network path selection". In: *IEEE J. Select. Areas Commun.* 24.3 (2006), pp. 659–672.

[BZV96]   T. Berger, Zhen Zhang, and H. Viswanathan. "The CEO problem [multiterminal source coding]". In: *IEEE Trans. Inform. Theory* 42.3 (May 1996), pp. 887–902.

[CAM13]   Meng Cheng, K. Anwar, and T. Matsumoto. "Outage based power allocation: Slepian-Wolf relaying viewpoint". In: *Globecom Workshops (GC Wkshps), 2013 IEEE*. Dec. 2013, pp. 807–811.

[Cov75]   T. M. Cover. "A proof of the data compression theorem of Slepian and Wolf for ergodic sources (Corresp.)" In: *IEEE Trans. Inform. Theory* 21.2 (1975), pp. 226–228.

[CT06]   Thomas M. Cover and Joy A. Thomas. *Elements of Information theory 2nd Edition*. USA: John Wiley & Sons, Inc., 2006.

[D11]   ICT-619555 RESCUE Deliverable D1.1. *System Scenarios and Technical Requirements*. 2014.

[DG09]   Pier Luigi Dragotti and Michael Gastpar. *Distributed Source Coding: Theory, Algorithms and Applications*. Academic Press, 2009.

[ETS14]   ETSI. *Intelligent Transport Systems (ITS); Vehicular Communications; GeoNetworking; Part 4: Geographical Addressing and Forwarding for Point-to-point and Point-to-multipoint Communications; Sub-part 1: Media-Independent Functionality (ETSI EN 302 636-4-1 V1.2.1)*. July 2014.

[Fes14]   A. Festag. "Cooperative Intelligent Transport Systems (C-ITS) Standards in Europe". In: *Communication Magazin* 12.52 (Dec. 2014).

[FL13]   H. Fares and C. Langlais. "Iterative joint source-relay channel decoding for the noisy decod-and-forward protocol". In: *IEEE VTC'13 Fall*. 2013, pp. 1–5.

[GK11]   A.E. Gamal and Y.H. Kim. *Network Information Theory*. Cambridge Univ. Press, 2011.

[GZ05]   J. Garcia-Frias and Ying Zhao. "Near-Shannon/Slepian-Wolf performance for unknown correlated sources over AWGN channels". In: *IEEE Trans. Commun.* 53.4 (Apr. 2005), pp. 555–559.

[HBP08]   J. Haghighat, H. Behroozi, and D. V. Plant. "Joint decoding and data fusion in wireless sensor networks using turbo codes". In: *Proc. IEEE 19th Int. Symp. Personal, Indoor and Mobile Radio Communications PIMRC*. Cannes, France, Spt. 2008, pp. 1–5.

[HKA08]   Kyu-Sung Hwang, Young-chai Ko, and M.-S. Alouini. "Outage probability of cooperative diversity systems with opportunistic relaying based on decode-and-forward". In: *IEEE Trans. Wireless Commun.* 7.12 (2008), pp. 5100–5107.

[HZA+13]   Xin He, Xiaobo Zhou, K. Anwar, and T. Matsumoto. "Estimation of Observation Error Probability in Wireless Sensor Networks". In: *IEEE Commun. Lett.* 17.6 (June 2013), pp. 1073–1076.

[HZF04]   P. Herhold, E. Zimmermann, and G. Fettweis. "A simple cooperative extension to wireless relaying". In: *Communications, 2004 International Zurich Seminar on*. 2004, pp. 36–39.

[IH11]   O. Iscan and C. Hausl. "Iterative Network and Channel Decoding for the Relay Channel with Multiple Sources". In: *Proc. IEEE 74th Veh. Technology Conf. (VTC Fall)*. San Francisco, CA, May 2011, pp. 1–5.

[KK06]   Ho Van Khuong and Hyung-Yun Kong. "LLR-Based Decode-and-Forward Protocol for Relay Networks and Closed-Form BER Expressions". In: *IEICE Trans. Fundam. Electron. Commun. Comput. Sci.* E89-A.6 (June 2006), pp. 1832–1841.

[KNP11]   K. Kosek-Szott, M. Natkaniec, and A. R. Pach. "A Simple but Accurate Throughput Model for IEEE 802.11 EDCA in Saturation and Non-saturation Conditions". In: *Computer Networks* 55 (2011), pp. 622–635.

[KNS+13]   K. Kosek-Szott, M. Natkaniec, S. Szott, A Krasilov, A Lyakhov, A Safonov, and I Tinnirello. "What's new for QoS in IEEE 802.11?" In: *Network, IEEE* 27 (2013), pp. 95–104. ISSN: 0890-8044.

[Küh15]   S. Kühlmorgen. "Performance Evaluation of ETSI GeoNetworking for Vehicular Ad hoc Networks". In: *Accepted for IEEE VTC Sprin* (Mar. 2015).

[LRW+98]   Jeffrey C. Lagarias, James A. Reeds, Margaret H. Wright, and Paul E. Wright. "Convergence Properties of the Nelder-Mead Simplex Method in Low Dimensions". In: *SIAM Journal of Optimization* 9.1 (1998), pp. 112–147.

[LTW04]   J.N. Laneman, D. N. C. Tse, and G. W. Wornell. "Cooperative diversity in wireless networks: Efficient protocols and outage behavior". In: *IEEE Trans. Inform. Theory* 50.12 (2004), pp. 3062–3080.

[LZA+14]   Pen-Shun Lu, Xiaobo Zhou, Khoirul Anwar, and Tad Matsumoto. "Joint Adaptive Network-Channel Coding for Energy-Efficient Multiple Access Relaying". In: *IEEE Trans. Veh. Technol.* 63.5 (June 2014), pp. 2298–2305.

[Meu71]   E. C. van der Meulen. "Three-terminal Communication channels". In: *Advanced Applied Probability* 3 (1971), pp. 120–154.

[NP00]   M. Natkaniec and A.R. Pach. "An analysis of the backoff mechanism used in IEEE 802.11 networks". In: *Computers and Communications, 2000. Proceedings. ISCC 2000. Fifth IEEE Symposium on*. 2000.

[OAF+08]   F.A. Onat, A. Adinoyi, Yijia Fan, H. Yanikomeroglu, J.S. Thompson, and I.D. Marsland. "Threshold Selection for SNR-based Selective Digital Relaying in Cooperative Wireless Networks". In: *IEEE Trans. Wireless Commun.* 7.11 (2008), pp. 4226–4237.

[PAR08]   R.C. Palat, A. Annamalai, and J.H. Reed. "Log-Likelihood-Ratio based Selective Decode and Forward Cooperative Communication". In: *Vehicular Technology Conference, 2008. VTC Spring 2008. IEEE*. 2008, pp. 615–618.

[RYA11]   A. Razi, K. Yasami, and A. Abedi. "On minimum number of wireless sensors required for reliable binary source estimation". In: *Proc. IEEE Wireless Communications and Networking Conf. (WCNC)*. Quintana-Roo, Mexico, Mar. 2011, pp. 1852–1857.

[SBS96]   M. Schwartz, W. R. Bennett, and S. Stein. "Communication Systems and Techniques". In: *IEEE Commun. Mag.* 34.5 (1996).

[Sha08]   L.F. Shampine. "Matlab program for quadrature in 2D". In: *Applied Mathematics and Computation* 202.1 (2008), pp. 266–274. ISSN: 0096-3003.

[Sha48]   C. E. Shannon. "A Mathematical Theory of Communications". In: *Bell Systems Technical Journal* 27 (1948), pp. 379–423, 623–656.

[Sha59]   C. E. Shannon. "Coding theorems for a discrete source with a fidelity criterion". In: *IRE Nat. Conv. Rec., Pt. 4*. 1959, pp. 142–163.

[SKM04]   L. Sankaranarayanan, G. Kramer, and Narayan B. Mandayam. "Hierarchical sensor networks: capacity bounds and cooperative strategies using the multiple-access relay channel model". In: *Sensor and Ad Hoc Communications and Networks, 2004. IEEE SECON 2004. 2004 First Annual IEEE Communications Society Conference on*. Oct. 2004, pp. 191–199.

[SW73]   D. Slepian and J. Wolf. "Noiseless coding of correlated information sources". In: *IEEE Trans. Inform. Theory* 19.4 (July 1973), pp. 471–480.

[Tun78]   Sui-Yin Tung. "Multiterminal Source Coding". PhD thesis. Cornell University, 1978.

[VFC+14] Francisco J Vazquez-Araujo, Oscar Fresnedo, Luis Castedo, and Javier Garcia-Frias. "Analog Joint Source-Channel Coding over MIMO channels". In: *Eurasip J. on Wireless Commun. and Netw.* 2014:25 (2014).

[Wan93]   Y. H. Wang. "On the number of successes in independent trials". In: *Statistica Sinica* 3.2 (1993), pp. 295–312.

[WK07]   D. H. Woldegebreal and H. Karl. "Multiple-Access Relay Channel with Network Coding and Non-Ideal Source-Relay Channels". In: *Proc. 4th Int. Symp. Wireless Communication Systems ISWCS 2007*. 2007, pp. 732–736.

[WMF15]   Albrecht Wolf, Maximilian Matth, and Gerhard Fettweis. "Improved Source Correlation Estimation in Wireless Sensor Networks". In: *IEEE International Conference on Communications* (2015), pp. 1–6.

[XLC04]   Zixiang Xiong, A. D. Liveris, and S. Cheng. "Distributed source coding for sensor networks". In: *IEEE Signal Processing Mag.* 21.5 (Sept. 2004), pp. 80–94.

[YAD+11] Jiazi Yi, Asmaa Adnane, Sylvain David, and Benoît Parrein. "Multipath optimized link state routing for mobile ad hoc networks". In: *Ad Hoc Networks* 9 (2011), pp. 28–47. ISSN: 1570-8705.

[YG11]   R. Youssef and A. Graell i Amat. "Distributed Serially Concatenated Codes for Multi-Source Cooperative Relay Networks". In: *IEEE Trans. Wireless Commun.* 10.1 (2011), pp. 253–263.

[ZA06]   Guang-Chong Zhu and F. Alajaji. "Joint source-channel Turbo coding for binary Markov sources". In: *IEEE Trans. Wireless Commun.* 5.5 (2006), pp. 1065–1075.

[ZCH+14] Xiaobo Zhou, Meng Cheng, Xin He, Khoirul Anwar, and Tad Matsumoto. "Outage Analysis of Decode-and-Forward Relaying System Allowing Intra-link Errors". In: *Proc. 20th European Wireless Conf. (EW 2014)*. Barcelona, Spain, 14-16 May 2014.

[ZHA+12] Xiaobo Zhou, Xin He, Khoirul Anwar, and Tad Matsumoto. "GREAT-CEO: larGe scale distRibuted dEcision mAking Technique for wireless Chief Executive Officer problems". In: *IEICE Trans. on Commun.* E95-B.12 (Dec. 2012), pp. 3654–3662.

[ZLA+14] Xiaobo Zhou, Pen-Shun Lu, K. Anwar, and T. Matsumoto. "Correlated Sources Transmission in Orthogonal Multiple Access Relay Channel: Theoretical Analysis and Performance Evaluation". In: *IEEE Trans. Wireless Commun.* 13.3 (Mar. 2014), pp. 1424–1435.

Appendix A   Proof of $\mathscr{R}_{SCwH}(p) \geq \mathscr{R}_{SW}(p)$

According to (3.6) and (3.8), $\mathscr{R}_{SCwH}(p) \geq \mathscr{R}_{SW}(p)$ is equivalent to $f_1(x) \leq f_2(x)$, where

$$f_1(x) = \begin{cases} H_b(p), & \text{for } x \geq 1, \\ H_b[H_b^{-1}(1-x)*p], & \text{for } 0 \leq x \leq 1, \end{cases} \tag{A.1}$$

and

$$f_2(x) = \begin{cases} H_b(p), & \text{for } x \geq 1, \\ 1 + H_b(p) - x, & \text{for } H_b(p) \leq x \leq 1, \\ 1, & \text{for } 0 \leq x \leq H_b(p), \end{cases} \tag{A.2}$$

are the boundaries for the sets of the inequalities for $\mathscr{R}_{SCwH}(p)$ and $\mathscr{R}_{SW}(p)$, respectively. It is obviously that $f_1(x) = f_2(x)$ for $x \geq 1$. For $0 \leq x \leq H_b(p)$, $f_1(x) \leq f_2(x)$ since $H_b[H_b^{-1}(1-x)*p] \leq 1$ always holds. For $H_b(p) \leq x \leq 1$, by setting $H_b^{-1}(1-x) = \alpha$, it is easily to obtain

$$\begin{aligned} f_2(x) - f_1(x) &= 1 + H_b(p) - x - H_b(\alpha*p) \\ &= H_b(\alpha) + H_b(p) - H_b(\alpha*p). \end{aligned} \tag{A.3}$$

To prove $f_2(x) - f_1(x) \geq 0$ for $H_b(p) \leq x \leq 1$, we consider the joint entropy of two binary random variable X and Y, where X follows a Bernoulli distribution with parameter α, and Y is the observation of X over a BSC with a crossover probability p. The joint entropy of X and Y can be expressed as

$$\begin{aligned} H(X,Y) &= H(X) + H(Y|X) \\ &= H(Y) + H(X|Y), \end{aligned} \tag{A.4}$$

where $H(X) = H_b(\alpha)$, $H(Y) = H_b(\alpha*p)$ and $H(Y|X) = H_b(p)$. From (A.4), we get

$$\begin{aligned} H(X|Y) &= H(X) + H(Y|X) - H(Y) \\ &= H_b(\alpha) + H_b(p) - H_b(\alpha*p) \\ &\geq 0. \end{aligned} \tag{A.5}$$

Hence, it can be concluded that $f_2(x) - f_1(x) \geq 0$ for $H_b(p) \leq x \leq 1$.

In summary, $f_1(x) \leq f_2(x)$ for $x \geq 0$, and $\mathscr{R}_{SCwH}(p) \geq \mathscr{R}_{SW}(p)$ has been proven.

Appendix B   Derivation of Eqations (3.14)-(3.21)

As mentioned Section 3.3.2, the intra-link error probability p and the rates R_1, R_2 can be transformed into the instantaneous channel SNR of their corresponding links using the $\Phi^{-1}(\cdot)$ function with $\Phi^{-1}(0) = 0$. The joint pdf of γ_0, γ_1 and γ_2 can be expressed as $p(\gamma_0, \gamma_1, \gamma_2) = p(\gamma_0) \cdot p(\gamma_1) \cdot p(\gamma_2)$ because the three links are statistically independent with each other. Moreover, $p(\gamma_i) = \frac{1}{\Gamma_i} \exp(-\frac{\gamma_i}{\Gamma_i})$, $i \in \{0, 1, 2\}$ due to the block Rayleigh fading assumptions. With these conditions, Equation (3.15) can be calculated as

$$
\begin{aligned}
P_{1,b} &= \Pr\{p = 0, (R_1, R_2) \in \mathscr{R}_b\} \\
&= \Pr\{p = 0, 0 \le R_2 \le 1, 0 \le R_1 \le H_b(H_b^{-1}(1 - R_2) * p)\} \\
&= \Pr\{\gamma_0 \ge \Phi_1^{-1}(1), \Phi_2^{-1}(0) \le \gamma_2 \le \Phi_2^{-1}(1), \Phi_1^{-1}(0) \le \gamma_1 \le \Phi_1^{-1}[1 - \Phi_2(\gamma_2)]\} \\
&= \int_{\Phi_1^{-1}(1)}^{\Phi_1^{-1}(\infty)} \int_0^{\Phi_2^{-1}(1)} \int_0^{\Phi_1^{-1}[1 - \Phi_2(\gamma_2)]} p(\gamma_0, \gamma_1, \gamma_2) d\gamma_1 d\gamma_2 d\gamma_0 \\
&= \int_0^{\Phi_2^{-1}(1)} \int_0^{\Phi_1^{-1}[1 - \Phi_2(\gamma_2)]} \left\{ p(\gamma_1) \cdot p(\gamma_2) \cdot \int_{\Phi_1^{-1}(1)}^{\Phi_1^{-1}(\infty)} p(\gamma_0) d\gamma_0 \right\} d\gamma_1 d\gamma_2 \\
&= \int_0^{\Phi_2^{-1}(1)} \int_{\Phi_1^{-1}(0)}^{\Phi_1^{-1}[1 - \Phi_2(\gamma_2)]} \left\{ p(\gamma_1) \cdot p(\gamma_2) \cdot \exp\left[-\frac{\Phi_1^{-1}(1)}{\Gamma_0} \right] \right\} d\gamma_1 d\gamma_2 \\
&= \exp\left[-\frac{\Phi_1^{-1}(1)}{\Gamma_0} \right] \cdot \int_0^{\Phi_2^{-1}(1)} \left\{ p(\gamma_2) \cdot \int_{\Phi_1^{-1}(0)}^{\Phi_1^{-1}[1 - \Phi_2(\gamma_2)]} p(\gamma_1) d\gamma_1 \right\} d\gamma_2 \\
&= \exp\left[-\frac{\Phi_1^{-1}(1)}{\Gamma_0} \right] \cdot \int_0^{\Phi_2^{-1}(1)} \left\{ p(\gamma_2) \cdot \left[1 - \exp(-\frac{\Phi_1^{-1}[1 - \Phi_2(\gamma_2)]}{\Gamma_1}) \right] \right\} d\gamma_2 \\
&= \frac{1}{\Gamma_2} \exp\left[-\frac{\Phi_1^{-1}(1)}{\Gamma_0} \right] \int_0^{\Phi_2^{-1}(1)} \exp(-\frac{\gamma_2}{\Gamma_2}) \cdot \left[1 - \exp(-\frac{\Phi_1^{-1}[1 - \Phi_2(\gamma_2)]}{\Gamma_1}) \right] d\gamma_2.
\end{aligned}
\tag{B.1}
$$

Equations (3.14), (3.16), (3.17), (3.18), (3.19), (3.20) and (3.21) can be calculated in the same way.

Appendix C   Approximation of the Inverse Binary Entropy Function

The binary entropy function is defined as

$$H_b(x) = z = -x\log_2 x - (1-x)\log_2(1-x). \tag{C.1}$$

For $0 \le x \le 0.5$, $H_b(x)$ is monotonically increasing and therefore has a unique inverse function

$$x = H_b^{-1}(z). \tag{C.2}$$

However, it may not be possible to derive the explicit expressions of $H_b^{-1}(z)$, according to Equation (C.1). By using a curve fitting technique [LRW+98], it can be well approximated by

$$H_b^{-1}(z) \approx (2^{c_1 z^{c_2}} - 2^{-c_3 z^{c_4}})^{c_5}, \tag{C.3}$$

with $c_1 = 0.6794$, $c_2 = 0.7244$, $c_3 = 0.1357$, $c_4 = 21.8026$ and $c_5 = 1.9920$. The numerically calculated $H_b^{-1}(z)$ and its approximated curves are shown in Figgure C.1.
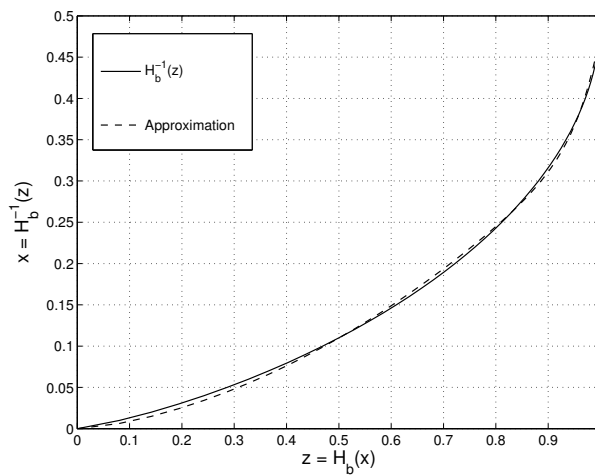
Figure C.1: The inverse binary entropy function and its approximation.

Appendix D   Slepian-Wolf inadmissible region closed-form expressions for high SNR

For Rayleigh fading channels the pdf (cf. Eq. (4.18)) can be applied in Eq. (4.39) with corresponding limits. From this it follows that

$$P_1 = 1 - \int_{2^{R_{c1}H(\mathbf{u}_1|\mathbf{u}_2,\mathbf{u}_3)}-1}^{\infty} \int_{2^{R_{c2}H(\mathbf{u}_2|\mathbf{u}_1,\mathbf{u}_3)}-1}^{\infty} \int_{2^{R_{c3}H(\mathbf{u}_3|\mathbf{u}_1,\mathbf{u}_2)}-1}^{\infty} \frac{1}{\Gamma_1}e^{-\frac{\gamma_1}{\Gamma_1}}\frac{1}{\Gamma_2}e^{-\frac{\gamma_2}{\Gamma_2}}\frac{1}{\Gamma_3}e^{-\frac{\gamma_3}{\Gamma_3}}\,d\gamma_3 d\gamma_2 d\gamma_1 \tag{D.1}$$

$$= 1 - e^{-\frac{2^{R_{c1}H(\mathbf{u}_1|\mathbf{u}_2,\mathbf{u}_3)}-1}{\Gamma_1}-\frac{2^{R_{c2}H(\mathbf{u}_2|\mathbf{u}_1,\mathbf{u}_3)}-1}{\Gamma_2}-\frac{2^{R_{c3}H(\mathbf{u}_3|\mathbf{u}_1,\mathbf{u}_2)}-1}{\Gamma_3}}. \tag{D.2}$$

For high-SNR the exponential function can approximated be the MacLaurin series and thus, the probability simplifies to

$$P_1 \approx \frac{2^{R_{c1}H(\mathbf{u}_1|\mathbf{u}_2,\mathbf{u}_3)}-1}{\Gamma_1} + \frac{2^{R_{c2}H(\mathbf{u}_2|\mathbf{u}_1,\mathbf{u}_3)}-1}{\Gamma_2} + \frac{2^{R_{c3}H(\mathbf{u}_3|\mathbf{u}_1,\mathbf{u}_2)}-1}{\Gamma_3}, \tag{D.3}$$

with the assumption $R_{c1} = R_{c2} = R_{c3} = R_c$, P_1 can be finalized to

$$= \frac{2^{R_cH(\mathbf{u}_1|\mathbf{u}_2,\mathbf{u}_3)}-1}{\Gamma_1} + \frac{2^{R_cH(\mathbf{u}_2|\mathbf{u}_1,\mathbf{u}_3)}-1}{\Gamma_2} + \frac{2^{R_cH(\mathbf{u}_3|\mathbf{u}_1,\mathbf{u}_2)}-1}{\Gamma_3}. \tag{D.4}$$

For probabilities P_2, P_3 and P_4 the pdf (cf. Eq. (4.18)) of Rayleigh fading channels can be applied to Eq. (4.40) - Eq. (4.42). With $(l,i,j,k) \in \{(2,1,2,3),(3,3,1,2),(4,2,3,1)\}$ the probabilities can be formulated to

$$P_l = \int_{2^{R_{ci}H(\mathbf{u}_i)}-1}^{\infty} \int_{2^{R_{cj}H(\mathbf{u}_j|\mathbf{u}_i,\mathbf{u}_k)}-1}^{2^{R_{cj}H(\mathbf{u}_i|\mathbf{u}_j)}-1} \int_{2^{R_{ck}H(\mathbf{u}_k|\mathbf{u}_i,\mathbf{u}_j)}-1}^{2^{R_{ck}H(\mathbf{u}_j,\mathbf{u}_k|\mathbf{u}_i)-\frac{R_{ck}}{R_{cj}}\log_2(\gamma_j+1)}-1} \frac{1}{\Gamma_i}e^{-\frac{\gamma_i}{\Gamma_i}}\frac{1}{\Gamma_j}e^{-\frac{\gamma_j}{\Gamma_j}}\frac{1}{\Gamma_k}e^{-\frac{\gamma_k}{\Gamma_k}}\,d\gamma_i d\gamma_j d\gamma_k,$$

The integral of γ_i and γ_k can be solved due to no limit-dependencies in other integrals and expressed as

$$P_l = \frac{1}{\Gamma_j}e^{-\frac{2^{R_{ci}H(\mathbf{u}_i)}-1}{\Gamma_i}}e^{-\frac{2^{R_{ck}H(\mathbf{u}_k|\mathbf{u}_i,\mathbf{u}_j)}-1}{\Gamma_k}}\int_{2^{R_{cj}H(\mathbf{u}_j|\mathbf{u}_j,\mathbf{u}_k)}-1}^{2^{R_{cj}H(\mathbf{u}_i|\mathbf{u}_j)}-1}e^{-\frac{\gamma_j}{\Gamma_j}}\left(1-e^{\frac{2^{R_{ck}H(\mathbf{u}_k|\mathbf{u}_i,\mathbf{u}_j)}}{\Gamma_k}+\frac{2^{R_{ck}H(\mathbf{u}_j,\mathbf{u}_k|\mathbf{u}_i)-\frac{R_{ck}}{R_{cj}}\log_2(\gamma_j+1)}}{\Gamma_k}}\right)d\gamma_j.$$

For high-SNR the exponential function can approximated be the MacLaurin series and thus, the probability simplifies to

$$\approx \frac{1}{\Gamma_j}\left(1-\frac{2^{R_{ci}H(\mathbf{u}_i)}-1}{\Gamma_i}-\frac{2^{R_{ck}H(\mathbf{u}_k|\mathbf{u}_i,\mathbf{u}_j)}-1}{\Gamma_k}\right)$$

$$\times \int_{2^{R_{cj}H(\mathbf{u}_j|\mathbf{u}_j,\mathbf{u}_k)}-1}^{2^{R_{cj}H(\mathbf{u}_i|\mathbf{u}_j)}-1}\left(1-\frac{\gamma_j}{\Gamma_j}\right)\left(\frac{2^{R_{ck}H(\mathbf{u}_k|\mathbf{u}_i,\mathbf{u}_j)}}{\Gamma_k}-\frac{2^{R_{ck}H(\mathbf{u}_j,\mathbf{u}_k|\mathbf{u}_i)-\frac{R_{ck}}{R_{cj}}\log_2(\gamma_j+1)}}{\Gamma_k}\right)d\gamma_j.$$

The integral for γ_j is solved with assumption $R_{ci} = R_{cj} = R_{ck} = R_c$ and the probability can be eventually expressed as

$$= \frac{(\Gamma_i - 2^{R_c} + 1)\left(-\Gamma_k + 2^{R_cH(\mathbf{u}_k|\mathbf{u}_i,\mathbf{u}_j)}-1\right)}{2\Gamma_i\Gamma_j^2\Gamma_k^2}\left(\left(2^{R_cH(\mathbf{u}_i|\mathbf{u}_j)}-2^{R_cH(\mathbf{u}_j|\mathbf{u}_i,\mathbf{u}_k)}\right)\right. \tag{D.5}$$

$$\times \left(-2^{R_c(H(\mathbf{u}_i,\mathbf{u}_j,\mathbf{u}_k)-1)}+2^{R_cH(\mathbf{u}_j,\mathbf{u}_k|\mathbf{u}_i)+1}-2^{R_c(H(\mathbf{u}_j|\mathbf{u}_i,\mathbf{u}_k)+H(\mathbf{u}_k|\mathbf{u}_i,\mathbf{u}_j))}+\Gamma_j 2^{R_cH(\mathbf{u}_k|\mathbf{u}_i,\mathbf{u}_j)+1}+2^{R_cH(\mathbf{u}_k|\mathbf{u}_i,\mathbf{u}_j)+1}\right)$$

$$\left. +(\Gamma_j+1)2^{R_cH(\mathbf{u}_j,\mathbf{u}_k|\mathbf{u}_i)+1}\log\left[2^{R_c(H(\mathbf{u}_j|\mathbf{u}_i,\mathbf{u}_k)-H(\mathbf{u}_i|\mathbf{u}_j))}\right]\right). \tag{D.6}$$

For probability P_{5a} the Rayleigh fading channel pdf is applied in Eq. (4.44) and formulated to

$$P_{5a} = \int_{2^{R_{c1}H(\mathbf{u}_1|\mathbf{u}_2,\mathbf{u}_3)}-1}^{2^{R_{c1}H(\mathbf{u}_1)}-1} \int_{2^{R_{c3}H(\mathbf{u}_3|\mathbf{u}_1,\mathbf{u}_2)}-1}^{2^{R_{c3}(H(\mathbf{u}_1|\mathbf{u}_3))-\frac{R_{c3}}{R_{c1}}\log_2(\gamma_1+1)}-1}$$
$$\int_{2^{R_{c2}H(\mathbf{u}_2|\mathbf{u}_1,\mathbf{u}_3)}-1}^{2^{R_{c2}H(\mathbf{u}_1,\mathbf{u}_2,\mathbf{u}_3)-\frac{R_{c2}}{R_{c1}}\log_2(\gamma_1+1)-\frac{R_{c2}}{R_{c3}}\log_2(\gamma_3+1)}-1} \frac{1}{\Gamma_1}e^{-\frac{\gamma_1}{\Gamma_1}}\frac{1}{\Gamma_2}e^{-\frac{\gamma_2}{\Gamma_2}}\frac{1}{\Gamma_3}e^{-\frac{\gamma_3}{\Gamma_3}}\, d\gamma_3 d\gamma_2 d\gamma_1.$$

The integral of γ_2 can be solved due to no limit-dependencies in other integrals and expressed as

$$=\frac{1}{\Gamma_1\Gamma_3}e^{-\frac{2^{R_{c2}H(\mathbf{u}_2|\mathbf{u}_1,\mathbf{u}_3)}-1}{\Gamma_2}}\int_{2^{R_{c1}H(\mathbf{u}_1|\mathbf{u}_2,\mathbf{u}_3)}-1}^{2^{R_{c1}H(\mathbf{u}_1)}-1}\int_{2^{R_{c3}H(\mathbf{u}_3|\mathbf{u}_1,\mathbf{u}_2)}-1}^{2^{R_{c3}(H(\mathbf{u}_1|\mathbf{u}_3))-\frac{R_{c3}}{R_{c1}}\log_2(\gamma_1+1)}-1}e^{-\frac{\gamma_1}{\Gamma_1}}e^{-\frac{\gamma_3}{\Gamma_3}}$$
$$\times\left(1-e^{\frac{2^{R_{c2}H(\mathbf{u}_2|\mathbf{u}_1,\mathbf{u}_3)}}{\Gamma_2}}-\frac{2^{R_{c2}H(\mathbf{u}_1,\mathbf{u}_2,\mathbf{u}_3)-\frac{R_{c2}}{R_{c1}}\log_2(\gamma_1+1)-\frac{R_{c2}}{R_{c3}}\log_2(\gamma_3+1)}}{\Gamma_2}\right)d\gamma_3 d\gamma_1 \tag{D.7}$$

For high-SNR the exponential function can approximated be the MacLaurin series and thus, the probability simplifies to

$$\approx\frac{1}{\Gamma_1\Gamma_3}\left(1-\frac{2^{R_{c2}H(\mathbf{u}_2|\mathbf{u}_1,\mathbf{u}_3)}-1}{\Gamma_2}\right)\int_{2^{R_{c1}H(\mathbf{u}_1|\mathbf{u}_2,\mathbf{u}_3)}-1}^{2^{R_{c1}H(\mathbf{u}_1)}-1}\left(1-\frac{\gamma_1}{\Gamma_1}\right) \tag{D.8}$$
$$\int_{2^{R_{c3}H(\mathbf{u}_3|\mathbf{u}_1,\mathbf{u}_2)}-1}^{2^{R_{c3}(H(\mathbf{u}_1|\mathbf{u}_3))-\frac{R_{c3}}{R_{c1}}\log_2(\gamma_1+1)}-1}\left(1-\frac{\gamma_3}{\Gamma_3}\right)\left(\frac{2^{R_{c2}H(\mathbf{u}_1,\mathbf{u}_2,\mathbf{u}_3)-\frac{R_{c2}}{R_{c1}}\log_2(\gamma_1+1)-\frac{R_{c2}}{R_{c3}}\log_2(\gamma_3+1)}}{\Gamma_2}-\frac{2^{R_{c2}H(\mathbf{u}_2|\mathbf{u}_1,\mathbf{u}_3)}}{\Gamma_2}\right)d\gamma_3 d\gamma_1.$$
$$\tag{D.9}$$

With assumption $R_{c1}=R_{c2}=R_{c3}=R_c$ the equation is transposed to

$$=\frac{1}{\Gamma_1\Gamma_2\Gamma_3}\left(1-\frac{2^{R_cH(\mathbf{u}_2|\mathbf{u}_1,\mathbf{u}_3)}-1}{\Gamma_2}\right)\int_{2^{R_cH(\mathbf{u}_1|\mathbf{u}_2,\mathbf{u}_3)}-1}^{2^{R_c}-1}\left(1-\frac{\gamma_1}{\Gamma_1}\right)$$
$$\int_{2^{R_cH(\mathbf{u}_3|\mathbf{u}_1,\mathbf{u}_2)}-1}^{2^{\frac{R_cH(\mathbf{u}_1|\mathbf{u}_3)}{(\gamma_1+1)}}-1}\left(1-\frac{\gamma_3}{\Gamma_3}\right)\left(2^{\frac{R_cH(\mathbf{u}_1,\mathbf{u}_2,\mathbf{u}_3)}{(\gamma_1+1)(\gamma_3+1)}}-2^{R_cH(\mathbf{u}_2|\mathbf{u}_1,\mathbf{u}_3)}\right)d\gamma_3 d\gamma_1, \tag{D.10}$$

The integrals for γ_1 and γ_3 are solved and the probability can be eventually expressed as

$$=-\frac{1}{\Gamma_1\Gamma_2\Gamma_3}\left(2^{R_c(H(\mathbf{u}_1|\mathbf{u}_2,\mathbf{u}_3)+H(\mathbf{u}_2|\mathbf{u}_1,\mathbf{u}_3)+H(\mathbf{u}_3|\mathbf{u}_1,\mathbf{u}_2))}-2^{R_c(H(\mathbf{u}_1)+H(\mathbf{u}_2|\mathbf{u}_1,\mathbf{u}_3)+H(\mathbf{u}_3|\mathbf{u}_1,\mathbf{u}_2))}\right.$$
$$+2^{R_cH(\mathbf{u}_1,\mathbf{u}_2,\mathbf{u}_3)}\log\left[2^{R_cH(\mathbf{u}_1|\mathbf{u}_2,\mathbf{u}_3)}\right]\left(\log\left[2^{-\frac{R_cH(\mathbf{u}_1|\mathbf{u}_2,\mathbf{u}_3)}{2}}2^{R_c(-H(\mathbf{u}_2|\mathbf{u}_1,\mathbf{u}_2)+H(\mathbf{u}_3|\mathbf{u}_1,\mathbf{u}_2)-H(\mathbf{u}_1,\mathbf{u}_2,\mathbf{u}_3))}\right]-1\right)$$
$$\left.+2^{R_cH(\mathbf{u}_1,\mathbf{u}_2,\mathbf{u}_3)}\log\left[2^{R_cH(\mathbf{u}_1)}\right]\left(\log\left[2^{\frac{R_cH(\mathbf{u}_1)}{2}}2^{R_c(H(\mathbf{u}_2|\mathbf{u}_1,\mathbf{u}_3)-H(\mathbf{u}_1,\mathbf{u}_2,\mathbf{u}_3)+H(\mathbf{u}_3|\mathbf{u}_1,\mathbf{u}_2))}\right]+1\right)\right). \tag{D.11}$$

For probability P_{5b} the Rayleigh fading channel pdf is applied in Eq. (4.45) and formulated to

$$P_{5b} = \int_{2^{R_{c1}H(\mathbf{u}_1|\mathbf{u}_2,\mathbf{u}_3)}-1}^{2^{R_{c1}H(\mathbf{u}_1|\mathbf{u}_2)}-1} \int_{2^{R_{c3}H(\mathbf{u}_3|\mathbf{u}_1,\mathbf{u}_2)}-1}^{2^{R_{c3}(H(\mathbf{u}_1,\mathbf{u}_2,\mathbf{u}_3)-H(\mathbf{u}_2))-\frac{R_{c3}}{R_{c1}}\log_2(\gamma_1+1)}-1}$$
$$\int_{2^{R_{c2}H(\mathbf{u}_2)}-1}^{2^{R_{c2}H(\mathbf{u}_1,\mathbf{u}_2,\mathbf{u}_3)-\frac{R_{c2}}{R_{c1}}\log_2(\gamma_1+1)-\frac{R_{c2}}{R_{c3}}\log_2(\gamma_3+1)}-1} \frac{1}{\Gamma_1}e^{-\frac{\gamma_1}{\Gamma_1}}\frac{1}{\Gamma_2}e^{-\frac{\gamma_2}{\Gamma_2}}\frac{1}{\Gamma_3}e^{-\frac{\gamma_3}{\Gamma_3}}\, d\gamma_3 d\gamma_2 d\gamma_1.$$

The integral of γ_2 can be solved due to no limit-dependencies in other integrals and expressed as

$$
=\frac{1}{\Gamma_1\Gamma_3}e^{-\frac{2^{R_{c2}H(\mathbf{u}_2)}-1}{\Gamma_2}}\int_{2^{R_{c1}H(\mathbf{u}_1|\mathbf{u}_2,\mathbf{u}_3)}-1}^{2^{R_{c1}H(\mathbf{u}_1|\mathbf{u}_2)}-1}\int_{2^{R_{c3}H(\mathbf{u}_3|\mathbf{u}_1,\mathbf{u}_2)}-1}^{2^{R_{c3}(H(\mathbf{u}_1,\mathbf{u}_2,\mathbf{u}_3)-H(\mathbf{u}_2))-\frac{R_{c3}}{R_{c1}}\log_2(\gamma_1+1)}-1}e^{-\frac{\gamma_1}{\Gamma_1}}e^{-\frac{\gamma_3}{\Gamma_3}}
$$

$$
\times\left(1-e^{\frac{2^{R_{c2}H(\mathbf{u}_2)}}{\Gamma_2}}-\frac{2^{R_{c2}H(\mathbf{u}_1,\mathbf{u}_2,\mathbf{u}_3)-\frac{R_{c2}}{R_{c1}}\log_2(\gamma_1+1)-\frac{R_{c2}}{R_{c3}}\log_2(\gamma_3+1)}}{\Gamma_2}\right)d\gamma_3 d\gamma_1. \tag{D.12}
$$

For high-SNR the exponential function can approximated be the MacLaurin series and thus, the probability simplifies to

$$
\approx\frac{1}{\Gamma_1\Gamma_3}\left(1-\frac{2^{R_{c2}H(\mathbf{u}_2)}-1}{\Gamma_2}\right)\int_{2^{R_{c1}H(\mathbf{u}_1|\mathbf{u}_2,\mathbf{u}_3)}-1}^{2^{R_{c1}H(\mathbf{u}_1|\mathbf{u}_2)}-1}\left(1-\frac{\gamma_1}{\Gamma_1}\right)
$$

$$
\int_{2^{R_{c3}H(\mathbf{u}_3|\mathbf{u}_1,\mathbf{u}_2)}-1}^{2^{R_{c3}(H(\mathbf{u}_1,\mathbf{u}_2,\mathbf{u}_3)-H(\mathbf{u}_2))-\frac{R_{c3}}{R_{c1}}\log_2(\gamma_1+1)}-1}\left(1-\frac{\gamma_3}{\Gamma_3}\right)\left(\frac{2^{R_{c2}H(\mathbf{u}_1,\mathbf{u}_2,\mathbf{u}_3)-\frac{R_{c2}}{R_{c1}}\log_2(\gamma_1+1)-\frac{R_{c2}}{R_{c3}}\log_2(\gamma_3+1)}}{\Gamma_2}-\frac{2^{R_{c2}H(\mathbf{u}_2)}}{\Gamma_2}\right)d\gamma_3 d\gamma_1.
$$

With assumption $R_{c1}=R_{c2}=R_{c3}=R_c$ the equation is transposed to

$$
=\frac{1}{\Gamma_1\Gamma_2\Gamma_3}\left(1-\frac{2^{R_c}-1}{\Gamma_2}\right)\int_{2^{R_cH(\mathbf{u}_1|\mathbf{u}_2,\mathbf{u}_3)}-1}^{2^{R_cH(\mathbf{u}_1|\mathbf{u}_2)}-1}\left(1-\frac{\gamma_1}{\Gamma_1}\right)\int_{2^{R_cH(\mathbf{u}_3|\mathbf{u}_1,\mathbf{u}_2)}-1}^{2^{\frac{R_c(H(\mathbf{u}_1,\mathbf{u}_2,\mathbf{u}_3)-H(\mathbf{u}_2))}{(\gamma_1+1)}}-1}\left(1-\frac{\gamma_3}{\Gamma_3}\right)\left(2^{\frac{R_cH(\mathbf{u}_1,\mathbf{u}_2,\mathbf{u}_3)}{(\gamma_1+1)(\gamma_3+1)}}-2^{R_c}\right)d\gamma_3 d\gamma_1.
$$

$$\tag{D.13}$$

The integrals for γ_1 and γ_3 are solved and the probability can be eventually expressed as

$$
=\frac{2^{R_cH(\mathbf{u}_1,\mathbf{u}_2,\mathbf{u}_3)}}{\Gamma_1\Gamma_2\Gamma_3}\left(1-2^{R_c(H(\mathbf{u}_1|\mathbf{u}_2,\mathbf{u}_3)-H(\mathbf{u}_1|\mathbf{u}_2))}\right.
$$

$$
\left.+\log\left[2^{R_cH(\mathbf{u}_1|\mathbf{u}_2)}\right]\left(\log\left[2^{\frac{R_cH(\mathbf{u}_1|\mathbf{u}_2)}{2}}\right]-1\right)+\log\left[2^{R_cH(\mathbf{u}_1|\mathbf{u}_2,\mathbf{u}_3)}\right]\left(1-\log\left[2^{\frac{R_cH(\mathbf{u}_1|\mathbf{u}_2,\mathbf{u}_3)}{2}}2^{R_c(H(\mathbf{u}_1|\mathbf{u}_2))}\right]\right)\right)\right).
$$

$$\tag{D.14}$$

For probability P_{5c} the Rayleigh fading channel pdf is applied in Eq. (4.46) and formulated to

$$
P_{5c}=\int_{2^{R_{c1}H(\mathbf{u}_1|\mathbf{u}_2,\mathbf{u}_3)}-1}^{2^{R_{c1}H(\mathbf{u}_1|\mathbf{u}_3)}-1}\int_{2^{R_{c3}H(\mathbf{u}_3|\mathbf{u}_1,\mathbf{u}_2)}-1}^{2^{R_{c3}(H(\mathbf{u}_1|\mathbf{u}_3)+H(\mathbf{u}_3))-\frac{R_{c3}}{R_{c1}}\log_2(\gamma_1+1)}-1}
$$

$$
\int_{2^{R_{c2}H(\mathbf{u}_2|\mathbf{u}_1,\mathbf{u}_3)}-1}^{2^{R_{c2}H(\mathbf{u}_1,\mathbf{u}_2,\mathbf{u}_3)-\frac{R_{c2}}{R_{c1}}\log_2(\gamma_1+1)-\frac{R_{c2}}{R_{c3}}\log_2(\gamma_3+1)}-1}\frac{1}{\Gamma_1}e^{-\frac{\gamma_1}{\Gamma_1}}\frac{1}{\Gamma_2}e^{-\frac{\gamma_2}{\Gamma_2}}\frac{1}{\Gamma_3}e^{-\frac{\gamma_3}{\Gamma_3}}d\gamma_3 d\gamma_2 d\gamma_1.
$$

The integral of γ_2 can be solved due to no limit-dependencies in other integrals and expressed as

$$
=\frac{1}{\Gamma_1\Gamma_3}e^{-\frac{2^{R_{c2}H(\mathbf{u}_2|\mathbf{u}_1,\mathbf{u}_3)}-1}{\Gamma_2}}\int_{2^{R_{c1}H(\mathbf{u}_1|\mathbf{u}_2,\mathbf{u}_3)}-1}^{2^{R_{c1}H(\mathbf{u}_1|\mathbf{u}_3)}-1}\int_{2^{R_{c3}H(\mathbf{u}_3|\mathbf{u}_1,\mathbf{u}_2)}-1}^{2^{R_{c3}(H(\mathbf{u}_1|\mathbf{u}_3)+H(\mathbf{u}_3))-\frac{R_{c3}}{R_{c1}}\log_2(\gamma_1+1)}-1}e^{-\frac{\gamma_1}{\Gamma_1}}e^{-\frac{\gamma_3}{\Gamma_3}}
$$

$$
\times\left(1-e^{\frac{2^{R_{c2}H(\mathbf{u}_2|\mathbf{u}_1,\mathbf{u}_3)}}{\Gamma_2}}-\frac{2^{R_{c2}H(\mathbf{u}_1,\mathbf{u}_2,\mathbf{u}_3)-\frac{R_{c2}}{R_{c1}}\log_2(\gamma_1+1)-\frac{R_{c2}}{R_{c3}}\log_2(\gamma_3+1)}}{\Gamma_2}\right)d\gamma_3 d\gamma_1. \tag{D.15}
$$

For high-SNR the exponential function can approximated be the MacLaurin series and thus, the probability simplifies to

$$
\approx\frac{1}{\Gamma_1\Gamma_3}\left(1-\frac{2^{R_{c2}H(\mathbf{u}_2|\mathbf{u}_1,\mathbf{u}_3)}-1}{\Gamma_2}\right)\int_{2^{R_{c1}H(\mathbf{u}_1|\mathbf{u}_2,\mathbf{u}_3)}-1}^{2^{R_{c1}H(\mathbf{u}_1|\mathbf{u}_3)}-1}\left(1-\frac{\gamma_1}{\Gamma_1}\right)
$$

$$
\int_{2^{R_{c3}H(\mathbf{u}_3|\mathbf{u}_1,\mathbf{u}_2)}-1}^{2^{R_{c3}(H(\mathbf{u}_1|\mathbf{u}_3)+H(\mathbf{u}_3))-\frac{R_{c3}}{R_{c1}}\log_2(\gamma_1+1)}-1}\left(1-\frac{\gamma_3}{\Gamma_3}\right)\left(\frac{2^{R_{c2}H(\mathbf{u}_1,\mathbf{u}_2,\mathbf{u}_3)-\frac{R_{c2}}{R_{c1}}\log_2(\gamma_1+1)-\frac{R_{c2}}{R_{c3}}\log_2(\gamma_3+1)}}{\Gamma_2}-\frac{2^{R_{c2}H(\mathbf{u}_2|\mathbf{u}_1,\mathbf{u}_3)}}{\Gamma_2}\right)d\gamma_3 d\gamma_1.
$$

With assumption $R_{c1} = R_{c2} = R_{c3} = R_c$ the equation is transposed to

$$= \frac{1}{\Gamma_1 \Gamma_2 \Gamma_3} \left(1 - \frac{2^{R_c H(\mathbf{u}_2|\mathbf{u}_1,\mathbf{u}_3)} - 1}{\Gamma_2} \right) \int_{2^{R_c H(\mathbf{u}_1|\mathbf{u}_2,\mathbf{u}_3)}-1}^{2^{R_c H(\mathbf{u}_1|\mathbf{u}_3)}-1} \left(1 - \frac{\gamma_1}{\Gamma_1} \right)$$

$$\int_{2^{R_c H(\mathbf{u}_3|\mathbf{u}_1,\mathbf{u}_2)}-1}^{2^{\frac{R_c(H(\mathbf{u}_1|\mathbf{u}_3)+H(\mathbf{u}_3))}{(\gamma_1+1)}}-1} \left(1 - \frac{\gamma_3}{\Gamma_3} \right) \left(\frac{2^{R_c H(\mathbf{u}_1,\mathbf{u}_2,\mathbf{u}_3)}}{(\gamma_3+1)(\gamma_1+1)} - 2^{R_c H(\mathbf{u}_2|\mathbf{u}_1,\mathbf{u}_3)} \right) d\gamma_3 d\gamma_1,$$

The integrals for γ_1 and γ_3 are solved and the probability can be eventually expressed as

$$= \frac{1}{\Gamma_1 \Gamma_2 \Gamma_3} \left(2^{R_c(H(\mathbf{u}_1|\mathbf{u}_3)+H(\mathbf{u}_2|\mathbf{u}_1,\mathbf{u}_3)+H(\mathbf{u}_3|\mathbf{u}_1,\mathbf{u}_2))} - 2^{R_c(H(\mathbf{u}_1|\mathbf{u}_2,\mathbf{u}_3)+H(\mathbf{u}_2|\mathbf{u}_1,\mathbf{u}_3)+H(\mathbf{u}_3|\mathbf{u}_1,\mathbf{u}_2))} \right.$$

$$+ 2^{R_c H(\mathbf{u}_1,\mathbf{u}_2,\mathbf{u}_3)} \log \left[2^{R_c H(\mathbf{u}_1|\mathbf{u}_3)} \right] \left(\log \left[2^{\frac{R_c H(\mathbf{u}_1|\mathbf{u}_3)}{2}} 2^{R_c(H(\mathbf{u}_3)-H(\mathbf{u}_3|\mathbf{u}_1,\mathbf{u}_2))} \right] - 1 \right)$$

$$\left. + 2^{R_c H(\mathbf{u}_1,\mathbf{u}_2,\mathbf{u}_3)} \log \left[2^{R_c H(\mathbf{u}_1|\mathbf{u}_2,\mathbf{u}_3)} \right] \left(1 - \log \left[2^{-\frac{R_c H(\mathbf{u}_1|\mathbf{u}_2,\mathbf{u}_3)}{2}} 2^{R_c(H(\mathbf{u}_3)+H(\mathbf{u}_1|\mathbf{u}_3)H(\mathbf{u}_3|\mathbf{u}_1,\mathbf{u}_2))} \right] \right) \right) \tag{D.16}$$

Appendix E   Derivation of Equation (6.5)

We first show some results about the entropy of the modulus-2 addition of two independent binary variable X and Y. Assume X and Y follow the Bernoulli distributions with parameters p_x and p_y, respectively, i.e., $X \sim \text{Bern}(p_x)$ and $Y \sim \text{Bern}(p_y)$. We can easily get the probability distribution for the modulus-2 addition of X and Y as

$$\begin{cases} p(X \oplus Y = 0) & = p(X = 0)p(Y = 0) + p(X = 1)p(Y = 1) & = (1 - p_x)(1 - p_y) + p_x p_y & = 1 - p_x * p_y, \\ p(X \oplus Y = 1) & = p(X = 0)p(Y = 1) + p(X = 1)p(Y = 0) & = (1 - p_x)p_y + p_x(1 - p_y) & = p_x * p_y, \end{cases}$$
$$\text{(E.1)}$$

where $p_x * p_y = (1 - p_x)p_y + p_x(1 - p_y)$. Therefore, the entropy of $X \oplus Y$ is $H(X \oplus Y) = H_b(p_x * p_y)$. There are two special cases:

- If $p_x = 0$, $H(X \oplus Y) = H_b(0 * p_y) = p_y$.

- If $p_x = 1$, $H(X \oplus Y) = H_b(0.5 * p_y) = H_b(0.5) = 1$.

These results will be used in the derivation of Equation (6.5),
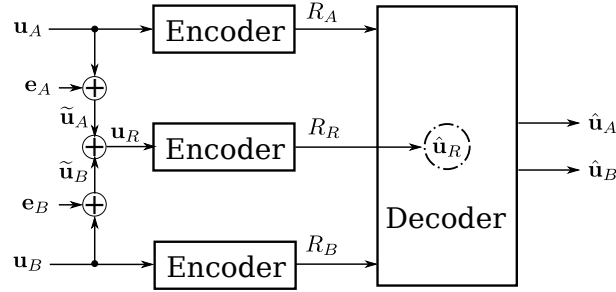
Figure E.1: The equivalent model of MARC-IE, where $\oplus$ indicates modulus-2 addition.

Now consider the equivalent system model of MARC-IE shown in Figure E.1, where vectors $\mathbf{e}_A$, $\mathbf{e}_B$ and are i.i.d. drawn from Bernoulli distributions with parameters p_A and p_B, respectively. The relationship between $\mathbf{u}_R$ and $\hat{\mathbf{u}}_R$ can be expressed as $\hat{\mathbf{u}}_R = \mathbf{u}_R \oplus \mathbf{e}_R$, where $\mathbf{e}_R$ is also i.i.d. drawn from Bernoulli distributions with parameters p_R. The mutual information between $\mathbf{u}_R$ and $\hat{\mathbf{u}}_R$) is

$$I(\mathbf{u}_R; \hat{\mathbf{u}}_R) = H(\hat{\mathbf{u}}_R) - H(\hat{\mathbf{u}}_R | \mathbf{u}_R) \tag{E.2}$$
$$= H(\widetilde{\mathbf{u}}_A \oplus \widetilde{\mathbf{u}}_B \oplus \mathbf{e}_R) - H_b(p_R) \tag{E.3}$$
$$= H(\mathbf{u}_A \oplus \mathbf{e}_A \oplus \mathbf{u}_B \oplus \mathbf{e}_B \oplus \mathbf{e}_R) - H_b(p_R) \tag{E.4}$$
$$\stackrel{(a)}{=} 1 - H_b(p_R), \tag{E.5}$$

where (a) follows the results presented above.

By using the chain rule, the joint entropy of $H(\mathbf{u}_A, \mathbf{u}_B, \mathbf{u}_R, \hat{\mathbf{u}}_R)$ can be represented as

$$H(\mathbf{u}_A, \mathbf{u}_B, \mathbf{u}_R, \hat{\mathbf{u}}_R) = H(\mathbf{u}_A, \mathbf{u}_B) + H(\mathbf{u}_R | \mathbf{u}_A, \mathbf{u}_B) + H(\hat{\mathbf{u}}_R | \mathbf{u}_A, \mathbf{u}_B, \mathbf{u}_R) \tag{E.6}$$
$$= H(\hat{\mathbf{u}}_R) + H(\mathbf{u}_A, \mathbf{u}_B | \hat{\mathbf{u}}_R) + H(\mathbf{u}_R | \mathbf{u}_A, \mathbf{u}_B, \hat{\mathbf{u}}_R). \tag{E.7}$$

Then we have

$$H(\mathbf{u}_A, \mathbf{u}_B | \hat{\mathbf{u}}_R) = H(\mathbf{u}_A, \mathbf{u}_B) + H(\mathbf{u}_R | \mathbf{u}_A, \mathbf{u}_B) + H(\hat{\mathbf{u}}_R | \mathbf{u}_A, \mathbf{u}_B, \mathbf{u}_R) - H(\hat{\mathbf{u}}_R) - H(\mathbf{u}_R | \mathbf{u}_A, \mathbf{u}_B, \hat{\mathbf{u}}_R). \tag{E.8}$$

Note the conditional mutual information $I(\mathbf{u}_R; \hat{\mathbf{u}}_R | \mathbf{u}_A, \mathbf{u}_B)$ can be expressed by the chain rule, as

$$I(\mathbf{u}_R; \hat{\mathbf{u}}_R | \mathbf{u}_A, \mathbf{u}_B) = H(\mathbf{u}_R | \mathbf{u}_A, \mathbf{u}_B) - H(\mathbf{u}_R | \mathbf{u}_A, \mathbf{u}_B, \hat{\mathbf{u}}_R)$$
$$= H(\hat{\mathbf{u}}_R | \mathbf{u}_A, \mathbf{u}_B) - H(\hat{\mathbf{u}}_R | \mathbf{u}_A, \mathbf{u}_B, \mathbf{u}_R). \tag{E.9}$$

By substituting $H(\mathbf{u}_R|\mathbf{u}_A,\mathbf{u}_B)$ of (E.9) into (E.8), $H(\mathbf{u}_A,\mathbf{u}_B|\hat{\mathbf{u}}_R)$ can be rewritten as

$$H(\mathbf{u}_A,\mathbf{u}_B|\hat{\mathbf{u}}_R) = H(\mathbf{u}_A,\mathbf{u}_B) + H(\hat{\mathbf{u}}_R|\mathbf{u}_A,\mathbf{u}_B) - H(\hat{\mathbf{u}}_R), \qquad (E.10)$$

where the conditional entropy $H(\hat{\mathbf{u}}_R|\mathbf{u}_A,\mathbf{u}_B)$ is calculated as

$$
\begin{aligned}
H(\hat{\mathbf{u}}_R|\mathbf{u}_A,\mathbf{u}_B) &= H(\mathbf{u}_A \oplus \mathbf{e}_A \oplus \mathbf{u}_B \oplus \mathbf{e}_B \oplus \mathbf{e}_R|\mathbf{u}_A,\mathbf{u}_B) \\
&= H(\mathbf{e}_A \oplus \mathbf{e}_B \oplus \mathbf{e}_R) \\
&= H_b(p_A * p_B * p_R). \qquad (E.11)
\end{aligned}
$$

Therefore, $H(\mathbf{u}_A,\mathbf{u}_B|\hat{\mathbf{u}}_R)$ shown in the third inequality of (6.5) can be obtained by substituting (E.11) into (E.10), as

$$
\begin{aligned}
H(\mathbf{u}_A,\mathbf{u}_B|\hat{\mathbf{u}}_R) &= H(\mathbf{u}_A,\mathbf{u}_B) + H(e_A \oplus e_B \oplus e_R) - H(\hat{\mathbf{u}}_R) \\
&= H(\mathbf{u}_A) + H(\mathbf{u}_B) + H_b(p_A * p_B * p_R) - H_b(\hat{\mathbf{u}}_R) \\
&= 1 + H_b(p_A * p_B * p_R). \qquad (E.12)
\end{aligned}
$$

The conditional entropy $H(\mathbf{u}_A,\mathbf{u}_B|\hat{\mathbf{u}}_R)$ in (E.12) can also alternatively be expressed by the chain rule, as

$$
\begin{aligned}
H(\mathbf{u}_A,\mathbf{u}_B|\hat{\mathbf{u}}_R) &= H(\mathbf{u}_B|\mathbf{u}_A,\hat{\mathbf{u}}_R) + H(\mathbf{u}_A|\hat{\mathbf{u}}_R) \\
&= H(\mathbf{u}_A|\mathbf{u}_B,\hat{\mathbf{u}}_R) + H(\mathbf{u}_B|\hat{\mathbf{u}}_R). \qquad (E.13)
\end{aligned}
$$

Since $\hat{\mathbf{u}}_R$ is composed of $\mathbf{u}_A$, the conditional entropy $H(\mathbf{u}_A|\hat{\mathbf{u}}_R)$ in (E.13) can be calculated as

$$
\begin{aligned}
H(\mathbf{u}_A|\hat{\mathbf{u}}_R) &= H(\mathbf{u}_A|\mathbf{u}_A \oplus \mathbf{e}_A \oplus \mathbf{u}_B \oplus \mathbf{e}_B \oplus \mathbf{e}_R) \\
&= H(\mathbf{e}_A \oplus \mathbf{u}_B \oplus \mathbf{e}_B \oplus \mathbf{e}_R) \\
&= 1. \qquad (E.14)
\end{aligned}
$$

Therefore, we can obtain $H(\mathbf{u}_B|\mathbf{u}_A,\hat{\mathbf{u}}_R)$, shown in the second inequality of (6.5), by substituting (E.14) into (E.13), as

$$
\begin{aligned}
H(\mathbf{u}_B|\mathbf{u}_A,\hat{\mathbf{u}}_R) &= H(\mathbf{u}_A,\mathbf{u}_B|\hat{\mathbf{u}}_R) - H(\mathbf{u}_A|\hat{\mathbf{u}}_R) \\
&= H_b(p_A * p_B * p_R). \qquad (E.15)
\end{aligned}
$$

The conditional entropy $H(\mathbf{u}_A|\mathbf{u}_B,\hat{\mathbf{u}}_R)$ shown in the first inequality of (6.5) is obtained in the same way.

Appendix F   Rate-distortion Region Visualization

Similar to the time sharing concept, the rate-distortion region is divided into three parts, as

(a) for some $0 \leq \tilde{d} \leq d_2$

$$\begin{cases} R_1 & \geq & H_b(d_1 * p_1 * p_2 * \tilde{d}) - H_b(d_1), \\ R_2 & \geq & 1 - H_b(\tilde{d}), \end{cases} \tag{F.1}$$

(b) for some $0 \leq \tilde{d} \leq d_1$

$$\begin{cases} R_2 & \geq & H_b(d_2 * p_1 * p_2 * \tilde{d}) - H_b(d_2) \\ R_1 & \geq & 1 - H_b(\tilde{d}); \end{cases} \tag{F.2}$$

(c)

$$R_{\text{sum}} \geq 1 + H_b(d_1 * p_1 * p_2 * d_2) - H_b(d_1) - H_b(d_2), \tag{F.3}$$

where $\tilde{d}$ is a dummy variable. We calculate the rates R_1, R_2 as well as R_{sum} with given d_1 and d_2, respectively, and then plot the rate-distortion region by combining the three parts shown above.

Appendix G   Sum Rate of Multiple Users Case

In general, the sum rate requirement R_{sum} in the Berger-Tung inner bound is given as

$$R_{\text{sum}} \geq I(\mathbf{u}_1, \mathbf{u}_2, \cdots, \mathbf{u}_K; \mathbf{v}_1, \mathbf{v}_2, \cdots, \mathbf{v}_K), \tag{G.1}$$

however, deriving this mutual information is not easy, instead, we assume $d_1, d_2, \cdots, d_K$ are relatively small. Thus, we only need to calculate the joint entropy $H(\mathbf{U})$ to obtain the sum rate.

Given the fact that u_k, $k = 1, \cdots, K$ is the result of passing u through a BSC with crossover probability p_k, where u_k and u represent the realizations of $\mathbf{u}_k$ and $\mathbf{u}$, respectively, the joint probability $\Pr(u_1, u_2, \cdots, u_K)$ is formulated as

$$\Pr(u_1, u_2, \cdots, u_K) = \Pr(u = 0) \prod_{i \in \mathbb{A}} (1 - p_i) \prod_{j \in \mathbb{A}^C} p_j + \Pr(u = 1) \prod_{i \in \mathbb{A}} p_i \prod_{j \in \mathbb{A}^C} (1 - p_j), \tag{G.2}$$

where $\mathbb{A}$ is the set of the index k if $u_k = 0$, $k = 1, \cdots, K$ and $\mathbb{A}^C$ is the complementary set of the set $\mathbb{A}$. For example, setting $K = 3$ with $u_1 = 0$, $u_2 = 1$ and $u_3 = 0$, the set $\mathbb{A}$ is equal to $\{1, 3\}$ and $\mathbb{A}^C = \{2\}$.

Therefore, the joint entropy $H(\mathbf{U})$ which is equivalent to the information rate R_{sum} is calculated as

$$H(\mathbf{U}) = - \sum_{u_k \in \{0,1\}} \Pr(u_1, u_2, \cdots, u_K) \log_2(\Pr(u_1, u_2, \cdots, u_K)). \tag{G.3}$$